From the Department of Neurology
of the University of Lübeck
Director: Prof. Dr. med. Thomas F. Münte

Neural processing of food stimuli: Influence of reward, homeostasis, habit, and attention

Dissertation for Fulfillment of Requirements
for the Doctoral Degree
of the University of Lübeck
from the Department of Natural Sciences

Submitted by
Mushfa Yousuf

Lübeck 2019

1st Referee: Prof. Dr. Thomas F. Münte

2nd Referee: Prof. Dr. Tömme Noesselt

Date of oral examination: 14-06-2019

Approved for printing. Lübeck, 17-06-2019

Table of contents

Zusammenfassung

Beim Menschen gilt Nahrung als effektiver Primärverstärker, während Geld ein Sekundärverstärker ist, der seinen Wert erst durch Lernerfahrung erhält. In der ersten Studie (Kapitel 2) versuchten wir, die neuronalen Regionen zu identifizieren, die die Verarbeitung von Nahrungsverstärkern unterstützen, sie mit den neuronalen Grundlagen von monetären Verstärkern zu vergleichen und ihre Modulation durch unterschiedliche Stoffwechselzustände (Hunger vs. Sättigung) zu untersuchen. Zwanzig gesunde männliche Probanden wurden in zwei experimentellen Sitzungen unter Verwendung funktioneller Magnetresonanztomographie getestet, einmal hungrig und einmal satt. Die Probanden nahmen an einer assoziativen Lernaufgabe teil und konnten in separaten Blöcken Lebensmittel- oder Geldbelohnungen erhalten. Sowohl Nahrungsmittel- als auch monetäre Belohnungen führten zu erhöhter kortikaler Aktivität im ventralen Striatum, dem medialen Orbitofrontalkortex und der Amygdala - Regionen, die bereits zuvor mit der Verarbeitung von Belohnungen in Verbindung gebracht wurden. Nahrungsmittelbelohungen aktivierten außerdem den operculären Teil des unteren Frontalgyrus und die Insula, die zusammen als primärer Geschmackskortex bezeichnet werden. Darüber hinaus wurden in Reaktion auf negatives Feedback (hier Belohnungsausfall) Aktivierungen der vorderen Insula, der supplementär motorischen Rinde sowie des lateralen präfrontalen Kortex beobachtet. Darüber hinaus konnte eine Interaktion zwischen dem Stoffwechselzustand und der Art der Belohnung im supramarginalen Gyrus (SMG) und anderen motorischen und sensorischen Regionen festgestellt werden. Schließlich konnte durch funktionelle Konnektivitätsanalyse eine Korrelation zwischen SMG und mesolimbischen Regionen, wie dem Hippocampus, Mittelhirn und dem cingulären Kortex, für die Hunger-Bedingung gezeigt werden. Für die Interaktion zwischen Stoffwechselzustand und Art der

Belohnung konnte ebenfalls eine Korrelation zwischen SMG und ventralem Striatum festgestellt werden. Während kortikale Regionen, die allgemein mit Belohnung in Verbindung gebracht werden, verschiedene Belohnungsreize verarbeiten, deuten unsere Ergebnisse darauf hin, dass der SMG möglicherweise eine Schlüsselrolle bei der Integration von Stoffwechselzuständen und Art der verfügbaren Belohnung spielt.

Die zweite Studie (Kapitel 3) diente dem Ziel, durch ein Belohnungsabwertungsverfahren die elektrophysiologischen Komponenten zu identifizieren, die mit zielgerichtetem versus gewohnheitsmäßiges Verhalten in Verbindung stehen. Wir analysierten Datensätze von 35 gesunden Probanden, die in einem bekannten, für die Untersuchung von Gewohnheitsbildung entwickelten Paradigma („fabulous fruit game“ getestet wurden. In Übereinstimmung mit früheren Untersuchungen zeigten die Teilnehmer im Verhalten eine Sensitivität für die Belohnungsabwertung, was als Kennzeichen zielgerichteter kognitiver Kontrolle gilt. In den elektrophysiologischen Daten beobachteten wir geringere N2- und erhöhte ERN-Amplituden nach Verhaltensfehlern ("slips of action") in Bedingungen, die sowohl das zielgerichtete als auch das gewohnheitsmäßige System betrafen. Probanden, die mehr Sensitivität gegenüber Belohnungsabwertung zeigten, hatten größere Differenzen in der Abnahme der N2 und der Zunahme der ERN. Außerdem zeigen wir, wie spezifische neurophysiologische Lernsignale, nämlich ERN und Feedback-bezogene P3, die nachfolgende Sensitivität gegenüber Belohnungsabwertung vorhersagen können. Unsere Ergebnisse deuten darauf hin, dass die N2- und ERN-Komponenten als Indikatoren für eine zielgerichtete vs. gewohnheitsmäßige kognitive Kontrolle verwendet werden können, und unterstreichen die Bedeutung der ERN als elektrophysiologisches Merkmal im Kontext von zielgerichtetem Verhalten.

In der dritten Studie (Kapitel 4) wollten wir mithilfe der funktionellen Magnetresonanztomographie frühere Ergebnisse zur N2pc-Komponente mit einem Bildgebungsansatz untermauern. Diese früheren Ergebnisse deuteten darauf hin, dass Nahrungsmittelstimuli die Aufmerksamkeit auf sich ziehen, was durch eine höhere Amplitude der kontralateralen N2 Komponente (N2pc) angezeigt wird. Zwanzig gesunde Teilnehmer führten eine selektive Aufmerksamkeitsaufgabe mit bilateralen Stimuli durch. Jeder Stimulus umfasste zwei Bilder, eines links und eines rechts eines Fixierungssymbols (ein nach links oder rechts zeigender Pfeil), das anzeigte, auf welche Seite die Aufmerksamkeit gerichtet werden sollte. Die Bilder überlagernd wurden grüne vertikale Balken dargeboten. Die Aufgabenstellung der Probanden war, die Größe des Balkens auf der durch den Pfeil angezeigten zu beachtenden Seite zu überprüfen und eine Taste für einen etwas kleineren Balken zu drücken. Die Bilder hinter den Balken konnten 4 verschiedene Konfigurationen aufweisen: (i) Objekte auf beiden Seiten, (ii) Nahrungsbilder auf der beachteten Seite / Objekt auf der unbeachteten Seite, (iii) Objekt auf der beachteten Seite / Essen auf der unbeachteten Seite und (iv) Nahrungsbilder auf beiden Seiten. Die Verhaltensdaten zeigen, dass die Reaktionszeit der Teilnehmer auf das Ziel länger war, wenn auf der abgelenkten Seite ein Lebensmittelbild angezeigt wurde verglichen mit Gegenständen. In Bezug auf die funktionelle Aktivität zeigen unsere Daten eine signifikant erhöhte Aktivität im extrastriären Kortex der kontralateralen und ipsilateralen (in Bezug auf die beachtete Seite), wenn Nahrung verglichen mit den Objektbildern auf der beachteten bzw. der unbeachteten Seite erschien. Diese Ergebnisse legen nahe, dass Lebensmittel aufgrund ihrer belohnenden Eigenschaften stärker Aufmerksamkeit auf sich ziehen als andere Objekte.

Abstract

In humans, food is considered a powerful primary reinforcer, whereas money is a secondary reinforcer, as it gains value through the learning experience. In the first study (chapter 2), we aimed to identify the neural regions supporting the processing of food-related reinforcers, relate it to the neural underpinnings of monetary reinforcers, and explore their modulation by metabolic state (hunger vs satiety). Twenty healthy male participants were tested in two experimental sessions, once hungry and once satiated, using functional magnetic resonance imaging. Participants performed an associative learning task, receiving food or monetary rewards (in the form of images) on separate blocks. Irrespective of incentive type, both food, and monetary rewards engaged ventral striatum, medial orbitofrontal cortex and amygdala, regions that have been previously associated with reward processing. Food incentives additionally engaged the opercular part of the inferior frontal gyrus and the insula, collectively known as a primary gustatory cortex. Moreover, in response to negative feedback (here, reward omission), robust activation was observed in the anterior insula, supplementary motor area and lateral parts of the prefrontal cortex, including middle and inferior frontal gyrus. Furthermore, the interaction between metabolic state and incentive type resulted in supramarginal gyrus (SMG) activity, among other motor and sensory-related regions. Finally, functional connectivity analysis showed a correlation in the hungry state between the SMG and mesolimbic regions, including the hippocampus, midbrain, and cingulate areas. Also, the interaction between metabolic state and incentive type revealed coupling between SMG and ventral striatum. Whereas general purpose reward-related regions process incentives of different kinds, the current results suggest that the SMG might play a key role in integrating the information related to current metabolic state and available incentive type.

In the second study (chapter 3), we aimed to identify the electrophysiological components associated with goal-directed vs habitual performance using an outcome devaluation procedure. Datasets from thirty-five healthy participants were analyzed using the 'fabulous fruit game' paradigm that has been used to pinpoint the transition from goal-directed to habitual behavior. Behaviorally, in line with previous research, participants displayed sensitivity to outcome devaluation, a hallmark of goal-directed control. Electrophysiologically, decreased N2 and increased error-related negativity (ERN) amplitudes were associated to slips of action in conditions that could potentially engage both the goal-directed and habitual systems, with participants that displayed more sensitivity to devaluation also showing larger difference-N2 decreases and difference-ERN increases. Furthermore, we show how specific neurophysiological learning signals, namely ERN and feedback-locked P3, could predict subsequent sensitivity to devaluation. Our findings indicate that the N2 and ERN components can be used as indices of goal-directed vs habitual control and emphasize the importance of the ERN as an electrophysiological trait in the context of goal-directed behavior.

In the third study (chapter 4), using functional magnetic resonance imaging, we aimed to corroborate previous N2pc findings, suggesting that food stimuli attract attention to their location and evoke contralateral activity on the posterior side of the scalp, the so called N2pc. Twenty healthy participants performed a selective attention task with a bilateral stimuli setup. In each trial two images are presented, one on the left and one on the right side of the (</>) fixation symbol. The fixation symbol (a left or right-pointing arrow) indicates the side to which attention needed to be directed covertly, i.e. without moving the eyes. Green vertical bars were superimposed on both images. The bars were task-relevant in that participants had to press a button whenever the bar on the attended side was slightly smaller than the standard bar. Four different stimulus configurations were used: (i) objects on both sides, (ii) food on the attended

side/object on the unattended side, (iii) object on the attended side/food on the unattended side, and (iv) food on both sides. The behavioral data demonstrated that participants' response time to targets was longer when a food image appeared on the distracted side as compared to object items indicating attention capture. Regarding functional activity, our data reveals significant activity in the contralateral and ipsilateral (with respect to attended side) extrastriate cortex when food relative to object image appeared on the attended and distracted side, respectively. These results suggest that food compared to other items attract and bias spatial attention likely because of its rewarding properties.

1 Introduction

1.1 General outline of the Thesis

Food, among other stimuli (e.g., sexual contact, sleep, water), is considered a primary reinforce, because it possesses characteristics that are necessary to sustain life. Its value is inherently adopted by organisms, which are naturally responsive to it (Krajbich et al. 2015; Schultz 2002; Vilkka 1997). In contrast to primary reinforcers, secondary reinforcers do not possess innate value, but this is instead learned through experience (Ryan and Deci 2000). Among secondary reinforcers (e.g., praise, reprimands, tokens), money is known to be a particularly potent one (Delgado et al. 2006).

This research aims to further our understanding of the neural mechanisms underlying reward, homeostasis, habit formation, and attention in response to food stimuli. In the current introductory chapter, I briefly explain the neural regions, along with their functional significance, that previously have been shown to be involved in processing of the aforementioned cognitive processes.

1.2 Neural responses to food and monetary stimuli in the context of reward processing

In everyday life, reward plays a critical role and acts as a reinforcer, encouraging organisms to alter their behavior. In affective neuroscience, the reward is often operationalized as a pleasant or valuable stimulus that motivates organisms to engage in a specific behavior (Schultz 2015). Several functional magnetic resonance imaging (fMRI) studies have assessed neural responses to visual food stimuli. Compared to nonfood objects, visualization of food stimuli elicited activation

in the opercular part of the inferior frontal gyrus (IFG) and insular cortex (Porubská et al. 2006; Simmons et al. 2005; Doherty et al. 2001). The majority of functional imaging studies on humans have identified the insular and frontal opercular regions as primary gustatory cortex, which has been shown to be responsible for the identification of tastes and the processing of taste intensity (Kringelbach et al. 2004; Small et al. 2003). The primary gustatory cortex has also been thought to be part of a network involved in representing and processing conceptual knowledge about food (Simmons et al. 2005; de Araujo et al. 2003a). It has been proposed that any damage to these regions can lead to an inability to recognize different tastes (Pritchard et al. 1999). Other areas that have also been found to be active on the visualization of food compared to nonfood objects include the visual cortex, limbic structures such as the amygdala and the parahippocampal gyrus, and prefrontal regions such as the orbitofrontal cortex (OFC; Grimm et al. 2012; Schur et al. 2009). In particular, the caudolateral part of OFC, also referred to as a secondary gustatory cortex, represent the reward center for taste and is believed to be responsible for projecting the sensation of taste to other regions in the OFC (de Araujo et al. 2003b; Gottfried et al. 2003). Neurons with taste responses can be found in many areas of the OFC and are thought to project to several regions of the ventral forebrain, including amygdala and hypothalamus (Rolls 2000). One primate study has shown that the hypothalamic neurons might receive input from these OFC neurons and make them respond to taste and sight of food if the monkey is hungry (Rolls 1999). Anatomically, it has also been shown that the efferent connections of the primary gustatory cortex are projecting to the secondary gustatory cortex (Oliveira-Maia et al. 2011). Furthermore, studies have also demonstrated that both primary and secondary gustatory cortices are activated not only during the tasting of actual foods but also might become active and produce taste responses while participants view food pictures (Simmons et al. 2005; Killgore et al. 2003).

Moreover, OFC activity has been reported to increase with the pleasantness rating of food stimuli (Kringelbach et al. 2003; de Araujo et al. 2003a).

Most fMRI studies to date have used either passive viewing of food pictures or passive food delivery to measure neural responses to food rewards. In paradigms using images, subjects passively view images of food and nonfood items in block or event-related designs (e.g. Leidy et al. 2011; Schienle et al. 2009; Killgore et al. 2003), whereas, in the case of passive delivery, food or liquid (e.g., juice, milkshake, chocolate) is orally delivered to subjects inside the scanner (e.g. Felsted et al. 2010; Rolls and McCabe 2007; Berns et al. 2001). Neural activity showed a very similar pattern in both types of paradigms, although with some variations in intensity and location of peak activity. Significant activation was reported in primary gustatory cortex, secondary gustatory cortex, ventral striatum (VS) and amygdala (Jacobson et al. 2010; Plassmann et al. 2008; Rolls 2006; Killgore et al. 2003). The secondary gustatory cortex has been thought to receive input from the amygdala (Morris and Dolan 2001), serving as an intermediate region between primary and secondary gustatory cortices (Jacobson et al. 2010). The amygdala is a part of the limbic system and responds to a range of biologically relevant stimuli, such as faces or other fear inducing stimuli (Kim et al. 2016; Pishnamazi et al. 2016). Amygdala has also been suggested to play a critical role in learning and recognition of the biological significance of food-related items (Sescousse et al. 2013; Morris and Dolan 2001). Few fMRI studies on food have shown an activation in the amygdala by food-related stimuli, such as odors and tastes as well as with sensations from the gastrointestinal tract (Sescousse et al. 2013; Dagher 2012).

As with the primary reinforcer food, neuroimaging research has also focused on brain responses to the powerful secondary reinforcer money. Previous fMRI studies have typically assessed brain activity to monetary reward using contingency or incentive paradigms. In

contingency tasks, participants learn probabilistic relations between stimuli and reward by trial and error (e.g. Jiang et al. 2014; Daniel and Pollmann 2010; Koch et al. 2008; Knutson et al. 2003), whereas in incentive tasks, subjects perform an elementary cognitive task in order to receive a reward (e.g. Bjork et al. 2010; Spreckelmeyer et al. 2009; Knutson and Greer 2008; Knutson et al. 2000). These studies have identified several brain regions implicated in reward processing, including striatum, OFC, amygdala and insula (Fujiwara et al. 2009; Völlm et al. 2007; Nieuwenhuis et al. 2005; Delgado et al. 2000; Knutson et al. 2000). Distinct functional roles have been attributed to these neuronal regions. For instance, the striatum is an integral component of the reward circuitry and is thought to play an essential role in processing a wide range of stimuli that can act as a reinforcer (Haber and Knutson 2010; Elliott et al. 2003). Another core component of the reward circuitry is the OFC. The OFC is implicated in reward processing, goal selection and incentive motivation (Arana et al. 2003; Gottfried et al. 2003). Several studies have further suggested a functional demarcation between medial and lateral OFC, with the former responding more strongly to reward and the latter being more sensitive to punishment. Regarding amygdala, studies have demonstrated an increase in activation to reward stimuli, irrespective of the kind of incentive delivered to the participants as rewarding feedback (Haber and Knutson 2010; Elliott et al. 2003). Evidence from experimental neurophysiology and neuropsychology suggested that amygdala output pathways have been strongly connected to VS and OFC. Along with these two regions, several other brain regions, e.g. the midbrain dopaminergic system and the basal forebrain, assist the amygdala in carrying out its reward-related functions (Murray 2007; Ramirez and Savage 2007).

Moreover, some of the studies mentioned above on monetary rewards have also investigated the influence of punishment and omission of reward on the neuronal regions. For example, activation in the striatum increased with the delivery of monetary reward (Delgado et

al. 2000). Conversely, activation in the striatum decreased following punishment or omission of monetary reward (Jiang et al. 2014; Delgado et al. 2003). Also, further studies have shown the involvement of the insula in learning the negative value of a stimuli. In addition, neuroimaging studies have shown an increase of activation in insula in the face of a potential monetary loss. The insula plays a vital role in combining effective processing, behavior, and decision-making. Anatomically, the insula has bidirectional connections with the numerous brain regions that are implicated in reward processing, such as OFC, VS, and amygdala. In previous studies, the activation of the insula has been associated with a wide variety of positive and negative affective processes, but most frequently related to aversive events, such as loud noise, disgust images and stale-smells (Palminteri et al. 2012; Knutson et al. 2003; O'Doherty et al. 2003).

1.3 Neural responses to food in hunger vs satiety

To better understand socially relevant clinical and non-clinical behaviors such as overeating, previous neuroimaging studies have assessed neural responses to food stimuli in different motivational (hungry vs satiated) states. Activation in the hippocampus, amygdala, inferior parietal lobule (IPL) and insula has been demonstrated when normal-weight participants viewed food images in a hungry compared to satiated state (Dagher 2012; van der Laan et al. 2011; Führer et al. 2008). Also, the hunger state showed increased activation in areas associated with selective attention and the processing of visual cues, such as extrastriate cortex and fusiform gyrus (S. Frank et al. 2010; Führer et al. 2008; Uher et al. 2006). Furthermore, it has been suggested that fasting often increases activation in VS and OFC in response to high-calorie compared to low-calorie food items (Pursey et al. 2014; Goldstone et al. 2009). The VS and OFC

were consistently shown to be involved in the cognitive processing of reward and stimuli salience (Sescousse et al. 2013).

1.4 Neural regions involved in the formation of goal-directed and habitual behavior

The neural regions underlying goal-directed and habitual behavior have been extensively investigated, and several essential neural networks have been shown to be involved. Evidence from both human and animal studies (Mannella et al. 2013; de Wit et al. 2009; Goto and Grace 2005; Yin et al. 2005) has suggested that goal-directed behavior relies on the neural networks comprising ventromedial prefrontal cortex (vmPFC), caudate nucleus, limbic structures including amygdala and hippocampus, and VS. The VS, which is also described as the region for limbic-to-motor interface (Mogenson et al. 1980), integrates limbic-dependent information concerning reward and motivation, and prefrontal-dependent cognitive functions to select appropriate goal-directed responses (Goto and Grace 2005; Grace 2000; Mogenson et al. 1980). The habitual behavior, in contrast, is believed to be rooted in the network involving posterior putamen and motor cortex (Tricomi et al. 2009; Yin et al. 2004). A diffusion tensor imaging study (de Wit et al. 2012b) has demonstrated a relationship between properties of the white matter tract connecting posterior putamen and premotor cortex and habitual responding, whereas properties of the tract connecting caudate nucleus and vmPFC were related to goal-directed responding, corroborating dissociable corticostriatal pathways underlying these behaviors. The vmPFC is considered a critical region for implementing goal-directed behavior. The vmPFC has shown to be involved in monitoring already learned correct responses and also in inhibiting these responses when the associated value of outcomes are no longer desirable (Haber 2011). Previous human

functional neuroimaging studies have reported a positive correlation between the vmPFC activation and goal-directed outcomes (McNamee et al. 2015; de Wit et al. 2009; Valentin et al. 2007). A recent human lesion study (Reber et al. 2017) has tested the relevance of vmPFC in the execution of goal-directed responses during an outcome devaluation test stage. Compared to healthy subjects and patients with non-vmPFC brain lesions, the patients with vmPFC lesion were unable to reduce their instrumental responses to the devalued outcomes, indicating their incapability of adopting changes in response→outcome contingencies flexibly.

The dual-system theory has also been formalized within computational models of reinforcement learning (RL). A model-based method (thought to subserve goal-directed behavior) maps the responses to their potential outcomes, whereas a model-free method (considered to serve habitual behavior) updates expectation based on retrospective experience (Huys et al. 2013). One study (Gläscher et al. 2010) has attempted to identify the neuronal signals underlying these computational models using a stochastic task. It has been reported that a model-based prediction error (PE) signal is encoded by the prefrontal-parietal cortices, whereas a model-free PE signal is encoded in the VS. However, in a more recent study (Daw et al. 2011), a sequential decision task has been used, and they reported that both model-free and model-based PE signals are encoded within prefrontal cortex and VS. Other studies have also reported a correlation between activity in the caudate nucleus and model-free PE signal (Haruno and Kawato 2006; O'Doherty et al. 2004).

Both human and animal studies (de Wit et al. 2012a; Cheer et al. 2007; Goto and Grace 2005) have also directed attention to the importance of dopamine (DA) in the formation and implementation of goal-directed and habitual behavior. DAergic projections from the ventral tegmental area (VTA) to the ventral corticostriatal network (i.e. vmPFC and VS) play a vital role

in the formation and modulation of goal-directed behavior (Cheer et al. 2007; Goto and Grace 2005). In contrast, DAergic projections from the substantia nigra pars compacta to dorsal striatum, particularly to the putamen, play an essential role in the formation of habits (Hernandez et al. 2015), and lesions to this pathway may prevent habit formation (Faure et al. 2005). One animal study (Hitchcott et al. 2007) has demonstrated that infusion of DA in the vmPFC shifts the habitual responses to goal-directed responses by restoring the response→outcome relationship bidirectionally, that is, increasing and decreasing responses to the valued and devalued outcomes, respectively.

In humans, the role of DA in RL has been extensively documented using the actor-critic RL model (San Martín 2012; Joel et al. 2002; Barto 1995). The actor component of this model is associated with regions that affect the motor cortex, such as the amygdala and dorsal striatum, and is considered to be involved in adopting optimal policies to perform the actions when facing particular stimuli. The anterior cingulate cortex (ACC) is regarded as a control filter which chooses the most appropriate strategies for these motor-related regions in a given situation. The critic component, in contrast, is associated with VS and believed to be involved in evaluating ongoing stimuli and in predicting whether any future outcomes will be desirable or not. After revising the prediction, the critic component computes a positive or negative PE signal that reflects whether the outcome is better or worse than expected, respectively. The empirical evidence relates this PE signal to phasic increase (for positive) or decrease (for negative) in the midbrain DA activity (San Martín 2012). The DA-related PE signals from VS (critic) communicates with ACC to guide the motor-related regions (actor) to execute optimal responses when facing specific stimuli.

1.5 Neural regions involved during selective visual attention

Selective visual attention prioritizes the cognitive processing of motivational items by filtering out other information that is competing for visual processing in a given environment (Moore and Zirnsak 2017; Desimone and Duncan 1995). Food is considered to have a strong influence on attention as it possesses not only the nutritional properties but also hedonic properties that make it perceptually more salient relative to other items (Castellanos et al. 2009; Robinson and Berridge 1993). Using a visual-search task, it has been previously demonstrated that food-related stimuli biased attention towards their location as compared to other objects (Schmidt et al. 2016; Mogg et al. 1998). The attentional bias towards food cues has been frequently investigated using the N2pc (an abbreviation of N2-posterior-contralateral) component (Jenkins et al. 2018; Maheux and Jolicœur 2017; Kumar et al. 2016). Relative to the attended hemifield, N2pc amplitude has shown to be more negative at the contralateral posterior parietal electrodes than at ipsilateral electrode (Verleger et al. 2012; Hopf et al. 2000). The sources of N2pc are located in extrastriate cortex (Hopf et al. 2000; Luck et al. 1997). Extrastriate cortex comprises a large number of areas dedicated to the processing of specific visual features and functions (Binder et al. 2009; Felleman 2009).

1.6 Outline of the Thesis

Chapter 2: In this chapter, we to aimed identify the common and distinct brain regions underlying the processing of food and monetary incentives in different metabolic states. To directly compare both incentive types, we used an associative learning task, in which participants received either food or monetary feedback in the form of images.

Chapter 3: In this chapter, we adapted a well-established behavioral and neuroimaging outcome devaluation paradigm to identify the electrophysiological markers of goal-directed vs habitual control during a devaluation test.

Chapter 4: In this chapter we aimed to corroborate previous N2pc findings using functional resonance imaging. We adapted a selective visual attention paradigm with a bilateral stimuli setup.

2 Neural processing of food and monetary rewards is modulated by metabolic state

2.1 Introduction

Ingestive behavior is driven by internal physiological factors, such as glucose, insulin or leptin blood levels, and external factors, such as time of day, environment, cultural or religious influences, food preferences or stress levels (DiLeone 2009; Saper et al. 2002; Plata-Salamán 1991). The communication between central and peripheral (gut, liver, adipose tissue) physiological mechanisms is supported by neural and humoral signals (Schwartz et al. 2000), which regulate food intake depending on hunger and satiety, a process termed homeostatic regulation (Balthasar 2006; Erlanson-Albertsson 2005). In humans, food intake also depends on hedonic factors (Nestler and Lutter 2009; Kringelbach 2004; Saper et al. 2002), which can precipitate eating behavior even when satiated. Thus, exposure to highly palatable food stimuli may inhibit satiation signals leading to overconsumption of food because of its rewarding properties (Keen-Rhinehart et al. 2013; Beaver et al. 2006; Weaver and Brittin 2001).

Investigating the neural responses to food stimuli in different metabolic states (hunger vs. satiety) might help to better understand overeating behavior. Previous research has shown that, compared to satiated participants, hungry participants showed significantly greater activity in the primary visual cortex, IPL, fusiform gyrus, insula, parahippocampal gyrus and amygdala in response to food images (Führer et al. 2008; Mohanty et al. 2008). Food-related stimuli (most often pictures of food) give rise to activity within insular-opercular areas (primary gustatory cortex), caudolateral regions of the OFC associated with taste reward (secondary gustatory cortex), amygdala and VS (Jacobson et al. 2010; Plassmann et al. 2008; Rolls 2006; Killgore et al. 2003). Evidence from experimental neurophysiology and neuropsychology has demonstrated

that the amygdala output pathways are strongly connected to VS and OFC (Dietrich et al. 2016; Stoeckel et al. 2009). The caudolateral OFC receives input from the amygdala (Morris and Dolan 2001), which is thought to be an intermediate region between the primary and secondary gustatory cortices (Jacobson et al. 2010). Moreover, OFC activity has been reported to increase with the pleasantness rating of food stimuli (de Araujo et al. 2003a; Kringelbach et al. 2003). Indeed, the OFC has been shown to be implicated in reward processing, goal selection and incentive motivation (Arana et al. 2003; Gottfried et al. 2003). Together with other brain regions including striatum, amygdala and insula, the OFC is an essential part of the network implicated in monetary reward processing (Fujiwara et al. 2009; Völlm et al. 2007; Nieuwenhuis et al. 2005; Delgado et al. 2000; Knutson et al. 2000). Moreover, in healthy participants, it has been reported that fasting increases responses to high-calorie food stimuli within OFC, striatum and insula, as well as visual areas (Pursey et al. 2014). In particular, the striatum is considered an integral component of the reward circuitry, playing an important role in processing a wide range of reinforcers (Elliott et al. 2003; Haber and Knutson 2010). Striatum activity has been shown to increase with the delivery of monetary reward (Delgado et al. 2000) and decrease following punishment or omission of monetary reward (Delgado et al. 2003).

To date, most fMRI research has focused on the neural activity elicited by either food or monetary reinforcers, but there is a dearth of studies directly comparing both incentive types. In one such study, it was shown that a neural network comprising insula, striatum and ACC covaried with PE for both appetitive and aversive drinks, whereas activity in pallidum, precentral gyrus, middle and inferior frontal gyrus, and middle cingulate cortex covaried with PE for monetary reward (Metereau and Dreher 2012). Using an incentive delay task, (Simon et al. 2014) reported increased OFC, posterior cingulate and inferior lateral PFC activity associated to the anticipation of food compared to monetary incentives, as well as significant lateral OFC and

occipital activity associated to the reception of food compared to money, whereas no brain region showed increased activity associated to monetary compared to food rewards. Recently, it has been shown that the striatum is more sensitive to food reward in obese compared to overweight and normal weight participants, whereas amygdala and medial frontal cortex are more sensitive to monetary reward in overweight compared to normal weight and obese participants (Verdejo-Román et al. 2017b). Excess weight (obesity or overweight) has further been associated with decreased functional connectivity during the processing of food rewards in a network involving mainly frontal and striatal areas and increased functional connectivity during the processing of monetary rewards in a network comprising frontal and parietal regions (Verdejo-Román et al. 2017a). In a meta-analysis, (Sescousse et al. 2013) found a common network recruited by food, erotic and monetary rewards comprising VS, ventromedial PFC, amygdala and anterior insula, although with some variation in magnitude and peak activity. The VS and the evolutionary newer regions in the anterior OFC were reliably more activated by monetary than food reward, whereas the anterior insula and the phylogenetically older regions in the posterior OFC, along with the somatosensory cortex, were reliably more activated by food than monetary reward.

The purpose of present study was to identify the common and distinct brain regions underlying the processing of food and monetary incentives in different metabolic states. To directly compare both incentive types, we used an associative learning task, in which participants received either food or monetary feedback in the form of images. Behaviorally, we hypothesized that participants would make more correct responses and respond faster when receiving food feedback in the hungry state, and when receiving monetary feedback in the satiated sate. Regarding functional activity, we hypothesized increased activation in the primary and secondary gustatory cortices during the reception of food reward, and that the activity in these regions would be enhanced in the hungry state. We also anticipated that both VS and medial OFC would

show increased activation following rewards compared to nonrewards, regardless incentive type. However, we expected increased activation in these regions associated to monetary compared to food reward when satiated.

2.2 Materials and Methods

2.2.1 Participants

Twenty-six men were recruited from the student population in Lübeck. Data from 20 participants (age range 18–29 years, *M* = 23.6, *SD* = 3.3) were analyzed in this study. Data of the remaining six subjects were discarded after the first session, because they either did not understand the task (*n* = 4) or showed excessive head motion (*n* = 2). The body max index (BMI) of the included participants was between 20 and 26 (*M* = 23.3, *SD* = 1.5). All were right handed, had normal or corrected to normal vision, had no history of neurological or psychiatric disorders, and were not taking any medication at the time. One participant was ovo-lactose vegetarian and three were smokers. The study had been approved by the local ethics committee of the University of Lübeck and informed consent was obtained from each subject before conducting the study. Participants were paid for their participation or received course credit.

2.2.2 Stimuli and Procedure

Participants performed an associative learning task, which comprised four experimental blocks of 64 trials. Each trial began with the presentation of a stimulus for 1 s. Participants were required to make a button press with either the right or left index finger. After interval of 1.5-11.5 s (*M* = 3.62, *SD* = 2.61), in which a fixation cross was shown, feedback was presented for 1 s. The next trial started after an inter-trial interval of 1.5-14 s (*M* = 3.65, *SD* = 2.98).

Within each experimental block, eight characters from the Japanese writing system (hiragana and katakana) were used as stimuli. Characters were different in each block. Participants were instructed to learn by trial-and-error whether each character was associated to a right or left button press. To ensure enough both positive and negative feedback trials, four stimuli were mapped to either a left/right button press on 100% of the trials, two were mapped to a left/right button press on 80% of the trials and to the opposite button on 20%, and the remaining two stimuli were mapped to each button on 50% of the trials. If they responded correctly, participants received feedback in the form of photograph of a purse showing three 1€ coins or a plate with two open-faced sandwiches (ham or cheese, depending on the subject's preference). If they responded incorrectly, feedback showed either an empty purse or an empty plate. If the participants failed to respond within 1200 ms of the onset of the stimulus, the message "Schneller!!" (faster!!) was presented. Participants were encouraged to learn the correct associations to maximize their wins, as they were told prior to the experiment that they would receive a proportion of the food and money they won. Monetary feedback was shown in two of the experimental blocks and food feedback in the other two. Presentation order was counterbalanced across participants and sessions.

In addition to the associative learning task, before the first and after every experimental block, participants were asked to rate the pleasantness (Wie angenehm findest Du dieses Bild? [How pleasant do you find this photograph?]), wanting (Wie gern würdest Du das angezeigte Essen/Geld jetzt bekommen? [How much would you like to receive the shown food/money right now?]) and gratification (Wie sehr würdest Du Dich über das angezeigte Essen/Geld jetzt freuen? [How happy would you feel right now about the depicted food/money?]) of the photographs used as feedback on a Likert scale ranging from 1 to 6. Also, before the first and after last experimental block, they were asked to rate their feelings of hunger (Wie hungrig fühlst Du Dich

gerade? [How hungry do you feel right now?]), satiation (Wie satt fühlst Du Dich gerade? [How full do you feel right now?]) and desire to eat (Wie stark ist gerade dein Wunsch zu essen? [How strong is your desire to eat right now?]). Both the associative learning task and the ratings were presented using Presentation software (Neurobehavioral System Inc., Albany, Ca) and visualized on MR compatible goggles inside the scanner.

Each participant took part in two experimental sessions, which took place with at least one-week interval. Participants were instructed to refrain from food and drink, except water, for at least six hours before the start of each session. In one of the sessions (henceforth satiated session) participants were provided with a full meal of 600 kcal (20% protein, 25% fat, 55% carbohydrate) 45 min before the start of the scan, whereas in the other session (henceforth hungry session) they remained in a food deprived state. Participants were not informed in advance that or whether they would get a meal in any of the sessions. The order of the sessions was counterbalanced across participants. At the end of each session, participants also received a fixed reward that they thought was performance related: three open-faced sandwiches and 4 € in the hungry session, and two open-faced sandwiches and 6 € in the satiated session.

2.2.3 MR Data Acquisition

Structural and functional imaging was performed on a 3-T Philips Ingenia MR scanner (Philips Medical Systems, Best, The Netherlands). Functional images were acquired in an interleaved fashion with a gradient-echo EPI sequence (voxel dimensions 2.5 × 2.5 × 2.5 mm, 47 slices, 80 × 80 matrix, TE = 28 ms, TR = 2.5 s, 160 mm field of view, 90° flip angle, 2.5 mm slice thickness). Four additional dummy volumes, which were then discarded, were acquired at the beginning of each experimental block to account for T1 equilibrium effects. Further, structural images were acquired using a T1-weighted sequence (voxel dimensions 1 × 1 × 1 mm,

180 slices, 240 × 240 matrix, TE = 3.577 ms, TR = 7.791 ms, 240 mm field of view, 8° flip angle, 1 mm slice thickness).

2.2.4 Behavioral Data Analysis

Behavioral data were analyzed using the R programming language (htts://www.r-project.org/) with the package ez (http://cran.r-project.org/web/packages/ez/). A repeated-measures ANOVA (rmANOVA) with the factors metabolic state (hungry, satiated) and incentive type (food, money) was calculated for the rate of correct responses. To analyze reaction times, an rmANOVA was computed with the factors metabolic state (hungry, satiated), incentive type (food, money) and correctness (error, correct). Degrees of freedom and *p*-values were Huynh-Feldt-corrected when necessary. Bonferroni-corrected post-hoc dependent t-tests were performed to analyze significant effects.

Ratings of hunger, satiation and desire to eat were analyzed separately using rmANOVAs with the factors metabolic state (hungry, satiated) and time point (T1: before the first run, T5: after the last run). Similarly, rmANOVAs with the factors metabolic state (hungry, satiated), time point (T1, T5), incentive type (food, money) and reward valence (reward, nonreward) were computed on the ratings of pleasantness, wanting and gratification. Degrees of freedom and *p*-values were Huynh-Feldt-corrected when necessary. Bonferroni-corrected post-hoc dependent t-tests were performed to analyze significant interactions.

2.2.5 fMRI Data Analysis

Part of the preprocessing was initially performed with FSLv5.0 (http://www.fmrib.ox.ac.uk/fsl) on a Debian-based operating system (Neurodebian 7.8.0) running on VirtualBox 5.0.0 to implement independent component analysis (ICA) based Automatic Removal of Motion Artifacts (ICA-AROMA; Pruim et al. 2015b) for head motion correction. ICA-AROMA offers a more efficient and robust method to reduce the movement artifacts in

fMRI data than other techniques (Pruim et al. 2015a). Data were further preprocessed and analyzed using SPM12 (http://www.fil.ion.ucl.ac.uk/spm/software/spm12/) running on MATLAB R2015a (Mathworks, Natick, US).

Estimation of realignment parameters, brain extraction and spatial smoothing are prerequisites for ICA-AROMA (Pruim et al. 2015b). Functional data were initially corrected for head movement by realigning to the middle volume using FMRIB's linear image registration tool (MCFLIRT; Jenkinson et al. 2002) to estimate the realignment parameters. Because FSL takes each functional run into account individually, realignment was performed for each experimental block independently. Brain extraction was then performed on the realigned data with the brain extraction tool (BET; Smith 2002) using a fractional intensity threshold of 0.3. Data were spatially smoothed with a 6-mm full width at half maximum (FWHM) Gaussian kernel.

The ICs classified as motion artifacts by ICA-AROMA were removed from the data that had been realigned using MCFLIRT. Note that the motion corrected data still contained skull and scalp, and were not smoothed, so as to continue preprocessing and analysis with SPM12 from this point onward.

The origins of structural and denoised functional volumes were first set manually at the anterior commissure to prevent normalization artifacts. Slice timing correction for each run was then carried out with reference to the middle slice by means of Fourier phase interpolation. Subsequently, volumes from all four functional runs were realigned spatially with respect to the first functional volume of the first run using rigid body transformation. The mean functional image of the four runs was then co-registered to the structural image of each subject. Normalization was performed using a **d**iffeomorphic **a**natomical **r**egistration through **e**xponentiated **l**ie algebra (DARTEL) template (Ashburner 2007). Segmentation of the structural images was performed to produce DARTEL-compatible grey and white matter images for the

tissue probability maps. A DARTEL template was then generated using the estimated grey and white matter of all subjects. Finally, functional data were normalized to MNI space using the parameters produced by the DARTEL template with a smoothing factor of 6-mm FWHM.

For each participant, an event related design matrix was created containing the conditions of interest: positive and negative monetary feedback, and positive and negative food feedback. This was done for each session (hungry and satiated) individually. Japanese character stimuli and missed feedback were modeled as effects of no interest. Low frequency noise was removed using a high-pass filter (cut-off 128 s). The standard SPM autoregressive AR(1) model was applied, and the onset regressors were convolved with the canonical hemodynamic response function. First-level contrast images were generated using a one-sample t-test for positive and negative feedback against the fixation cross, separately for each incentive type. On the group level, we conducted rmANOVAs with factors, namely metabolic state (hungry, satiated), incentive type (food, money), and reward valence (reward, nonreward). These analyses were specified as flexible factorial designs on SPM12 with each subject treated as a random effects variable. Main effects were tested using t-contrasts and two-way interactions using F-contrasts. The three-way interaction was tested using GLM Flex (http://nmr.mgh.harvard.edu/harvardagingbrain/People/AaronSchultz/Aarons_Scripts.html).

Furthermore, to better understand of the role of the regions associated with the interaction between metabolic state and incentive type, seed-based functional connectivity analyses were performed using the Beta Series Correlation toolbox (BASCO; Göttlich et al. 2015) running on SPM12. This toolbox is based on the approach introduced by Rissman et al. (2004). The seeds were based on the functionally activated clusters which were observed because of the above-mentioned interactions. Each cluster was delineated separately using the MarsBar region-of-interest toolbox (Brett et al. 2002; http://marsbar.sourceforge.net/). For each seed, the functional

connectivity analysis was also carried out separately. First, connectivity maps were estimated at the single-subject level by correlating the mean beta-series of the seed region to the beta-series of each voxel within the brain using the two contrasts of each incentive type individually: positive and negative feedback against the fixation cross. The resulting connectivity maps were Fisher z-transformed. The modulation of functional connectivity by metabolic state and incentive type was then investigated on the second-level using a two-way rmANOVA. The average beta- and z-values of significant clusters were extracted for plotting using the MarsBar region-of-interest toolbox (Brett et al. 2002).

An uncorrected voxel-level threshold of $p < .005$ was selected for all the analyses, with a family-wise error rate (FWE) corrected threshold of $p < .05$ at the cluster level. This voxel-level threshold was chosen to sufficiently avoid Type I errors while also reducing Types II errors (Lieberman and Cunningham 2009).

2.3 Results

2.3.1 Behavioral Results

An rmANOVA with factors metabolic state (hungry, satiated) and incentive type (food, money) was performed on the correct response rate. This showed a significant effect of incentive type, $F(1,19) = 12.93$, $\eta^2_G = .06$, $p = .002$, with significantly more correct responses when money (64.82±6.21 %) was used as an incentive than when food (60.80±9.25 %) was used. There was no significant effect of metabolic state nor interaction between incentive type and metabolic state, $p > .1$.

Reaction times were tested using an rmANOVA with factors metabolic state (hungry, satiated), incentive type (food, money) and correctness (correct, incorrect). This showed a significant effect of correctness, $F(1,19) = 116.22$, $\eta^2_G = .13$, $p < .001$, as well as significant

interactions between incentive type and correctness, $F(1,19) = 5.60$, $\eta^2_G = .01$, $p = .029$, and metabolic state, incentive type and correctness, $F(1,19) = 10.75$, $\eta^2_G = .01$, $p = .004$. All other effects and interactions were not statistically significant, $p > .1$. Bonferroni-corrected post-hoc t-tests were used to analyze the three-way interaction, demonstrating that this was driven by the fact that correct responses (hungry: food: 732±65 ms, money: 727±54 ms; satiated: 733±52 ms, money: 716±47 ms) were made significantly faster than incorrect responses (hungry: food: 768±69 ms, money: 763±54 ms; satiated: 765±52 ms, money: 780±53 ms) in all conditions (hungry: food: $p < .001$, money: $p = .012$; satiated: food: $p = .001$, money: $p < .001$).

Ratings of hunger, satiation and desire to eat before the first (T1) and after the last (T5) experimental block were analyzed using rmANOVAs with the factors metabolic state (hungry, satiated) and time point (T1, T5). Participants were significantly hungrier in the hungry (5.03±1.00) than the satiated session (1.80±0.91), $F(1,19) = 120.73$, $\eta^2_G = .75$, $p < .001$. Similarly, they reported a significantly higher desire to eat in the hungry (4.88±1.16) than in the satiated session (1.90±0.96), $F(1,19) = 115.03$, $\eta^2_G = .68$, $p < .001$. In both cases, there was neither an effect of time point nor an interaction between metabolic state or time point, $p > .05$. Participants were significantly more satiated in the satiated (4.53±0.88) than in the hungry session (1.80±0.88), $F(1,19) = 58.50$, $\eta^2_G = .63$, $p < .001$, and although overall the feeling of satiation decreased significantly over time (T1: 3.33±1.85, T5: 3.00±1.63), $F(1,19) = 7.12$, $\eta^2_G = .02$, $p = .015$, there was no significant interaction between metabolic state and time point, $p > .1$.

The ratings of the pleasantness, wanting and gratification of the feedback stimuli were tested using rmANOVAs with the factors metabolic state (hungry, satiated), time point (T1, T5), incentive type (food, money) and reward valence (reward, nonreward). Pleasantness ratings showed a significant effect of reward valence, $F(1,19) = 190.19$, $\eta^2_G = .66$, $p < .001$, as well as significant interactions between metabolic state and reward valence, $F(1,19) = 6.99$, $\eta^2_G = .02$, p

= .016, time point and reward valence, $F(1,19) = 34.11$, $\eta^2_G = .04$, $p < .001$, incentive type and reward valence, $F(1,19) = 6.17$, $\eta^2_G = .02$, $p = .023$, and metabolic state, incentive type and reward valence, $F(1,19) = 18.24$, $\eta^2_G = .04$, $p < .001$. All other effects and interactions were not statistically significant, $p > .05$. Bonferroni-corrected post-hoc t-tests were used to analyze the two-way interaction between metabolic state and reward valence (Table 2.1).

Wanting ratings showed significant effects of metabolic state, $F(1,19) = 15.98$, $\eta^2_G = .06$, $p = .001$, incentive type, $F(1,19) = 23.60$, $\eta^2_G = .10$, $p < .001$, and reward valence, $F(1,19) = 290.15$, $\eta^2_G = .72$, $p < .001$, as well as significant interactions between metabolic state and incentive type, $F(1,19) = 32.66$, $\eta^2_G = .09$, $p < .001$, between metabolic state and reward valence, $F(1,19) = 22.35$, $\eta^2_G = .10$, $p < .001$, between time point and reward valence, $F(1,19) = 30.85$, $\eta^2_G = .05$, $p < .001$, between incentive type and reward valence, $F(1,19) = 53.08$, $\eta^2_G = .11$, $p < .001$, between metabolic state, time point and reward valence, $F(1,19) = 5.85$, $\eta^2_G = .01$, $p = .026$, and between metabolic state, incentive type and reward valence, $F(1,19) = 36.43$, $\eta^2_G = .13$, $p < .001$. All other effects and interactions were not statistically significant, $p > .05$. Bonferroni-corrected post-hoc t-tests were used to analyze the two-way interactions between metabolic state and reward valence, and between metabolic state and incentive type (Table 2.1).

The gratification ratings showed significant effects of metabolic state, $F(1,19) = 11.24$, $\eta^2_G = .03$, $p = .003$, incentive type, $F(1,19) = 43.52$, $\eta^2_G = .11$, $p < .001$, and reward valence, $F(1,19) = 314.77$, $\eta^2_G = .74$, $p < .001$, as well as significant interactions between metabolic state and incentive type, $F(1,19) = 37.25$, $\eta^2_G = .10$, $p < .001$, time point and incentive type, $F(1,19) = 15.06$, $\eta^2_G = .02$, $p = .001$, metabolic state and reward valence, $F(1,19) = 16.42$, $\eta^2_G = .08$, $p = .001$, time point and reward valence, $F(1,19) = 25.72$, $\eta^2_G = .06$, $p < .001$, incentive type and reward valence, $F(1,19) = 37.98$, $\eta^2_G = .09$, $p < .001$, metabolic state, time point and reward valence, $F(1,19) = 5.80$, $\eta^2_G = .02$, $p = .026$, and metabolic state, incentive type and reward

valence, $F(1,19) = 13.85$, $\eta^2_G = .07$, $p = .001$. All other effects and interactions were not statistically significant, $p > .1$. Bonferroni-corrected post-hoc t-tests were performed to analyze the two-way significant interactions between metabolic state and reward valence, and between metabolic state and incentive type (Table 2.1).

Metabolic state	Incentive type	Reward valence	Pleasantness	Wanting	Gratification
Hungry	Food	Reward	5.15 (0.86)	5.38 (0.74)	5.18 (0.96)
		Nonreward	1.85 (0.77)	1.45 (0.96)	1.43 (0.64)
	Money	Reward	5.03 (1.12)	5.33 (0.83)	5.30 (0.91)
		Nonreward	2.05 (1.32)	1.53 (1.11)	1.40 (0.81)
Satiated	Food	Reward	4.08 (1.37)	2.80 (1.59)	3.08 (1.65)
		Nonreward	2.18 (1.08)	1.75 (1.08)	1.53 (0.82)
	Money	Reward	5.05 (0.90)	5.58 (0.50)	5.53 (0.51)
		Nonreward	1.78 (0.95)	1.58 (1.30)	1.75 (1.43)

Pairwise comparison	Pleasantness	Wanting	Gratification
Hungry reward vs. nonreward	<.001	<.001	<.001
Satiated reward vs. nonreward	<.001	<.001	<.001
Hungry vs. satiated reward	.018	<.001	<.001
Hungry vs. satiated nonreward	n.s.	n.s.	n.s.
Hungry food vs. money	---	n.s.	n.s.
Satiated food vs. money	---	<.001	<.001
Hungry vs. satiated food	---	<.001	<.001
Hungry vs. satiated money	---	n.s.	n.s.

Table 2.1 | Results of the behavioral post-hoc analyses. Mean (SD) rating and p-values of the pairwise comparisons used to analyze significant interactions of the behavioral rmANOVAs. All *p*-values are Bonferroni-corrected for the corresponding number of pairwise comparisons performed.

2.3.2 fMRI Results

Peak regions and coordinates are shown in Table 2.2.

No main effect of metabolic state was observed. Food compared to monetary incentives significantly increased activation within left medial cingulate gyrus, right insula and right

fusiform gyrus (Figure 2.1 A); whereas there was no significantly increased activation for money compared to food incentives. Reward feedback resulted in significant activations in the limbic, striatal and frontal areas, such as bilateral ACC, left medial OFC, right amygdala and bilateral VS (Figure 2.1 B); whereas nonreward feedback resulted in significant activations within limbic and frontoparietal regions, including right insula, bilateral supplementary motor area (SMA), right precuneus and bilateral IPL (Figure 2.1 C).

The interaction between metabolic state and reward valence demonstrated significant activity within the left dorsal putamen (Figure 2.2 A). The interaction between metabolic state and incentive type revealed significant activity within right SMG, right postcentral gyrus, left precuneus and bilateral SMA (Figure 2.2 C). The interaction between incentive type and reward valence, as well as the three-way interaction between metabolic state, incentive type and reward valence were not statistically significant.

2.3.3 Functional Connectivity Results

Peak regions and coordinates are shown in Table 2.3.

Only the right supramarginal gyrus (SMG) seed showed significant connectivity results. The rmANOVA revealed a significant coupling of the right SMG with right midbrain, bilateral midcingulate area and left hippocampus when participants were hungry as compared to when they were satiated (Figure 2.3 A). Viewing food compared to monetary incentives led to enhanced connectivity between the right SMG and right postcentral gyrus, right superior temporal gyrus and left middle occipital gyrus (Figure 2.3 B). The interaction between metabolic state and incentive type revealed significantly increased connectivity between the right SMG and ipsilateral VS (Figure 2.3 C).

Region	BA	x	y	z	k	Peak *t/F*	p_{FWE}-value
Metabolic state: Hungry > Satiated							
No significant clusters							
Metabolic state: Satiated > Hungry							
No significant clusters							
Incentive type: Food > Money							
R fusiform gyrus	19	28	-78	-15	76	5.46	.049
L SMA	32	-8	13	40	155	4.27	.033
R insula	13	45	0	0	180	4.20	< .001
R precentral gyrus	44	47	3	23	170	3.84	< .001
L putamen	*	-31	7	5	50	3.73	< .001
L superior parietal gyrus	7	-23	-66	43	201	3.40	.016
R putamen	*	29	7	5	35	3.01	< .001
R IFG	44	40	15	8	90	2.22	< .001
Incentive type: Money > Food							
No significant clusters							
Reward valence: Reward > Nonreward							
L medial OFC	10	0	58	-5	821	11.94	< .001
L VS	*	-13	3	-15	34	11.59	< .001
R VS	*	13	5	-15	40	9.02	< .001
L hippocampus	*	-22	-20	-15	235	8.24	< .001
L middle occipital gyrus	39	-38	-80	33	190	7.02	< .001
L medial frontal gyrus	10	-5	53	15	510	6.09	.031
R hippocampus	*	28	-35	-8	97	5.99	< .001
R anterior cingulate gyrus	32	5	43	3	579	5.05	< .001
L fusiform gyrus	37	-23	-40	-15	85	4.92	< .001
L anterior cingulate gyrus	32	-8	48	3	322	4.87	< .001
L superior temporal gyrus	22	-58	-5	-5	797	4.86	< .001
L amygdala	*	-25	-3	-20	105	4.62	< .001
L angular gyrus	39	-53	-70	33	269	4.54	< .001
R caudate	*	13	20	3	193	4.48	< .001
L middle temporal gyrus	22	-53	-10	-8	529	4.13	< .001
R putamen	*	23	13	-3	87	4.11	< .001
L putamen	*	-18	-13	-3	120	3.39	< .001
L caudate	*	-8	15	3	135	3.14	< .001
R amygdala	*	25	-3	-20	67	2.63	< .001

Table 2.2 | Whole-brain results for the three-factor rmANOVAs. Main effects: metabolic state, incentive type and reward valence, and the interactions: metabolic state × incentive type, metabolic state × reward valence, incentive type × reward valence and metabolic state × incentive type × reward valence. Peak *t*-values are reported for the main effects, and peak *F*-values for the interactions. All results are FWE-corrected at the cluster level, $p < .05$. Abbreviations: IFG: inferior frontal gyrus, IPL: inferior parietal lobule, MFG: middle frontal gyrus, OFC: orbitofrontal cortex, SMA: supplementary motor area, SMG: supramarginal gyrus, VS: ventral striatum, BA: Brodmann's area and *k*: cluster size. *No BA available.

Region	BA	x	y	z	k	Peak *t/F*	p_{FWE}-value
Reward valence: Nonreward > Reward							
R IFG	47	48	23	-10	246	7.99	< .001
L IPL	40	-38	-50	48	414	6.86	< .001
R MFG	10	33	58	5	546	6.30	< .001
L MFG	10	-30	53	8	347	5.76	< .001
R insula	13	40	18	-1	170	5.21	< .001
R SMA	6	13	10	63	223	5.05	< .001
L SMA	8	-8	15	50	387	4.62	< .001
R IPL	40	48	-48	50	235	4.57	< .001
R midcingulate area	32	8	10	38	109	4.41	< .001
R precuneus	7	8	-70	45	126	3.91	< .001
L superior medial frontal gyrus	8	-3	33	38	243	3.83	< .001
L precuneus	7	-8	-70	50	50	3.05	< .001
Metabolic state × Reward valence							
L putamen	*	-25	3	5	13	11.55	.009
Metabolic state × Incentive type							
R SMG	40	45	-30	38	67	22.24	.038
L precuneus	7	-10	-65	48	192	22.22	.004
R SMA	6	8	8	50	144	16.99	.019
L SMA	6	-8	8	46	43	11.21	.018
R postcentral gyrus	1	28	-35	45	77	13.33	.038
Incentive type × Reward valence							
No significant clusters							
Metabolic state × Incentive type × Reward valence							
No significant clusters							

Table 2.2 (continued) | Whole-brain results for the three-factor rmANOVAs. Main effects: metabolic state, incentive type and reward valence, and the interactions: metabolic state × incentive type, metabolic state × reward valence, incentive type × reward valence and metabolic state × incentive type × reward valence. Peak *t*-values are reported for the main effects, and peak *F*-values for the interactions. All results are FWE-corrected at the cluster level, p < .05. Abbreviations: IFG: inferior frontal gyrus, IPL: inferior parietal lobule, MFG: middle frontal gyrus, OFC: orbitofrontal cortex, SMA: supplementary motor area, SMG: supramarginal gyrus, VS: ventral striatum, BA: Brodmann's area and *k*: cluster size. *No BA available.

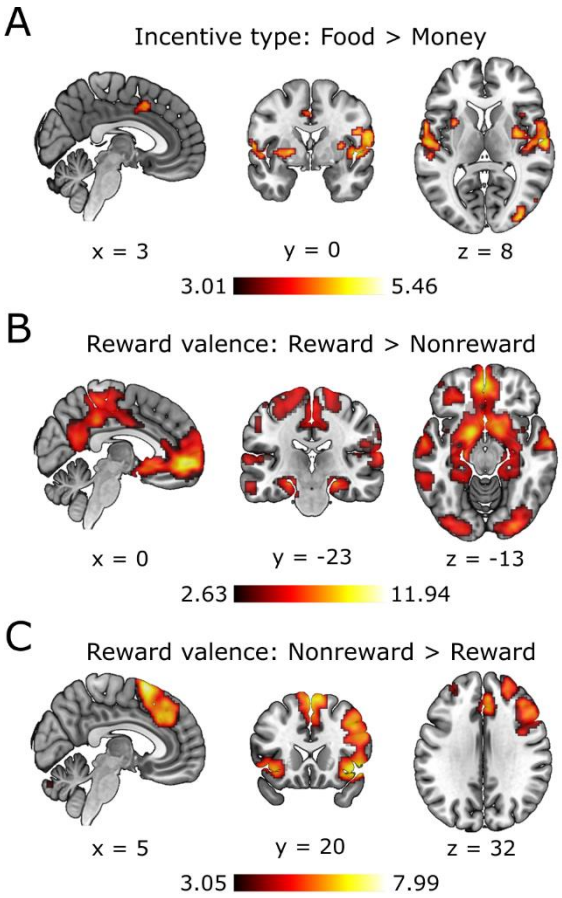

Figure 2.1 | Results of whole-brain main effects analyses. The *t*-values are thresholded at p <.05 (FWE corrected for multiple comparisons at the cluster level) and superimposed on a T1-weighted structural MNI template. Significant brain activations during the contrasts (A) food > money, (B) reward > nonreward, and (C) nonreward > reward.

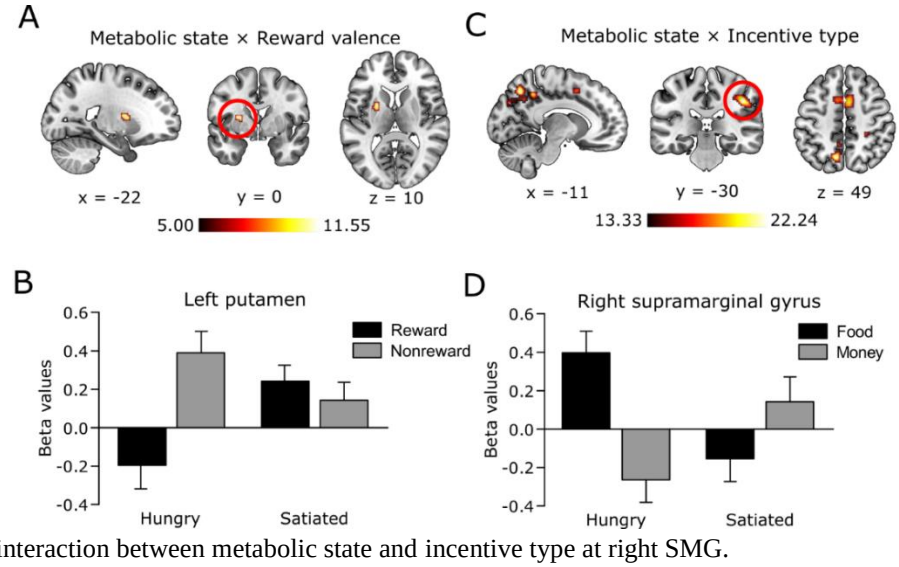

Figure 2.2 | Results of whole-brain interaction analyses. The *F*-values are thresholded at p <.05 (FWE corrected for multiple comparisons at the cluster level) and superimposed on a T1-weighted structural MNI template. Significant brain activations during the contrasts (A) metabolic state × reward valence, and (B) bar graph demonstrating the pattern of activation resulting from an interaction between metabolic state and reward valence at left putamen. (C) Metabolic state × incentive type, and (D) bar graph demonstrating the pattern of activation resulting from an interaction between metabolic state and incentive type at right SMG.

Region	BA	x	y	z	k	Peak *t/F*	p_{FWE}-value
Metabolic state: Hungry > Satiated							
L hippocampus	*	-28	-25	-10	109	5.62	< .001
R midbrain	*	5	-18	-15	144	4.40	< .001
R midcingulate area	31	12	-28	45	60	3.82	.031
L midcingulate area	31	-5	-23	45	50	3.44	.030
Metabolic state: Satiated > Hungry							
No significant clusters							
Incentive type: Food > Money							
R postcentral gyrus	1	60	-10	25	126	4.38	.001
R superior temporal gyrus	41	65	-18	5	87	4.27	.001
L middle occipital gyrus	18	-33	-85	10	42	3.44	.018
Incentive type: Money > Food							
No significant clusters							
Metabolic state × Incentive type							
R VS	*	15	3	-13	126	20.51	.044

Table 2.3 | Functional connectivity results for the two-factor rmANOVAs. Main effects: metabolic state and incentive type, and the interaction: metabolic state × incentive type. Peak *t*-values are reported for the main effects, and peak *F*-value for the two-way interaction. All results are FWE-corrected at the cluster level, p < .05. Abbreviations: VS: ventral striatum, BA: Brodmann's area and *k*: cluster size. *No BA available.

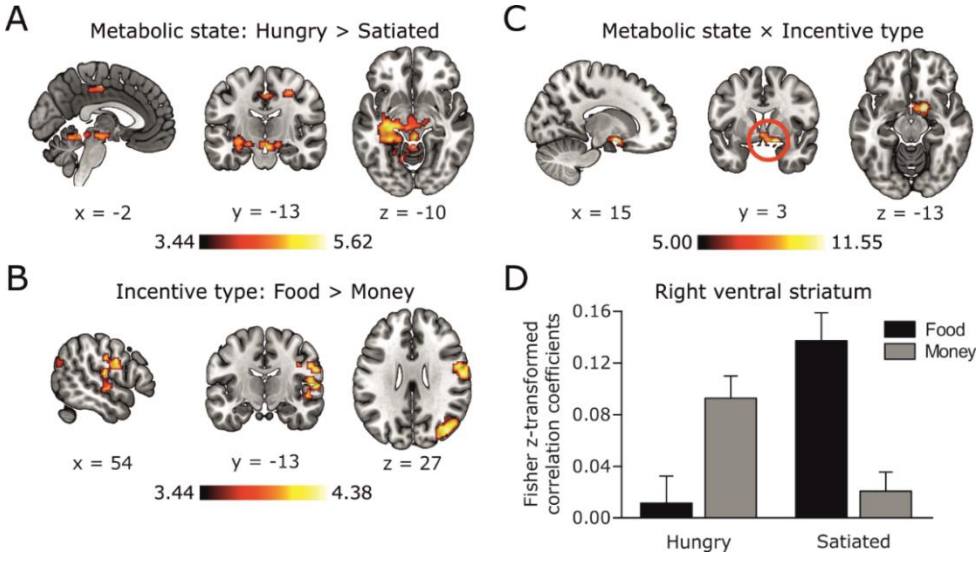

Figure 2.3 | Results of functional connectivity main effects analyses. The *t*-values are thresholded at p <.05 (FWE corrected for multiple comparisons at the cluster level) and superimposed on a T1-weighted structural MNI template. Depicted are areas showing significant connectivity to the SMG seed (A) hungry > satiated, (B) food > money, and (C) metabolic state × incentive type. (D) Bar graph demonstrating the connectivity pattern resulting from an interaction between metabolic state and incentive type in the right VS.

2.4 Discussion

The current data demonstrate that food compared to monetary incentives elicit increased activity within right putamen, insula and IFG, among other regions, whereas our analysis shows no brain region with greater activation for monetary feedback. In addition, rewards, irrespective of incentive type, result in increased activity in regions including left medial OFC, and bilateral striatum and amygdala; and nonrewards elicit activity in the right medial frontal gyrus (MFG) and anterior insula, left IFG, and bilateral SMA. Metabolic state modulates the effects of reward valence in the left dorsal putamen. Moreover, an interaction between metabolic state and incentive type is identified in the right SMG.

2.4.1 Effects of Incentive Type

The insula and opercular parts of the IFG show activation when food images are used as feedback. These have been identified as the primary gustatory cortex and have been frequently found to be active during the processing of food stimuli, both during ingestion and visual presentation (Blechert et al. 2016; Rolls 2016; Steward et al. 2016; Wright et al. 2016). Contrary to our expectations, however, we find no activation within the secondary gustatory cortex associated to food incentives.

The insula has been shown to be involved in the processing of different types of desirable (or craved for) stimuli, including food (Rolls et al. 1990), smoking (Brody et al. 2004), sexual (Kühn and Gallinat 2011) and gambling (Ko et al. 2009) cues. Remarkably, this region has been reported to respond more strongly to primary reinforcers, specifically erotica and food-related stimuli, than to monetary outcomes (Sescousse et al. 2013). Our own findings of increased activation in the insula following food compared to monetary rewards dovetail with this observation, as well as with previous studies reporting insula activation evoked by both actual

food and food images (Simon et al. 2014; Schienle et al. 2009). The anterior insula contains not only the primary gustatory cortex but also, more ventrally, autonomic-visceral functions with activation driven by salient stimuli regardless of their nature (rewarding, non-rewarding, novel; see Rolls 2016). According to Rolls (2016), the insula represents and integrates information about the external world (touch), intermediate milieu (taste and texture) and visceral and autonomic function. As food-related (but not monetary) stimuli invoke such representations, the increased activation of the insula in the current study is readily explained.

Interestingly, this effect of incentive type in the imaging data is not reflected in the behavioral data, with participants performing significantly better when money was used as an incentive, irrespective of metabolic state. Money is believed to be highly motivational, with numerous previous studies showing that participants perform better on cognitive tasks with monetary incentives (e.g. Dombrowe et al. 2011; Hübner and Schlösser 2010; Engelmann et al. 2009; Engelmann and Pessoa 2007). However, it remains under discussion whether non-monetary incentives have similar or distinct motivational effects on cognitive task performance (Krug and Braver 2014). Simon et al. (2014) used an incentive delay task to compare food to monetary feedback and, in line with our current observations, reported a neural network associated to food compared to money, but no significant results in the opposite contrast. Furthermore, these authors reported no significant differences in behavioral performance depending on incentive type. Indeed, it is worth noting that, although we find a significant difference in favor of monetary incentives, the effect size of this difference is small (Bakeman 2005), with both incentive types leading to correct response rates of between 60–65%. Moreover, as stated previously, the meta-analysis performed by Sescousse et al. (2013) has proved that the insula is more robustly activated by primary compared to secondary reinforcers. This agrees with previous studies suggesting that autonomic arousal induced by primary reinforcers results in

strong activation in the insula, among other regions (Kühn and Gallinat 2011; Critchley et al. 2002). It might be because of the critical role of primary reinforcers in homeostasis and survival. Hence, we speculate that while money might act as a strong motivator, translating into better task performance, the evolutionary relevance of food might result in a more potent neural response

2.4.2 Reward-Related Activations

Regardless of incentive type, reward outcomes lead to activation of typical reward-related regions, including VS, medial OFC and amygdala. The VS is thought to be a core area of the brain reward system. Studies using large-scale reverse inference have also indicated that the VS is more strongly involved in reward processing than other cognitive processes (Cauda et al. 2011; Yarkoni et al. 2011). VS activation has been frequently reported in response to various kinds of rewarding stimuli, suggesting its involvement in the processing of rewards irrespective of their nature (Sescousse et al. 2013). In contrast, the OFC is thought to be a more heterogeneous area, with some researchers suggesting a medial-lateral distinction (Friederich et al. 2013; Kühn and Gallinat 2011). In concert with the VS, medial OFC activity has usually been associated with incentive motivation, learning and memory of stimulus reward value; whereas lateral OFC activity has often been associated with punishment (Kringelbach 2005; Kringelbach and Rolls 2004). It is also worth noting that the caudolateral parts of the OFC contain the secondary gustatory cortex, highlighting the functional heterogeneity of the OFC. Moreover, medial and lateral OFC activation has been found to correlate with pleasantness ratings of odors and flavors (Rolls 2008). Regarding the amygdala, recent studies suggest that it is equally sensitive to positive and negative feedback (Bermudez et al. 2012; Murray 2007). The amygdala receives projections from various structures, especially from VS and OFC, areas that are strongly involved in the processing of rewards (Cho et al. 2013). A recent meta-analysis showed that the amygdala evenly responded to food and monetary outcomes (Sescousse et al. 2013). Our own findings are

in line with these observations, suggesting that a set of common regions responds to rewards irrespective of modality.

We show that the omission of rewards as a result of incorrect responses leads to an activation of the anterior insula, consistent with earlier findings indicating that this region is particularly sensitive to aversive events such as monetary loss, punishment or reward omission (Liljeholm et al. 2014; Knutson et al. 2007). Reward omission also engages the lateral prefrontal cortex, including MFG and IFG, and as well as the SMA, a network that has been previously identified in response to negative feedback stimuli (Camara et al. 2009).

2.4.3 Interactions with Metabolic State

Our analysis reveals an interaction between metabolic state and reward valence within the left dorsal putamen, with decreased activity for reward feedback when hungry and increased when satiated. The dominant anatomical connections of the dorsal putamen are sensorimotor and associative (Draganski et al. 2008; Lehéricy et al. 2004; Haber et al. 1994). Moreover, DAergic neurons from the substantia nigra pars compacta provide afferents to the dorsal putamen and are involved in developing and executing skilled motor responses (Robbins and Everitt 1992). It has been suggested that the VS mediates feedback-driven stimulus-action learning, whereas the dorsal striatum (dorsal putamen and caudate nucleus) mediates decision making after stimulus action associations have been learned (Hiebert et al. 2014), particularly through the integration of sensorimotor, cognitive and motivational information (Balleine et al. 2007). We assume that the hungry state decreases this post-learning effect, although our data does not permit clarifying the exact functional mechanism by which this occurs, for instance on a neurotransmitter level.

Of relevance in the present data set are activations in somatosensory and motor regions, specifically right SMG, left precuneus, right postcentral gyrus and bilateral SMA, which reflect

the interaction between metabolic state and incentive type. A similar pattern of activations has been previously reported in studies on interoceptive and exteroceptive awareness (Araujo et al. 2015; Kashkouli Nejad et al. 2015). To further elucidate this interaction, we carried out seed-to-whole-brain functional connectivity analyses, in which only the SMG seed reveals significant results. This region is believed to be key in the representation and evaluation of self-related states (Grosbras and Paus 2005), and it has been shown to display increased activity to both interoceptive and exteroceptive compared to autobiographical states (Araujo et al. 2015). In the context of our study, the right SMG activity associated to the interaction between metabolic state and incentive type might point to an integration of interoceptive and exteroceptive information: the extracted beta values demonstrate that this region is more sensitive to food incentives when hungry and to monetary incentives when satiated.

Our seed-based functional connectivity analysis shows that the SMG is correlated with midbrain and limbic regions in the hungry state, but there is no significant connectivity to any region when satiated. Within the midbrain, connectivity from the right SMG extended into the right VTA, one of the critical regions in the reward system (Block 2011). The VTA projects information to striatal and limbic regions via DA (Schultz et al. 1997). Furthermore, for food compared to monetary incentives, we observe functional connectivity between the right SMG and attentional network regions (right superior temporal gyrus and left middle occipital gyrus). The superior temporal gyrus is thought to be a site of multimodal sensory convergence, receiving signals from the dorsal and ventral streams for processing of auditory, visual and, most importantly, somatosensory information (Benarroch 2006). Hunger and satiety are two major components of interoceptive self-awareness that lead to initiation and cessation of food intake. The observed connectivity between the SMG and mesolimbic regions, including midbrain, hippocampus and cingulate gyrus, when hungry but not when satiated might be due to the feeling

of hunger being a very salient need that requires being fulfilled. Another main highlight of our connectivity analysis is the coupling between the right SMG and VS because of the interaction between metabolic state and incentive type. The SMG is positively correlated with the VS for both incentive types, but this coupling is enhanced for food when satiated and for money when hungry. Meta-analytic evidence suggests that VS activity is independent of incentive type, although with some variations in intensity (Sescousse et al. 2013). However, a recent study has shown increased VS activation when expecting food incentives in a hungry compared to satiated state, whereas the expectation of monetary incentives was not influenced by metabolic state (Simon et al. 2017). Our results appear to show that the SMG uncouples from the VS when processing the potentially most salient incentive in a given metabolic state, that is, food and monetary incentives when hungry and satiated, respectively. Taking into an account that functional connectivity does not reveal the causal influences of a region over another, we can only speculate given the activity of the SMG revealed by the task-based analysis and the correlation coefficients of the VS.

3 Electrophysiology of goal-directed vs habitual control during outcome devaluation

3.1 Introduction

According to the dual-system theory, instrumental learning behavior is controlled by two distinct systems: the goal-directed and the habit systems (Dezfouli and Balleine 2012; de Wit et al. 2009). Behavior is thought to be goal-directed when it reflects knowledge of the response-outcome relationship, and when the agent only responds to the stimulus (S) if the outcome (O) is currently motivationally relevant, i.e. the agent flexibly adapts responses (R) based on current desires and needs (de Wit et al. 2009). Therefore, S→O→R associative chains drive goal-directed action selection (Dickinson and Balleine 1994). In contrast, in habitual behavior, behavior is driven by the stimulus and is insensitive to goal value, with responses being enacted even when the outcome is not desirable. Thus, S→R associations alone drive habitual action selection (Dickinson and Weiskrantz 1985). Although habitual responding is advantageous in terms of efficiency, requiring less cognitive effort, it comes at the cost of flexibility, easily leading to so-called "slips of action" (de Wit et al. 2012b; Dayan 2009). For instance, when a commuter doesn't stop at the grocery store on their routine drive home, because the familiar route triggered the driver to continue despite the current need for groceries. Instrumental responding is thought to be initially goal-directed and under voluntary control but tends to become habitual (i.e. reflexive) with repeated practice (Dolan and Dayan 2013). Still, associations might form concurrently for goal-directed and habitual behavior, and both may contribute to an action (Balleine and Ostlund 2007). Therefore, one possible way to evaluate the relative balance between goal-directed and habitual control (Watson and de Wit 2018) is by testing sensitivity to the current value of outcomes using an outcome devaluation procedure, in which an action is first

paired with a desired outcome that is subsequently devalued, e.g. through sensory-specific satiation or aversive conditioning. Neuroimaging and lesion evidence suggest that the vmPFC is critical for implementing goal-directed behavior in outcome devaluation tasks (Reber et al. 2017; de Wit et al. 2012b; de Wit et al. 2009; Valentin et al. 2007), together with VS and the anterior caudate nucleus (Liljeholm et al. 2015; de Wit et al. 2012b; Balleine and O'Doherty 2009). Habitual behavior, in contrast, is believed to be controlled by a network involving posterior putamen and motor cortex (de Wit et al. 2012b; Balleine and O'Doherty 2009; Tricomi et al. 2009).

In the present study, we adapted a well-established behavioral and fMRI paradigm, the so-called 'fabulous fruit game' (de Wit et al. 2012b; de Wit et al. 2012a; de Wit et al. 2009), to investigate the event-related potentials (ERPs) underlying goal-directed and habitual behavior. This paradigm consists of an instrumental learning stage, in which participants learn stimulus-outcome pairs by trial-and-error, followed by two test stages: an outcome-devaluation test to assess knowledge of O→R contingencies, and a slips-of-action test that uses outcome devaluation in extinction to assess the relative balance between goal-directed and habitual control. In this test, some outcomes are devalued while others remain valuable; participants relying on goal-directed behavior should only respond to valuable outcomes while refraining from responding to devalued outcomes, whereas those relying on habits should continue to react to stimuli (de Wit et al. 2012b; de Wit et al. 2012a). The paradigm also employs three discriminative conditions. Briefly, in standard discriminations, different images serve as stimuli and outcomes, and performance can be supported both by goal-directed and habitual control (de Wit et al. 2012b); in contrast, in incongruent discriminations, the images serving as stimulus and outcome in one pair have the opposite function in another pair, so that performance can only be supported by the habit system as the elicited response conflict makes them hard to solve with goal-directed behavior (de Wit et

al. 2014); and finally, in congruent discriminations, the same image serves as stimulus and outcome, rendering active outcome retrieval unnecessary (de Wit et al. 2012a).

Given that the slips-of-action test is analogous to a go/nogo task, we expected that goal-directed vs habitual behavior could be reflected in the stimulus-locked N2 and P3 components. The N2 is a negative deflection of the ERP that peaks fronto-centrally between 200-400 ms and is larger on inhibitions compared to go trials (Enriquez-Geppert et al. 2010; Bekker et al. 2005; Kok et al. 2004; Bokura et al. 2001; Falkenstein et al. 1999; Eimer 1993) as well as on successful compared to unsuccessful inhibitions (Luus et al. 2007; Schmajuk et al. 2006; Roche et al. 2005), although some have reported increased amplitudes associated to failed response inhibition (e.g. Solbakk et al. 2014; Greenhouse and Wessel 2013). The nogo N2 has been suggested to reflect inhibitory processes (Rietdijk et al. 2014; Bekker et al. 2005; Falkenstein et al. 1999; Kopp et al. 1996), although others have posited that it might be better explained as a reflection of increased conflict (Randall and Smith 2011; Yeung et al. 2004; Donkers and van Boxtel 2004; Nieuwenhuis et al. 2003; Botvinick et al. 2001). Since, the inhibition of prepotent but goal-inappropriate responses is obviously essential for adaptive goal-directed behavior (Aron et al. 2014; Ridderinkhof et al. 2011), we hypothesized that conditions that could be resolved using goal-directed control would display larger N2 amplitudes associated to inhibitions to devalued outcomes on the slips-of-action test. Moreover, we expected reduced N2 amplitudes associated to slips of action (though probably still more negative amplitudes than for responses to valuable outcomes; e.g. Kok et al. 2004; Ramautar et al. 2004). Given the known modulation of the N2 amplitude by the speed-accuracy trade-off (Schmajuk et al. 2006; Falkenstein et al. 1999; Jodo and Kayama 1992), we hypothesized larger reductions in participants showing more relative goal-directed control as reflected by increased devaluation sensitivity, which would also perform the task more accurately.

The N2 is followed by a fronto-central P3, typically peaking between 300-600 ms, which has also been found to be increased on nogo compared to go trials (Rietdijk et al. 2014; Enriquez-Geppert et al. 2010; Roche et al. 2005; Bokura et al. 2001; Falkenstein et al. 1999) and on failed compared to successful inhibition trials (Roche et al. 2005; Kok et al. 2004), although others have found the opposite pattern (e.g. Greenhouse and Wessel 2013). The nogo P3 is believed to reflect post-response monitoring and evaluation of the inhibitory performance (Gajewski and Falkenstein 2013; Huster et al. 2013; Liotti et al. 2005; Bruin et al. 2001). Therefore, as for the N2, we expected larger P3 amplitudes associated to inhibitions to devalued outcomes in conditions that could be resolved through goal-directed behavior. However, in contrast to the N2, we hypothesized increased P3 amplitudes associated to slips of action, these being more prominent in participants with increased devaluation sensitivity.

We further expected slips of action to be reflected by the response-locked error-related negativity (ERN) and error positivity (P_E) complex. These are considered indices of performance monitoring, which is essential for optimal goal-directed behavior, entailing the detection and evaluation of error significance as well as guiding of behavior to avoid future mistakes (Ullsperger et al. 2014; Gruendler et al. 2011). The ERN is a fronto-centrally distributed negative deflection of the ERP that peaks approximately 50-80 ms post-response (van Veen and Carter 2002b; Holroyd et al. 1998; Gehring et al. 1993). This component has been most prominently linked to the monitoring of conflicts between response tendencies arising simultaneously (Yeung et al. 2004; Botvinick et al. 2001), and to PE in RL (Holroyd and Coles 2002) and predicted response-outcome models (Alexander and Brown 2011). ERN amplitude is not only increased under conditions of high response conflict (Larson et al. 2012; Gehring and Fencsik 2001), but also under negative affect (Hajcak et al. 2004), when errors are cognitively more significant (Hajcak et al. 2005) and, notably, preceding behavioral adjustments (Debener et al. 2005;

Gehring et al. 1993). We hypothesized that larger ERN amplitudes would be elicited in the standard and congruent conditions, which can be resolved with goal-directed control. However, if the ERN were to purely reflect conflict monitoring, it should be largest in the incongruent condition, which is characterized by eliciting response conflict. Furthermore, we expected that more relative goal-directed control, as reflected by increased devaluation sensitivity, would be associated to larger ERN amplitudes.

The ERN is followed by a centro-parietal P_E, a positive deflection in the ERP peaking 200-500 ms after the commission of an error (Overbeek et al. 2005; Falkenstein et al. 1991), which is widely considered to reflect error awareness and remedial action (Boldt and Yeung 2015; Steinhauser and Yeung 2010; Endrass et al. 2007; Nieuwenhuis et al. 2001). The P_E is larger when participants recognize their response was incorrect (Endrass et al. 2007; Endrass et al. 2005; Nieuwenhuis et al. 2001), with amplitude increasing with the degree of confidence that an error has been committed (Boldt and Yeung 2015). Importantly, the P_E has also been interpreted as an instance of the P3 component and related to the conscious processing of motivationally significant events (Ullsperger et al. 2014; Ridderinkhof et al. 2009). Therefore, we expected that increased P_E amplitudes would be associated with slips of action in conditions that can be resolved with goal-directed behavior (standard and congruent). We also anticipated that devaluation sensitivity would positively correlate with P_E amplitude, since more goal-directed control should be accompanied by increased error awareness.

Finally, we also aimed to assess whether goal-directed vs habitual behavior during the slips-of-action test could be predicted from behavior and/or ERPs in previous task stages. Specifically, we considered the response-locked ERN and P_E, and the outcome-locked feedback-related negativity (FRN; more recently termed reward positivity, RewP; see Holroyd et al. 2008)

and P3 from the instrumental learning stage. The FRN was initially described as peaking about 200-300 ms following negative feedback (Nieuwenhuis et al. 2004; Miltner et al. 1997) and sharing several characteristics, including scalp topography and putative neural generator, with the ERN (San Martín 2012; Gentsch et al. 2009). Originally, the RL theory (Holroyd and Coles 2002) posited that both response- and feedback-locked signals were two manifestations of the same ERN. More recent reformulations consider that the difference in ERPs to negative and positive feedback result from positive feedback: while task-related stimuli in general would elicit an N2, rewarding feedback would not, resulting in a RewP (Cockburn and Holroyd 2018; Holroyd and Umemoto 2016; Proudfit 2015; Holroyd et al. 2008). The ensuing centro-parietally distributed feedback-locked P3 peaks between 300-600 ms and has been associated with affective processing of the motivational salience of the feedback as well as context updating to maximize future rewards (Glazer et al. 2018; San Martín 2012; Polich 2007; Donchin 1981). We considered that these electrophysiological signals during learning might possess intrinsic characteristics that could be related to goal-directed vs habitual behavior at a later stage. Indeed, N2, ERN and FRN/RewP have been interpreted as electrophysiological indices of PE or surprise (Ullsperger et al. 2014; Alexander and Brown 2011; Holroyd et al. 2008), whereas the P_E and the P3 associated to both action-relevant stimuli and feedback have been suggested to reflect similar neural processes related to adaptive behavior and awareness of it (Ullsperger et al. 2014; Ridderinkhof et al. 2009). Behaviorally, however, we did not expect performance during the instrumental learning stage to predict devaluation sensitivity, but rather expected a positive relationship between O→R contingency knowledge in the outcome-devaluation test and devaluation sensitivity in the slips-of-action test.

3.2 Material and Methods

3.2.1 Participants

Forty participants (20 women) were recruited from the student population in Lübeck. Data sets from 35 participants (18 women, age range 18–30 years, *M* = 24.08, *SD* = 3.21) were analyzed in this study. The remaining five participants were excluded due to excessive artifacts. All participants were right-handed, had normal or corrected-to-normal vision, had no history of neurological or psychiatric disorders (self-report), and were not taking any medication at the time. Informed consent was obtained from each participant before conducting the study. Participants were paid for their participation or received course credit.

3.2.2 Stimuli and Procedure

Participants were trained and tested on an instrumental learning paradigm (de Wit et al. 2012b; de Wit et al. 2012a; de Wit et al. 2009), which was programmed and presented using Presentation software (Neurobehavioral System Inc., Albany, CA). Participants visualized the stimuli on a standard 24” PC monitor inside the EEG chamber. Fruit and vegetable images (henceforth, for simplification, vegetables) were used as stimuli.

The study consisted of four experimental runs, which were counterbalanced across participants. Each run used different stimulus images and consisted of three stages: instrumental learning, outcome-devaluation test and slips-of-action-test. The key features of each stage are described below. Participants were informed that they would earn points (1 point = 0.01€) in each run and were shown their score at the end of each stage. Each experimental run was scored independently, and the best score was selected for payment at the end of the experiment.

Stage 1: Instrumental learning

This stage comprised 72 trials divided in six mini-blocks. At the beginning of each trial, a vegetable was shown in front of a closed door (discriminative stimulus) in the center of the screen. Participants had to learn by trial and error, whether a right or left index finger button press (response) would open the door to a second vegetable (outcome) and were instructed to try to learn the stimulus-response-outcome associations. Participants were also informed that they would be rewarded for speed: responses made within 0-1000 ms would earn them five points and those within 1500-2000 ms three points. If they failed to respond within 2000 ms of stimulus onset, the message "Schneller!!" (Faster!!) was presented and they received no points. If an incorrect response was made, there was no vegetable behind the door and the participant received zero points. Points were always depicted over the open door.

A total of six stimulus-response-outcome associations were used in each experimental run and each was presented twice in random order in each mini-block. Participants were trained in three types of discrimination, with two discriminative stimuli each, one associated to a right and the other to a left button press. In standard discriminations, four vegetables were used, two serving as stimuli and the other two as their respective outcomes, e.g. onion-left response-banana and cherry-right response-broccoli. In congruent discriminations, the same vegetable served as both stimulus and outcome within the stimulus-response-outcome association, e.g. mandarin-left response-mandarin and avocado-right response-avocado. Finally, in incongruent discriminations, each vegetable stimulus functioned as outcome for the other, e.g. pear-left response-pumpkin and pumpkin-right response-pear.

Stage 2: Outcome-devaluation test

Following the instrumental learning stage, an outcome-devaluation test, during which EEG was not acquired, was carried out to assess the participant's knowledge of the O→R contingencies. This stage consisted of 12 trials, with each outcome tested twice in random order. On each trial, two open doors with outcome vegetables were presented vertically in the center of the screen. One had been previously associated to a left and the other to a right button press. However, a red cross superimposed on one of the doors indicated that that vegetable was devalued and no longer worth points. Participants were instructed to press the button previously associated to the valuable vegetable. Although points were given for correct responses, no feedback was delivered.

Stage 3: Slips-of-action test

The final stage consisted of six mini-blocks of 24 trials each. At the beginning of each mini-block, all six vegetable outcomes (behind open doors) were displayed for 5000 ms. A red cross was superimposed on two items that belonged to different discrimination types and button presses, indicating that these were now devalued and worth negative points. Subsequently, the discriminative stimuli (vegetables in front of closed doors) were shown. Each stimulus was shown for 2000 ms, with a 1000 ms inter-stimulus interval. Participants were instructed to press the appropriate button before the stimulus disappeared if it was associated with a valuable outcome and refrain from responding if it was associated with one of the two devalued outcomes. Although participants did not receive performance feedback, they were informed that they would still gain points for correct responses but lose one point for each response to a devalued item. Each discriminative stimulus was shown four times per mini-block and each outcome was devalued in two of the mini-blocks.

The slips-of-action test was used to assess the balance between habitual (S→R) and goal-directed (S→O→R) control. Under habitual control, it should be difficult to withhold a response leading to a devalued outcome; conversely, under goal-directed control, responses leading to devalued outcomes should be successfully inhibited. Performance in this stage was used to calculate the DSI: the difference between the percentage of responses to still valuable outcomes and the percentage of responses to devalued outcomes.

3.2.3 EEG Data Acquisition

The EEG signal was recorded from 29 scalp electrodes at a sampling rate of 500 Hz with a resolution of 0.1μV and bandpass-filtered between 0.1-70 Hz. Electrodes (Fp1/2, Fz, F3/4, F7/8, FC1/2, FC5/6, Cz, C3/4, T3/4, CP1/2, CP5/6, Pz, P3/4, P7/8, PO3/4, O1/2) were mounted on an elastic cap (EasyCap, BrainProducts GmbH, Munich, Germany) and distributed according to an extension of the international 10-20 system (Nuwer et al. 1998). Vertical and horizontal eye movements were recorded with electrodes placed above and below the right eye, and on the outer canthus of each eye. The right earlobe was used as an online reference. Impedances were kept below 5 kΩ.

3.2.4 Behavioral Data Analysis

Behavioral data were analyzed using the R programming language (htts://www.r-project.org/) with the packages PairedData (https://cran.r-project.org/web/packages/PairedData/), ez (http://cran.r-project.org/web/packages/ez/) and robustbase (https://cran.r-project.org/web/packages/robustbase/). Robust methods were used if assumptions for parametric tests were violated.

For each stage, one sample t-tests were performed for each discrimination type to assess whether participants' performance was above chance level. For the instrumental learning stage,

performance was assessed in the last mini-block, when the stimulus-response-outcome associations should be learnt. The overall percentage of correct responses was tested in the outcome-devaluation test. Chance level at the slips-of-action test has been posited to be at a DSI of 0 (de Wit et al. 2012b). However, the DSI of a participant relying fully on S→R associations and hence responding to all valuable and devalued outcomes would also be at 0 without performance being chance level. Therefore, for the slips-of-action test, tests were performed on the percentage of responses to valuable outcomes and of slips of action separately, both with expected chance levels of 50%.

To assess behavioral performance during the instrumental learning stage, repeated-measures ANOVAs (rmANOVA) with the factors discrimination type (standard, congruent, incongruent) and last mini-block (B6) were calculated for the rate of correct responses. Analogous rmANOVA was also performed with factor mini-block (B1-B6). The outcome-devaluation test was analyzed by means of a one-way rmANOVA with factor discrimination type on the rate of correct responses. Finally, the slips-of-action test was used to assess relative goal-directed and habitual control by calculating the DSI separately for the three types of discrimination. Incorrect responses (e.g. pressing the left button in a stimulus-right response-outcome association) were discarded. A DSI of 100 would indicate that the participant was driven exclusively by goal-directed control and a score of 0 would specify exclusive habitual control (de Wit et al. 2012b). A one-way rmANOVA with the factor discrimination type was performed on these indices.

Degrees of freedom and *p*-values were Huynh-Feldt-corrected when necessary. FDR-corrected post-hoc paired samples t-tests comparing standard to congruent and incongruent conditions were performed to explore the significant main effects and interactions. These post-hoc comparisons were chosen since habitual behavior is thought to predominate in incongruent

trials, whereas standard and congruent trials can be resolved through both goal-directed and habitual behavior (de Wit et al. 2011; de Wit et al. 2009); but the standard discrimination lacks the stimulus-outcome confound present in the other two discriminations (de Wit et al. 2012a).

3.2.5 EEG Data Analysis

EEG data were processed using EEGLAB (Delorme and Makeig 2004; http://sccn.ucsd.edu/eeglab) and ERPLAB (Lopez-Calderon and Luck 2014; http://erpinfo.org/erplab) running on MATLAB R2016b (Mathworks, Natick, US). Data recorded from scalp electrodes were re-referenced offline to the average signal from the two earlobe electrodes. Subsequently, data were downsampled to 250 Hz, highpass filtered at 0.5 Hz and notch-filtered at 50 Hz. Data were then segmented into epochs (-500 to 1200 ms) around the events of interest: time-locked to correct and incorrect responses, and positive and negative feedback for the instrumental learning task, and to stimuli followed by responses to still valuable outcomes, by inhibitions to devalued outcomes and by slips of action, as well as time-locked to responses to valuable outcomes and slips of action (responses to devalued outcomes) for the slips-of-action test. As in the behavioral analysis, incorrect responses were discarded. Independent component analysis was then performed to correct for ocular and cardiac artifacts (Jung et al. 2000). Epochs with voltage changes ±70 μV were discarded and participants with over 20% rejected epochs were excluded from analysis (five participants). The remaining epochs were then averaged separately for each condition. Response-locked ERPs were bandpass-filtered between 1-8 Hz (Krämer et al. 2007) and baseline corrected between -400 and -200 ms, as the ERN and P_E are known to emerge before the button press (Koelsch 2012). Stimulus- and feedback-locked ERPs were lowpass-filtered at 20 Hz (Chmielewski et al. 2015; Verleger et al. 2014; Warren and Holroyd 2012; Baker and Holroyd 2011; Moser and Simons 2009; Holroyd et

al. 2008; Hajcak et al. 2006) and baseline corrected between -200 and 0 ms. Individual averages were collapsed to calculate grand averages.

To assess statistical differences between conditions, the mean amplitudes of the midline electrodes (Fz, Cz, Pz) in the time-windows of interest were subjected to statistical analyses in R (htts://www.r-project.org/) using the abovementioned packages. Robust methods were used if assumptions for parametric tests were violated. Time-windows of interest were based on earlier publications and appropriateness was verified based on the visual inspection of the grand average waveforms. For the response-related effects during instrumental learning, the ERN was quantified between 20-120 ms and subjected to an rmANOVA with the factors discrimination type (standard, congruent, incongruent), correctness (correct and incorrect response) and electrode site (Fz, Cz, Pz). Since the ERP evidenced no P_E, this was not statistically analyzed. For feedback-related effects, FRN/RewP and P3 components were measured between 200-300 ms and 300-550 ms, respectively, and subjected to rmANOVAs with the factors discrimination type, feedback valence (positive, negative) and electrode site. Given that it was apparent that the negativity following negative feedback was more positive than its analogue following positive feedback, to further quantify the FRN/RewP, an rmANOVA was computed using the peak-to-peak difference at an individual level between the most negative peak between 200–300 ms post-feedback and the amplitude of the preceding positive peak. For the slips-of-action test, the stimulus-locked N2 and P3 components were quantified between 180-300 ms and 500-700 ms, respectively, and analyzed by means of rmANOVAs with the factors discrimination type, ensuing response (responses to valuable outcomes, inhibitions to devalued outcomes, slips of action) and electrode site. For the response-related effects, the ERN and P_E were quantified between 20-120 ms and 240-380 ms, respectively, and subjected to separate rmANOVAs with the factors discrimination type, correctness (responses to valuable outcomes and slips of action) and

electrode site. Degrees of freedom and *p*-values were Huynh-Feldt-corrected when necessary. FDR-corrected post-hoc paired samples t-tests comparing standard to congruent and incongruent conditions were performed to explore significant main effects and interactions (de Wit et al. 2012a; de Wit et al. 2011; de Wit et al. 2009).

3.2.6 Relationship between Behavioral and Electrophysiological Measures

As in previous studies (de Wit et al. 2012b; de Wit et al. 2012a), these analyses were performed only on measures from standard discriminations, which can be supported by both goal-directed and habitual systems (de Wit et al. 2009), in contrast to incongruent discriminations (de Wit et al. 2014) and without the confounders of congruent discriminations (de Wit et al. 2012a; de Wit et al. 2009).

Behavioral and electrophysiological measures of interest were subjected to linear regression analyses. If possible, robust regression (MM-estimation) was performed when assumptions for OLS regression were not met or significant outliers were present. Behavioral measures were rank-transformed (de Wit et al. 2012b) and tied ranked were treated with a permutation with increasing values at each index set of ties. As with the behavioral measures, only ERPs that had demonstrated significant interactions with the factor discrimination type were considered, i.e. N2 and ERN of the slips-of-action test. Because these ERPs were modulated by discrimination type and ensuing response/correctness, but without the influence of electrode site, the electrode Cz was chosen for analyses as it showed the largest dN2 and dERN on the scalp topographies (see Figures 3.5 and 3.6).

3.3 Results

3.3.1 Behavioral Results

Stage 1: Instrumental learning stage

One sample t-tests were performed on the correct response rate in the last mini-block to quantify whether participants' performance was better than chance for each discrimination type at the end of the learning stage (Figure 3.1). These showed that performance was above chance level for all discrimination types (see Table 3.1 for statistical values).

	M (*SD*)	t/t_y	df	*d*	*p*
Stage 1: Instrumental learning (last mini-block)					
Standard	98.04 % (5.83)	97.74	28	8.25	< 2.22e-16
Congruent	97.32% (5.09)	49.69	28	9.29	< 2.22e-16
Incongruent	92.86% (10.52)	31.34	28	4.07	< 2.22e-16
Stage 2: Outcome-devaluation test					
Standard	83.04% (18.91)	11.77	28	1.75	3.54e-12
Congruent	96.61% (6.13)	44.10	28	7.61	< 2.22e-16
Incongruent	61.07% (27.91)	2.49	28	0.40	.019
Stage 3: Slips-of-action test					
Standard - valuable	88.46% (13.22)	17.56	28	2.91	< 2.22e-16
Congruent - valuable	93.59% (7.48)	37.13	28	5.83	< 2.22e-16
Incongruent - valuable	80.22% (17.48)	11.08	28	1.73	9.46e-12
Standard - devalued	19.96% (19.54)	-13.32	28	1.54	1.84e-13
Congruent - devalued	18.80% (10.21)	-18.07	34	3.05	1.05e-18
Incongruent - devalued	20.58% (18.18)	-11.90	28	1.62	2.19e-12

Table 3.1 | Results from the one-sample t-tests carried out on the participants' performance for each discrimination type. For the slips-of-action test, these were performed separately on responses to valuable and devalued outcomes. Note that *t*-values can be the result of parametric t-tests or robust Yuen's t-tests; the latter resulted in 28 degrees of freedom (df). Effect sizes are represented by Cohen's *d* and *p*-values are FDR-corrected.

A one-way rmANOVA demonstrated significant differences between discrimination types on the percentage of correct responses in the last mini-block, $F(1,51) = 10.61$, $\eta^2_p = .24$, $p =$ 4.96e-4, with performance in the standard trials being significantly better than in the incongruent,

$t_y(28) = 3.53$, $d = 0.75$, $p = .003$, but not congruent condition, $t_y(28) = 1.22$, $d = 0.14$, $p > .1$ (FDR-corrected).

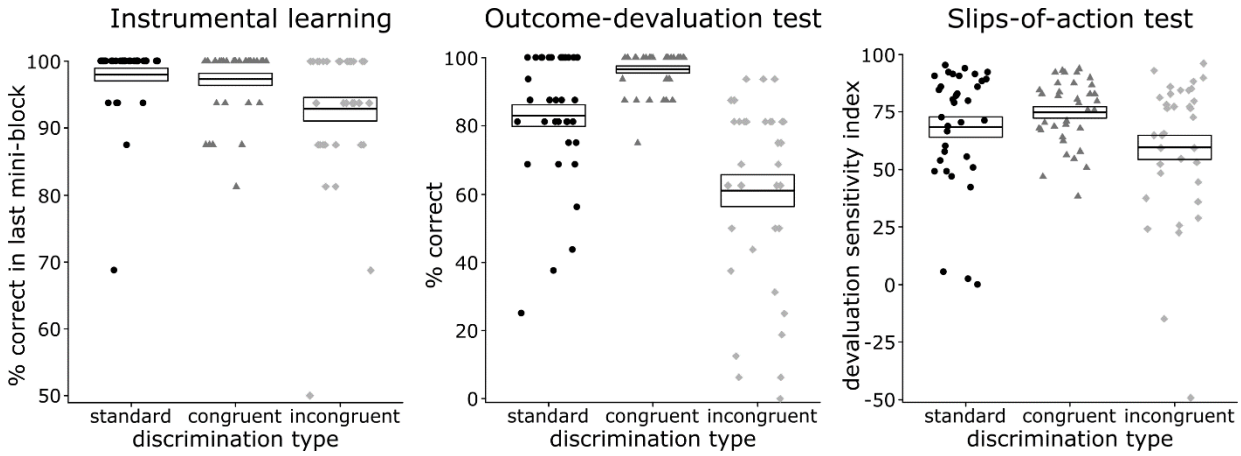

Figure 3.1 | Behavioral performance in the three stages of the task. Percentage of correct responses in the last mini-block of the instrumental learning stage (left), percentage of correct responses in the outcome-devaluation test (center) and devaluation sensitivity index (percentage of responses to valuable outcomes minus percentage of responses to devalued outcomes) in the slips-of-action test (right). Crossbars represent the mean (central line) plus-minus the standard error of the mean. Black dots, dark grey triangles and light diamonds represent individual participant's values in the standard, congruent and incongruent discriminations, respectively.

An rmANOVA with factors discrimination type (standard, congruent, incongruent) and mini-block (B1-B6) was performed on the correct response rate (Figure 3.2). This showed significant effects of discrimination type, $F(2,68) = 15.23$, $\eta^2_p = .31$, $p = 3.42e\text{-}6$, and mini-block, $F(3,110) = 226.50$, $\eta^2_p = .87$, $p = 1.88e\text{-}48$. The interaction between discrimination type and mini-block was not statistically significant, $F(8,271) = 1.93$, $\eta^2_p = .05$, $p = .056$. FDR-corrected (for the seven comparisons performed) post-hoc tests were performed to analyze the main effects of discrimination type and mini-block. The discriminative conditions were compared to each other using paired samples t-tests, demonstrating that performance was better for standard (89.32±6.74 %) compared to incongruent (84.87±10.32 %) trials, $t_y(28) = 4.20$, $d = 0.81$, $p = .001$, but not to the congruent condition (89.64±5.41 %), $t_y(28) = 0.15$, $d = 0.05$, $p > .1$. The main effect of mini-

block was analyzed by averaging the data over discrimination type and comparing each block with its succeeding block using paired samples t-test. These demonstrated that, except between mini-blocks B3 and B4, $t_y(28) = -1.50$, $d = 0.35$, $p > .1$, and B5 and B6, $t_y(28) = -1.69$, $d = 0.31$, $p > .1$, participants gradually improved their performance over time: from B1 (66.43±6.29 %) to B2 (83.69±10.57 %), $t_y(28) = -12.58$, $d = 2.07$, $p = 3.43e\text{-}12$; from B2 to B3 (91.37±9.52 %), $t_y(28) = -7.48$, $d = 1.29$, $p = 1.33e\text{-}7$; from B4 (93.21±6.26 %) to B5 (94.88±6.58 %), $t_y(28) = -4.05$, $d = 0.61$, $p = .001$.

An analogous rmANOVA was performed on the reaction times (Figure 3.2), showing significant effects of discrimination type, $F(2,68) = 38.79$, $\eta^2_p = .53$, $p = 5.77e\text{-}12$, and mini-block, $F(3,91) = 86.63$, $\eta^2_p = .72$, $p = 3.37e\text{-}25$, as well as a significant interaction between discrimination type and mini-block, $F(8,258) = 2.30$, $\eta^2_p = .06$, $p = .024$. As with the correct response rates, FDR-corrected (for the seven comparisons performed) post-hoc tests were performed to analyze the main effects of discrimination type and mini-block. These demonstrated that the main effect of discrimination type was due to reaction times being significantly faster for standard (690±108 ms) than incongruent (734±107 ms), $t_y(28) = -6.12$, $d = 0.93$, $p = 4.60e\text{-}6$, but slower than congruent (660±94 ms) trials, $t_y(28) = 4.12$, $d = 0.66$, $p = .001$. The post-hoc t-tests performed to elucidate the main effect of mini-block demonstrated that response times got significantly faster over time: from B1 (808±105 ms) to B2 (750±102 ms), $t_y(28) = 4.81$, $d = 0.83$, $p = 1.10e\text{-}4$; from B2 to B3 (691±106 ms), $t_y(28) = 7.41$, $d = 1.11$, $p = 3.14e\text{-}7$; from B3 to B4 (656±107 ms), $t_y(28) = 3.81$, $d = 0.76$, $p = .001$; from B4 to B5 (643±115 ms), $t_y(28) = 2.20$, $d = 0.31$, $p = .036$; and from B5 to B6 (620±108 ms), $t_y(28) = 3.20$, $d = 0.60$, $p = .004$.

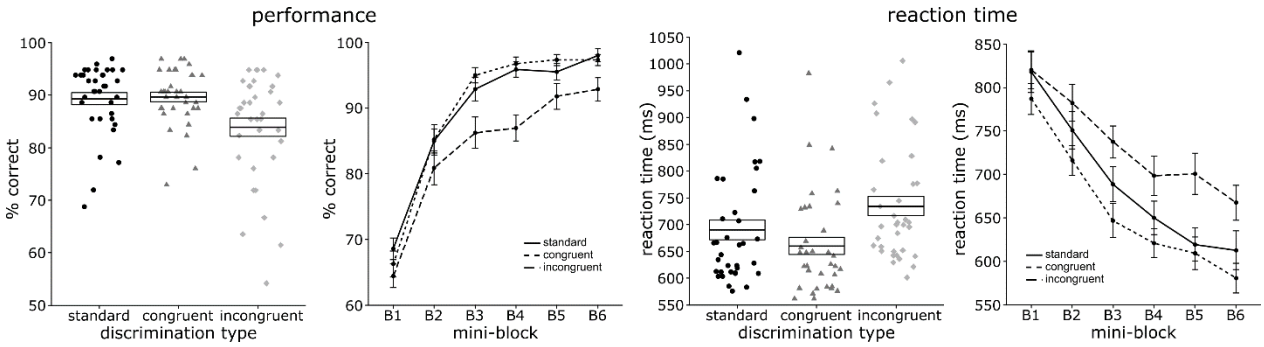

Figure 3.2 | Behavioral performance during the instrumental learning stage. Overall percentage of correct responses (outer left), percentage of correct responses in each mini-block (center left), overall reaction time (center right), and reaction time in each mini-block (outer right). Crossbars and error bars represent the mean (central line) plus-minus the standard error of the mean. Black dots/solid lines, dark grey triangles/dotted lines and light diamonds/dashed lines represent individual participant's values in the standard, congruent and incongruent discriminations, respectively.

Stage 2: Outcome-devaluation test

One sample t-tests were performed on the percentage of correct responses to quantify whether the participants' performance was better than chance for each discrimination type. These showed that performance was above chance level for all discrimination types (see Table 3.1 for statistical values).

A one-way rmANOVA showed a significant effect of discrimination type on the percentage of correct responses, $F(2,57) = 45.03$, $\eta^2_p = .57$, $p = 2.24e\text{-}11$ (Figure 3.1). Post-hoc paired samples t-tests demonstrated that participants had significantly better knowledge of O→R associations on congruent compared to standard, $t_y(28) = 3.97$, $d = 0.71$, $p = 4.53e\text{-}4$, and standard compared to incongruent discriminations, $t_y(28) = 6.21$, $d = 1.12$, $p = 2.09e\text{-}6$ (FDR-corrected).

Stage 3: Slips-of-action test

Firstly, one sample t-tests were performed on the percentage of responses to valuable and devalued outcomes separately to quantify whether the participants' performance was better than chance for each discrimination type. These showed that performance was better than chance level for all discrimination types for both valuable and devalued outcomes (see Table 3.1 for statistical values). Furthermore, the percentages of responses to valuable and to devalued outcomes were not related to each other in the case of standard (ρ = -.31) and congruent (ρ = -.33) trials, both p = .72. But in the case of the incongruent discriminations, participants who made more responses to valuable outcomes also responded significantly less to devalued outcomes, ρ = -.47, p = .014 (FDR-corrected).

The one-way rmANOVA computed on the DSI showed a significant effect of discrimination type, $F(2,54) = 8.93$, $\eta^2_p = .21$, $p = .001$ (Figure 3.1). Post-hoc paired samples t-tests demonstrated that participants displayed significantly more goal-directed control in standard (68.50±25.90 %) trials compared to the incongruent condition (59.64±31.43 %), $t_y(28) = 3.45$, $d = 0.58$, $p = .004$, but not compared to the congruent condition (74.80±14.37 %), $t_y(28) = -1.00$, $d = 0.29$, $p > .1$ (FDR-corrected).

3.3.2 EEG Results

Stage 1: Instrumental learning stage

Response-locked component.

The mean amplitude of the ERN was examined using an rmANOVA with factors discrimination type (standard, congruent, incongruent), correctness (correct, incorrect) and electrode site (Fz, Cz, Pz). This showed significant effects of discrimination type, $F(2,68) = 3.74$, $\eta^2_p = .10$, $p = .029$, correctness, $F(1,34) = 68.37$, $\eta^2_p = .67$, p = 1.19e-9, and electrode site,

$F(1,51) = 12.81$, $\eta^2_p = .27$, $p = 1.44e\text{-}4$, as well as a significant two-way interaction between correctness and electrode site, $F(1,45) = 13.21$, $\eta^2_p = .28$, $p = 2.24e\text{-}4$, and a three-way interaction between discrimination type, correctness and electrode site, $F(3,90) = 3.16$, $\eta^2_p = .08$, $p = .034$. All other interactions were not statistically significant, $p > .1$ (discrimination type × correctness: $F(2,68) = 1.37$, $\eta^2_p = .04$; discrimination type × electrode site: $F(3,102) = 0.50$, $\eta^2_p = .00$). FDR-corrected post-hoc paired samples t-tests were performed to analyze the three-way interaction. To this end, the amplitude difference between incorrect and correct responses was calculated, and the discriminative conditions were subsequently compared to each other at each electrode. However, although the difference ERN (dERN) was largest for all discriminations at Cz (Figure 3.3), there were no significant differences between discrimination types at any electrode, $p > .1$ (Fz: standard vs incongruent: $t_y(28) = -0.21$, $d = 0.00$; Fz: standard vs congruent: $t_y(28) = -0.01$, $d = 0.01$; Cz: standard vs incongruent: $t_y(28) = -1.51$, $d = 0.23$; Cz: standard vs congruent: $t_y(28) = 0.55$, $d = 0.12$; Pz: standard vs incongruent: $t_y(28) = -1.09$, $d = 0.18$; Pz: standard vs congruent: $t_y(28) = 1.06$, $d = 0.19$).

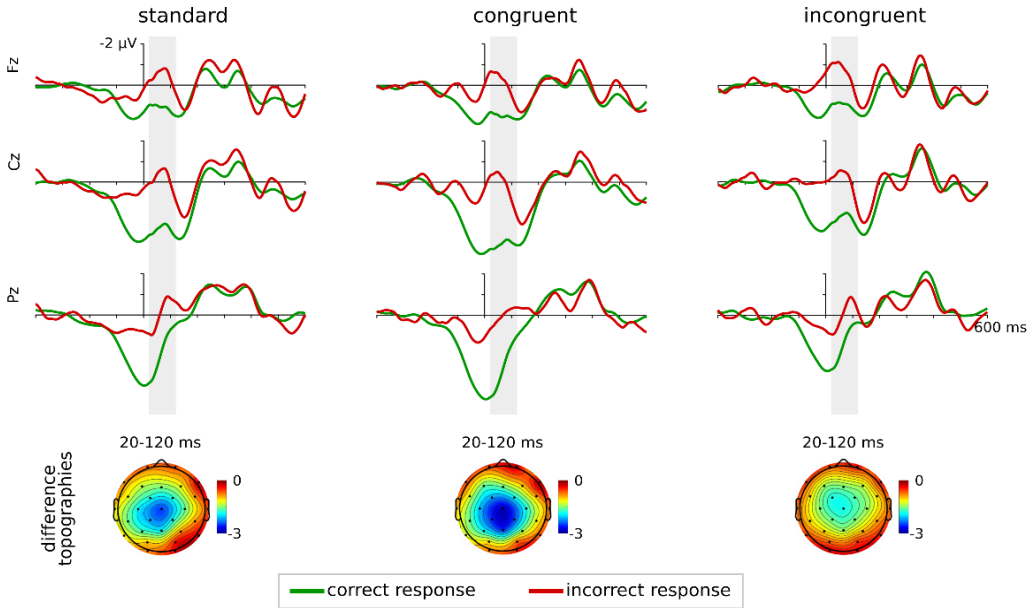

Figure 3.3 | Response-locked ERPs during the instrumental learning stage. ERPs at Fz, Cz and Pz time-locked to responses to correct (green line) and incorrect (red line) responses in standard (left), congruent (center) and incongruent (right) discriminations. Topographies depict the differences between incorrect and correct responses at the indicated time window.

Feedback-locked components.

The mean amplitude of the FRN/RewP was examined using an rmANOVA with factors discrimination type (standard, congruent, incongruent), feedback valence (positive, negative) and electrode site (Fz, Cz, Pz). This showed significant effects of discrimination type, $F(2,68) = 4.67$, $\eta^2_p = .12$, $p = .013$, feedback valence, $F(1,34) = 20.08$, $\eta^2_p = .37$, $p = 8.01e\text{-}5$, and electrode site, $F(1,40) = 53.12$, $\eta^2_p = .61$, $p = 1.66e\text{-}9$, as well as a significant two-way interaction between feedback valence and electrode site, $F(1,44) = 12.86$, $\eta^2_p = .27$, $p = 3.30e\text{-}4$, and a three-way interaction between discrimination type, feedback valence and electrode site, $F(2,85) = 10.00$, $\eta^2_p = .23$, $p = 3.46e\text{-}5$. All other interactions were not statistically significant, $p > .1$ (discrimination type × feedback valence: $F(2,68) = 0.75$, $\eta^2_p = .02$; discrimination type × electrode site: $F(3,90) = 0.91$, $\eta^2_p = .03$). FDR-corrected post-hoc paired samples t-tests were performed to analyze the three-way interaction. To this end, the difference between the mean amplitudes of negative and positive feedback was calculated, and the discriminative conditions were subsequently compared at each electrode. However, no significant differences were found in the difference ERP between discrimination types at any electrode (Figure 3.4), $p > .1$ (Fz: standard vs incongruent: $t_y(28) = 0.90$, $d = 0.19$; Fz: standard vs congruent: $t_y(28) = 1.41$, $d = 0.27$; Cz: standard vs incongruent: $t_y(28) = 1.52$, $d = 0.24$; Cz: standard vs congruent: $t_y(28) = 0.29$, $d = 0.13$; Pz: standard vs incongruent: $t_y(28) = 0.60$, $d = 0.13$; Pz: standard vs congruent: $t_y(28) = -2.21$, $d = 0.32$).

The rmANOVA with factors discrimination type (standard, congruent, incongruent), feedback valence (positive, negative), and electrode site (Fz, Cz, Pz) performed on the peak-to-peak amplitude of the FRN/RewP showed a significant effect of feedback valence, $F(1,34) = 5.31$, $\eta^2_p = .14$, $p = .027$, confirming the presence of a larger negativity following negative (-4.74±3.56 µV) compared to positive feedback (-3.45±2.13 µV). No other effects or interactions were statistically significant, $p > .1$ (discrimination type: $F(2,58) = 1.58$, $\eta^2_p = .04$; electrode site:

$F(1,48) = 1.43$, $\eta^2_p = .04$; discrimination type × feedback valence: $F(2,59) = 0.62$, $\eta^2_p = .02$; discrimination type × electrode site: $F(4,119) = 0.56$, $\eta^2_p = .02$; feedback valence × electrode site: $F(1,51) = 0.42$, $\eta^2_p = .01$; discrimination type × feedback valence × electrode site: $F(3,111) = 0.93$, $\eta^2_p = .03$).

An rmANOVA with factors discrimination type (standard, congruent, incongruent), feedback valence (positive, negative), and electrode site (Fz, Cz, Pz) was used to test the mean amplitude of the P3, revealing significant effects of feedback valence, $F(1,34) = 189.72$, $\eta^2_p = .85$, $p = 1.81e\text{-}15$, and electrode site, $F(1,42) = 155.68$, $\eta^2_p = .82$, $p = 4.55e\text{-}17$, as well as a two-way interaction between feedback valence and electrode site, $F(1,41) = 66.23$, $\eta^2_p = .66$, $p = 4.41e\text{-}11$, and a three-way interaction between discrimination type, feedback valence and electrode site, $F(3,95) = 10.77$, $\eta^2_p = .24$, $p = 6.44e\text{-}6$. All other effects and interactions were not statistically significant, $p > .1$ (discrimination type: $F(2,68) = 1.06$, $\eta^2_p = .03$; discrimination type × feedback valence: $F(2,68) = 0.56$, $\eta^2_p = .02$; discrimination type × electrode site: $F(2,79) = 0.43$, $\eta^2_p = .01$). Post-hoc paired samples t-tests were performed to analyze the three-way interaction. To this end, the difference between the mean amplitudes of negative and positive feedback was estimated, and the discriminative conditions were then compared to each at each electrode. However, although the difference P3 (dP3) was largest for all conditions at Pz (Figure 3.4), no comparison survived FDR-correction, $p > .1$ (Fz: standard vs incongruent: $t_y(28) = 0.24$, $d = 0.03$; Fz: standard vs congruent: $t(34) = 0.54$, $d = 0.09$; Cz: standard vs incongruent: $t_y(28) = -0.05$, $d = 0.07$; Cz: standard vs congruent: $t_y(28) = -0.28$, $d = 0.13$; Pz: standard vs incongruent: $t_y(28) = -0.80$, $d = 0.18$; Pz: standard vs congruent: $t_y(28) = -2.17$, $d = 0.46$).

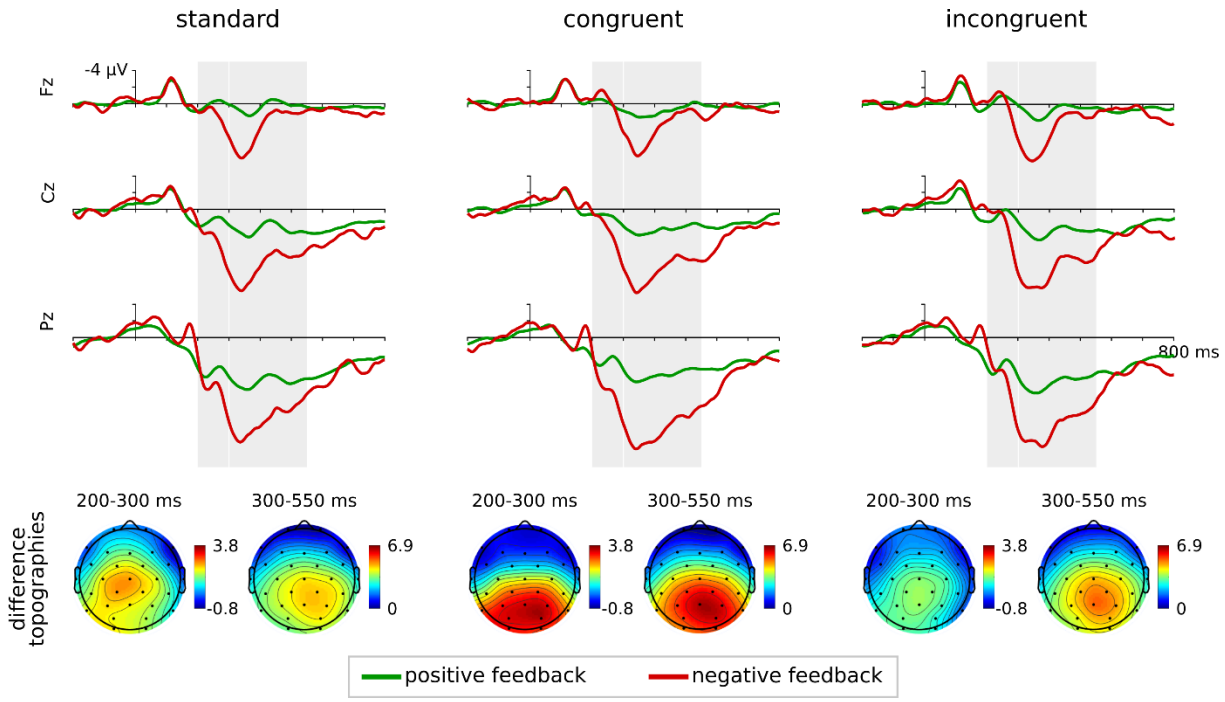

Figure 3.4 | Feedback-locked ERPs during the instrumental learning stage. ERPs at Fz, Cz and Pz time-locked to responses to positive (green line) and negative (red line) feedback in standard (left), congruent (center) and incongruent (right) discriminations. Topographies depict the differences between negative and positive feedback at the indicated time windows.

Stage 3: Slips-of-action test

Stimulus-locked components.

An rmANOVA with factors discrimination type (standard, congruent, incongruent), ensuing response (responses to valuable outcomes, inhibitions to devalued outcomes, slips of action) and electrode site (Fz, Cz, Pz) was performed on the mean amplitude of the N2. This revealed significant effects of ensuing response, $F(2,52) = 10.08$, $\eta^2_p = .23$, $p = .001$, and electrode site, $F(1,41) = 55.35$, $\eta^2_p = .62$, $p = 6.49e\text{-}10$, as well a two-way interaction between discrimination type and ensuing response, $F(2,77) = 6.09$, $\eta^2_p = .15$, $p = .002$. All other effects and interactions were not statistically significant, $p > .1$ (discrimination type: $F(2,68) = 0.42$, $\eta^2_p = .01$; discrimination type × electrode site: $F(3,87) = 1.79$, $\eta^2_p = .05$; ensuing response × electrode

site: $F(2,68) = 2.21$, $\eta^2_p = .06$; discrimination type × ensuing response × electrode site: $F(3,119) = 0.90$, $\eta^2_p = .03$). FDR-corrected post-hoc paired samples t-tests were performed to examine the two-way interaction between discrimination type and ensuing response. To this end, N2 amplitudes were first averaged across electrode sites. Subsequently, the differences (dN2) between inhibitions to devalued and responses to valuable outcomes, as well as between slips of action and responses to valuable outcomes were computed separately. Discrimination types were then compared for these dN2 values. This demonstrated that the dN2 for slips of action was significantly more positive for standard (2.10±2.81 µV) compared to incongruent discriminations (-0.41±2.32 µV), $t_y(28) = 3.20$, $d = 0.65$, $p = .014$ (Figure 3.5). No significant difference was found in the comparison between standard and congruent discriminations, $t_y(28) = 1.74$, $d = 0.36$, $p > .1$. No significant differences between discrimination types were observed in the dN2 for inhibitions to devalued outcomes, $p > .1$ (standard vs incongruent: $t_y(28) = 0.73$, $d = 0.07$; standard vs congruent: $t_y(28) = 0.65$, $d = 0.07$).

The mean P3 amplitude was examined using an rmANOVA with the factors discrimination type (standard, congruent, incongruent), ensuing response (responses to valuable outcomes, inhibitions to devalued outcomes, slips of action) and electrode site (Fz, Cz, Pz). This yielded significant effects of discrimination type, $F(2,60) = 6.75$, $\eta^2_p = .17$, $p = .003$, ensuing response, $F(2,61) = 18.06$, $\eta^2_p = .35$, $p = 1.72e\text{-}6$, and electrode site, $F(1,46) = 75.84$, $\eta^2_p = .69$, $p = 4.75e\text{-}13$, as well as a two-way interaction between ensuing response and electrode site, $F(3,86) = 5.99$, $\eta^2_p = .15$, $p = .002$. All other interactions were not statistically significant, $p > .1$ (discrimination type × ensuing response: $F(2,78) = 0.57$, $\eta^2_p = .02$; discrimination type × electrode site: $F(3,91) = 1.25$, $\eta^2_p = .04$; discrimination type × ensuing response × electrode site: $F(4,125) = 0.69$, $\eta^2_p = .02$). No post-hoc tests were carried out since there were no significant interactions with the factor discrimination type.

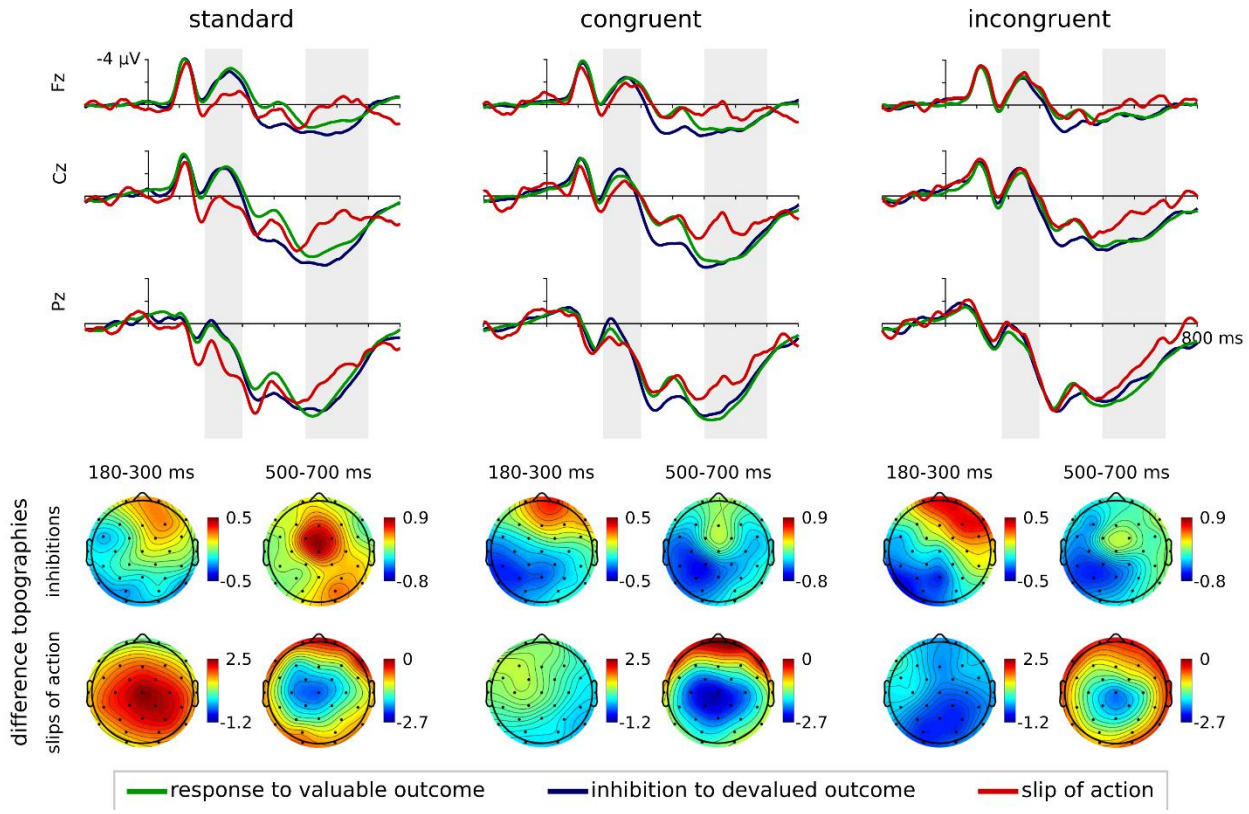

Figure 3.5 | Stimulus-locked ERPs during the slips-of-action test. ERPs at Fz, Cz and Pz time-locked to stimuli preceding responses to valuable outcomes (green line), preceding slips of action (red line) and preceding inhibitions to devalued outcomes (blue line) in standard (left), congruent (center) and incongruent (right) discriminations. Topographies depict the differences between stimuli preceding inhibitions to devalued and responses to valuable outcomes, and between stimuli preceding slips of action and responses to valuable outcomes at the indicated time windows.

Response-locked components.

An rmANOVA with factors discrimination type (standard, congruent, incongruent), correctness (responses to valuable outcomes, slips of action) and electrode site (Fz, Cz, Pz) was used to test the mean amplitude of the ERN, revealing significant effects of correctness, $F(1,34) = 88.12$, $\eta^2_p = .72$, $p = 5.74e\text{-}11$, and electrode site, $F(1,44) = 5.32$, $\eta^2_p = .14$, $p = .018$, as well as interactions between discrimination type and correctness, $F(2,68) = 4.61$, $\eta^2_p = .12$, $p = .013$, discrimination type and electrode site, $F(3,115) = 2.98$, $\eta^2_p = .08$, $p = .029$, and correctness and electrode site, $F(2,56) = 15.51$, $\eta^2_p = .31$, $p = 1.62e\text{-}5$. All other effects and interactions were not

statistically significant, $p > .1$ (discrimination type: $F(2,68) = 1.42$, $\eta^2_p = .04$; discrimination type × correctness × electrode site: $F(3,113) = 1.07$, $\eta^2_p = .03$). Post-hoc paired samples t-tests were performed to examine the two-way interaction between discrimination type and correctness. To this end, the ERPs were first averaged over the three electrode sites, the difference in ERN amplitude between slips of action and responses to valuable outcomes (dERN) was then computed and compared between discriminative conditions. This demonstrated that the amplitude of the dERN was significantly larger for the standard (-4.06±3.39 µV) compared to incongruent trials (-2.59±2.91 µV), $t_y(28) = -3.12$, $d = 0.44$, $p = .008$, but not compared to congruent trials (-3.89±2.13 µV), $t(28) = -0.33$, $d = 0.06$, $p > .1$ (FDR-corrected) (Figure 3.6).

An rmANOVA with factors discrimination type (standard, congruent, incongruent), correctness (responses to valuable outcomes, slips of action), and electrode site (Fz, Cz, Pz) was used to test the mean amplitude of the P_E, revealing a significant effect of correctness, $F(1,34) = 18.27$, $\eta^2_p = .35$, $p = 1.46e\text{-}4$, and electrode site, $F(1,49) = 62.33$, $\eta^2_p = .65$, $p = 2.82e\text{-}12$, as well as a two-way interaction between correctness and electrode site, $F(3,114) = 3.61$, $\eta^2_p = .10$, $p = .012$. All other effects and interactions were not statistically significant (discrimination type: $F(2,68) = 0.52$, $\eta^2_p = .01$, $p > .1$; discrimination type × correctness: $F(2,68) = 2.75$, $\eta^2_p = .07$, $p = .071$; correctness × electrode site: $F(2,54) = 1.94$, $\eta^2_p = .05$, $p > .1$; discrimination type × correctness × electrode site: $F(3,97) = 1.17$, $\eta^2_p = .03$, $p > .1$). No post-hoc tests were carried out since there was no significant interactions including the factor discrimination type.

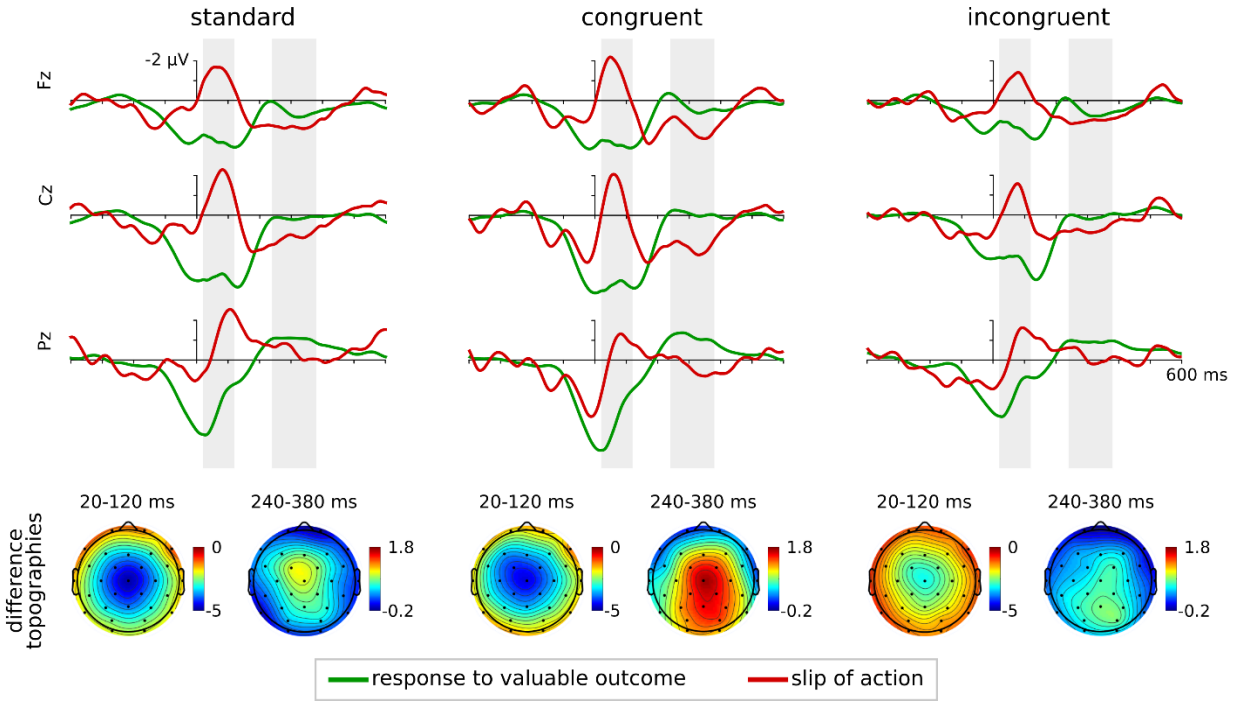

Figure 3.6 | Response-locked ERPs during the slips-of-action test. ERPs at Fz, Cz and Pz time-locked to responses to valuable outcomes (green line) and slips of action (red line) in standard (left), congruent (center) and incongruent (right) discriminations. Topographies depict the differences between slips of action and responses to valuable outcomes at the indicated time windows.

3.3.3 Relationship between Behavioral and Electrophysiological Measures (Standard Discrimination)

Can devaluation sensitivity predict the electrophysiological components from the slips-of-action test?

Since N2 and ERN have been associated to the monitoring of response conflict (van Veen and Carter 2002b; Botvinick et al. 2001; Gehring and Fencsik 2001), multiple regression models including the dN2 (for slips of action) and the dERN evoked by incongruent discriminations as predictors were considered, to account for the potential influence of response conflict in the ERPs elicited by the standard discrimination.

In the case of the dN2 (at Cz), the multiple regression model including the incongruent-dN2 was not statistically different from the simple regression model without it, $W_T(1,32) = 0.54$, $p > .1$, so the simple regression model was chosen. This demonstrated that the ranked DSI significantly predicted dN2 amplitude, W_T (1,33) = 17.09, p = 5.66e-6, with R^2 = .35 (Figure 3.7 A).

In the case of the dERN (at Cz), the multiple regression model including the incongruent-dERN was marginally better than the simple regression model without it, $F(1,32) = 3.61$, p = .066, so the multiple regression model was chosen, in order to better understand the possible influence of response conflict in the standard-dERN. The model using both ranked DSI and incongruent-dERN was statistically significant, $F(2,32) = 17.96$, p = 5.89e-6, with R^2 = .53. However, the ranked DSI significantly contributed to the model, t = -4.86, p = 2.98e-5, while the incongruent-dERN only showed a marginal contribution, t = 1.90, p = .066 (Figure 3.7 B).

Can behavior in the previous stages predict measures from the slips-of-action test?

The multivariate regression analysis performed on the ranked behavioral values showed that the overall correct response rate in the instrumental learning stage did not predict the correct response rate in the outcome-devaluation test or the DSI from the slips-of-action test, V = 0.12, $F(2,32) = 2.09$, $p > .1$ (outcome-devaluation test: R^2 = .00; slips-of-action test: R^2 = .07). In contrast, the correct response rate in the outcome-devaluation test strongly predicted the DSI from the slips-of-action test, $F(1,33) = 31.07$, p = 3.39e-6, with R^2 = .48 (Figure 3.7 C).

Multiple regression analysis showed that dN2 amplitude (at Cz) in the slips-of-action test could not be predicted by the performance in the previous stages, $F(2,32) = 2.32$, $p > .1$, R^2 = .13. However, performance in the outcome-devaluation test marginally contributed to the model, t =

1.94, $p = .062$, while instrumental learning performance showed no significant contribution, $t = -1.04$, $p > .1$.

An analogue analysis with dERN amplitude (at Cz) as regressand showed that the multiple regression model was statistically significant, $F(2,32) = 6.36$, $p = .005$, with $R^2 = .28$, but again not significantly different from a simple regression with just performance in the outcome-devaluation test as a predictor, $F(1,32) = 0.17$, $p > .1$. The simple regression analysis demonstrated that ranked performance in the outcome-devaluation test significantly predicted dERN amplitude in the slips-of-action test, $F(1,33) = 12.88$, $p = .001$, with $R^2 = .28$ (Figure 3.7 D).

Can electrophysiological components from the instrumental learning stage predict measures from the slips-of-action test?

Multiple regression analysis showed that the dERN and dP3 from the instrumental learning stage could significantly predict the ranked DSI from the slips-of-action test, $F(2,32) = 5.99$, $p = .006$, with $R^2 = .27$. The dP3, $t = 2.79$, $p = .009$, contributed more to the model than the dERN, $t = -2.48$, $p = .019$ (Figure 3.7 E).

Whereas neither ERP from the instrumental learning stage could predict the dN2 associated to slips of action, $W_T(2,32) = 2.19$, $p > .1$, with $R^2 = .04$, the analogous multiple regression model using the dERN from the slips-of-action test as a regressand was statistically significant, $F(2,32) = 5.52$, $p = .009$, with $R^2 = .26$. However, the dERN from the instrumental learning stage significantly contributed to the model, $t = 3.00$, $p = .005$, while the dP3 only showed a marginal contribution, $t = -1.91$, $p = .066$ (Figure 3.7 F).

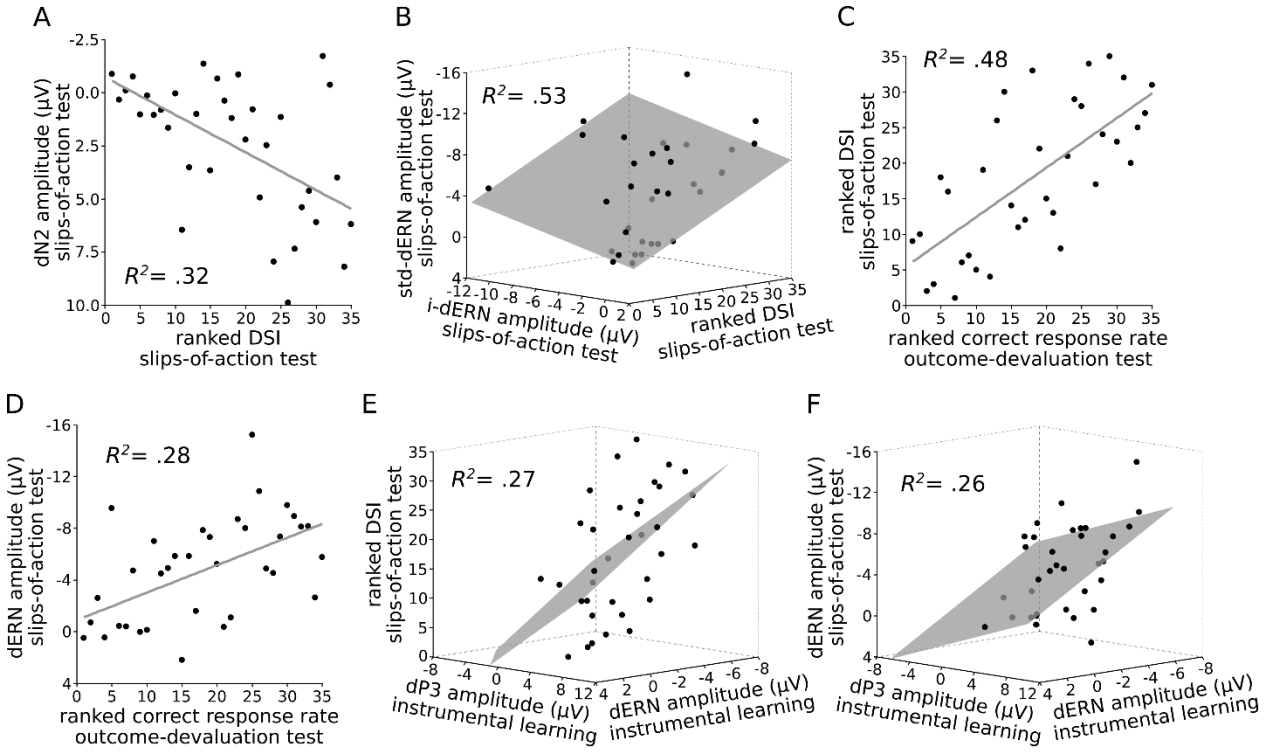

Figure 3.7 | Results of the regression analyses between behavioral and electrophysiological measures in the standard discrimination. (A) Participants showing more goal-directed control (higher devaluation sensitivity indices; DSI) had larger, positive-going dN2 amplitudes associated to slips of action in the slips-of-action test, p = 2.30e-4. (B) Participants showing more goal-directed control (higher DSI) had larger dERN amplitudes associated to slips of action in the slips-of-action test, p = 2.98e-5. The dERN associated to slips of action in incongruent discriminations (i-dERN) was not significantly correlated with the dERN in standard discriminations (std-dERN), p = .066. (C) Participants with better knowledge of the O→R contingencies (higher correct response rate) in the outcome-devaluation test subsequently showed more goal-directed control (higher DSI) in the slips-of-action test, p = 3.39e-6. (D) Participants with better knowledge of the O→R contingencies (higher correct response rate) in the outcome-devaluation test subsequently had larger dERN amplitudes associated to slips of action in the slips-of-action test, p = .001. (E) Participants with larger dERN amplitudes associated to incorrect responses, p = .019, and larger dP3 amplitudes associated to negative feedback, p = .009, in the instrumental learning stage subsequently showed more goal-directed control (higher DSI) in the slips-of-action test. (F) Participants with larger dERN amplitudes associated to incorrect responses in the instrumental learning stage subsequently had larger dERN amplitudes associated to slips of action in the slips-of-action test, p = .005. The dP3 associated to negative feedback from the instrumental learning stage was not significantly correlated with the dERN from the slips-of-action test, p = .066.

3.4 Discussion

In the present study, goal-directed vs habitual control was tested using an outcome devaluation procedure, in which participants were asked to flexibly adjust their behavior to changes in outcome value. On the behavioral level, our results are in line with previous studies using the fabulous fruit game (de Wit et al. 2012b; de Wit et al. 2009), demonstrating greater devaluation sensitivity, and thus increased goal-directed control, on standard compared to incongruent discriminations. On the electrophysiological level, this was reflected on the dN2 and dERN.

The data show that the N2 was modulated by both the ensuing response and discrimination type. Specifically, as anticipated, the N2 amplitude associated to slips of action was significantly smaller in standard than in incongruent discriminations. Similar N2 amplitudes were found on the congruent condition, which as standard discriminations can be solved by the goal-directed system (de Wit et al. 2012b). Moreover, the reduction in N2 amplitude in the standard condition was more pronounced with increasing sensitivity to devaluation, although it was unrelated to knowledge of the R→O contingencies in the outcome-devaluation test. These results appear consistent with the conflict monitoring account of the N2, which predicts that conflict-based recruitment of attentional control will result in increased N2 amplitude (Carter and van Veen 2007; Yeung and Cohen 2006; Yeung et al. 2004; Donkers and van Boxtel 2004; Nieuwenhuis et al. 2003; van Veen and Carter 2002a; Botvinick et al. 2001). In line with this prediction, the incongruent condition, which is designed to generate response conflict (de Wit et al. 2012b; de Wit et al. 2009), elicited larger N2 amplitudes than the other two conditions. Furthermore, the correlation between the N2 decrease and increased sensitivity to devaluation in the standard condition suggests that increased goal-directed control results in more efficient suppression of

irrelevant stimulus information (Yeung and Cohen 2006). Interestingly, contrary to our expectations, responses to valuable outcomes and inhibitions to devalued outcomes displayed similar N2 amplitudes across all discrimination types. Response inhibition typically elicits larger N2 amplitudes than response execution (Enriquez-Geppert et al. 2010; Bekker et al. 2005; Falkenstein et al. 1999), although factors such as increased frequency of nogo/stop trials (Enriquez-Geppert et al. 2010; Bekker et al. 2005; Ramautar et al. 2004) and poor task performance (Falkenstein et al. 1999) have been shown to reduce the amplitude of the nogo N2. Still, it is unlikely that these factors explain the similar N2 amplitudes in the slips-of-action test, given that participants performed well above chance level for all discrimination types, and the proportion of devalued outcomes was kept at 33% throughout the test. Yet the fact that the outcome value of the discriminative stimuli changed thorughout the blocks, i.e. devalued outcomes (nogo) became valuable (go) and vice versa from one block to the next, might be influencing the presentation of the associated N2 components, although our data do not permit clarifying the possible underlying functional mechanism.

In addition to the N2, the ERN in the slips-of-action test was modulated by both correctness (response to valuable outcome vs slip of action) and discrimination type, with dERN amplitude being significantly larger in standard compared to incongruent discriminations. Increased devaluation sensitivity in the slips-of-action test also predicted larger dERN amplitudes, as did better knowledge of the R→O contingencies in the outcome-devaluation test. The ERN is typically associated with erroneous responses and their affective, motivational or evaluative aspects (Proudfit et al. 2013; Aarts et al. 2013; Carbonnell and Falkenstein 2006; Nieuwenhuis et al. 2003), and has been linked to PE (Holroyd and Coles 2002; Alexander and Brown 2011) as well as to conflict monitoring (Botvinick 2007; Botvinick et al. 2001; but see Burle et al. 2008; Steinhauser et al. 2008; Carbonnell and Falkenstein 2006). Therefore, in order to account for the

potential effect of response conflict in our findings, we included the dERN elicited by incongruent discriminations in our analysis, since these are designed to generate response conflict (de Wit et al. 2012b; de Wit et al. 2009), showing that standard and incongruent dERN amplitudes did not significantly covary, thus discarding the possibility that dERN amplitude changes in standard discriminations were due to increased conflict monitoring. Rather they seem to be related to devaluation sensitivity as reflected by the DSI, and therefore to goal-directed control. Indeed, efficient error monitoring and post-error adaptation are essential for goal-directed behavior (Ullsperger et al. 2014), with research showing that patients with lesions to the medial OFC/vmPFC, key regions driving goal-directed behavior in outcome devaluation tasks (de Wit et al. 2012b; de Wit et al. 2009; Valentin et al. 2007), exhibit severely reduced ERN amplitudes with impaired error correction (Turken and Swick 2008). Input from the medial OFC/vmPFC has been considered as a candidate for PE calculation in midbrain DA neurons (Schoenbaum et al. 2009) and these regions are thought to be essential in implementing value-based choices (Henri-Bhargava et al. 2012; Camille et al. 2011; Fellows 2006). Therefore, the increased engagement of mOFC/vmPFC during goal-directed control (de Wit et al. 2009) might result in more negative PE signals being relayed from midbrain to dorsal ACC (Holroyd and Coles 2002) and hence in the observed association between enlarged ERN amplitudes and greater devaluation sensitivity.

In contrast to N2 and ERN, the analyses of the ensuing positivities, P3 and P_E respectively, did not reveal significant interactions with discrimination type. Contrary to our hypothesis, it appears that there was a reduction in P3 amplitude associated to slips of action compared to both responses to valuable outcomes and successful inhibitions to devalued outcomes on all discriminative conditions, although P3 amplitudes in the incongruent condition were overall reduced, as evidenced by the significant main effect of discrimination type. Similarly, the data showed a P_E following slips of action compared to responses to valuable outcomes, but its

amplitude was not influenced by discrimination type and thus equivalent regardless of the amount of goal-directed vs habitual control required. The P3 has been related to attentional processes and working memory updating (Polich 2007; Donchin 1981), while the P_E is widely believed to reflect error awareness (Boldt and Yeung 2015; Steinhauser and Yeung 2010; Endrass et al. 2007; Nieuwenhuis et al. 2001). It has been suggested that both components might be related, given their similar morphology and scalp distribution (Ullsperger et al. 2014; Ridderinkhof et al. 2009; O'Connell et al. 2007; Davies et al. 2001). Both P3 and P_E have been proposed to reflect neurocognitive processes implicated in the conscious processing of the motivational significance of the preceding stimulus or response (Ridderinkhof et al. 2009), with some reaserch suggesting that they might represent the accumulation of evidence that is compared against a criterion in the decision making process (Kelly and O'Connell 2013; O'Connell et al. 2012; Steinhauser and Yeung 2010; O'Connell et al. 2007). Somewhat in line with the current results, a recent study found increased P3 amplitudes associated to goal-directed behavior in a forced-choice RL task (Luque et al. 2017), which might explain why overall P3 amplitudes in the incongruent discrimination, which can only be resolved by the habit system (de Wit et al. 2012b; de Wit et al. 2009), were smaller than in the two conditions that can engage goal-directed control. However, the fact that both the stimulus- and rseponse-locked ERPs associated to the different types of actions (responses to valuable outcomes, inhibitions to devalued outcomes and slips of action) were not modulated by discrimination type could be related to participants having reached near-perfect performance during instrumental learning and having very good knowledge of the O→R contingencies, which could result in similar levels of decisional certainty across discrimination types in the slips-of-action test.

Finally, as expected, our data showed that instrumental learning behavior was unrelated to either behavioral or electrophysiological measures during the slips-of-action test, but we

considered relevant to explore whether electrophysiological signals during learning could predict participants' subsequent tendency towards habitual or goal-directed behavior. The dERN and post-feedback dP3 were selected as potential predictors, since they were modulated by the interaction between discrimination type and response correctness or feedback valence, respectively. The data show that devaluation sensitivity could be predicted by both ERPs from the learning phase, with participants with larger dERN and dP3 amplitudes during learning displaying more goal-directed behavior during the test stage. Previous research has associated larger ERN amplitudes with higher response control (Pailing et al. 2002) and a bias to learn to avoid negative events (Frank et al. 2005), and in the context of outcome evaluation and learning, negative outcomes have been shown to elicit larger P3 amplitudes when these lead to behavioral adjustment in the subsequent trial (Schiffer et al. 2017; Donaldson et al. 2016; Chase et al. 2011). Indeed, these are characteristics that seem essential for goal-directed behavior and could hence be at the core of participants' behavior when confronted to an outcome devaluation setting. Our analyses also show that larger dERN, but not dP3, amplitudes from the instrumental learning stage significantly predicted larger dERN amplitudes during the slips-of-action test. However, the ERPs elicited during learning could not predict the dN2 from the slips-of-action test, once again underscoring how N2 and ERN probably reflect different aspects of performance monitoring (Larson et al. 2014; Yeung and Cohen 2006; Falkenstein et al. 1999). Psychopathology and personality research suggest that variations in ERN amplitude are state-independent and rather related to trait differences (Boksem et al. 2008; Hajcak et al. 2008; Hall et al. 2007; Boksem et al. 2006; Potts et al. 2006; Ruchsow et al. 2005; Moser et al. 2005; Hajcak et al. 2004, 2003; Luu et al. 2000). This is in line with our ERN findings, which show that dERN amplitudes remain stable across tasks in the fabulous fruit game (see also Riesel et al. 2013) and are suggestive of an overarching cognitive control trait.

4 Functional evidence of biased attention towards food stimuli

4.1 Introduction

Motivational items, such as food, appear to have a strong influence on attention. It might be because of its nutritional and hedonic properties, which make it perceptually more salient and thus draw our attention in a bottom-up manner (Castellanos et al. 2009; Robinson and Berridge 1993). It has been previously demonstrated that food-related cues biased attention towards their location as compared to other items within the visual search array, and that this effect was enhanced in a hungry state (Mogg et al. 1998). Previous research has widely investigated the link between attentional bias towards food cues and eating behavior. For instance, one clinical study has established that heightened attention towards food cues may occur in obese individuals due to preoccupation with food intake (Braet and Crombez 2003). In general, an attentional bias towards food cues has been shown in both lean and obese individuals. However, obese individuals have been shown to direct their attention towards food cues stronger than lean individuals, especially in a hungry state (Nijs et al. 2010). In another study, it has been demonstrated that heightened attention towards healthy and unhealthy food cues predicted a decrease and increase in body mass index (BMI), respectively, over a one year period (Calitri et al. 2010).

The attentional bias towards food cues has been previously investigated using the N2pc (an abbreviation of N2-posterior-contralateral) component (Kumar et al. 2016), which is a reliable electrophysiological component indexing the allocation of covert attention in the visual environment (Eimer 1996; Luck and Hillyard 1994b, 1994a). Relative to attended hemifield, N2pc (peak latency between 180 and 300 ms) is typically estimated by taking the voltage difference of contralateral and ipsilateral electrodes (relative to the attended stimulus) located at the posterior scalp (e.g. PO7 and PO8), and the amplitude is generally more negative at the

contralateral electrode than at the ipsilateral electrode (Verleger et al. 2012). Evidence from a source localization study (Hopf et al. 2000) has suggested that N2pc, which arises from parieto-occipital regions, reflects two distinct neural mechanisms: an early shift of attention (180-200 ms) within visual search arrays reflected by a parietal source followed by a later stage of focused attention (220-240 ms) reflected by a source in extrastriate areas of occipital and temporal cortex. Previous studies in both animals and humans have shown the involvement of extrastriate cortex in selective attention, suggesting that this visual area preferentially process the selected information after filtering out the unwanted distracter information available in the visual field (Kastner and Ungerleider 2000; Desimone and Duncan 1995; Tsotsos 1990). In the context of attentional bias towards food cues, hunger enhanced the ERP to food (vs. control stimuli) in a time window of 180-310 ms over posterior sites (Stockburger et al. 2008).

Models of visual attention posit that it can be driven by exogenous and endogenous factors. For example, salient stimuli bias visual attention exogenously to their location in a bottom-up fashion. On the other hand, attention might also volitionally (endogenously) directed to a location in space in a top-down fashion (Hickey et al. 2010; Jonides 1981). Further on a behavioral level, it has been shown that a rapid shift of attention towards task-irrelevant salient stimuli and a slower shift of attention towards task-relevant target stimuli affects response times of participants (Hickey et al. 2010).

In the present study, we used fMRI to assess attentional bias towards food images. A selective attention paradigm with bilateral stimuli was adopted for this study in which one image appeared on the left and other on the right side of the fixation symbol at the same time. Participants were instructed to shift their covert attention either to the left or right side of the fixation symbol and respond when a target appeared on the attended side that was superimposed

on the task-irrelevant images. Four different combinations of bilateral stimuli were used, including a food image on the left and object image on the right side of the fixation symbol, and vice versa. These two combinations of bilateral stimuli were compared with two other bilateral control stimuli, that is, either object or food image appeared on both sides of the fixation symbol. Behaviorally, we hypothesized that participants would make slow responses to targets when a food distracter appeared on the unattended side compared to an object distracter. Regarding functional activity, we hypothesized that a food image that appears on the attended side would induce higher activation in the contralateral extrastriate cortex. Furthermore, a food item that appears on the unattended side would also capture attention and elicit higher activation in the ipsilateral extrastriate cortex relative to attended side.

4.2 Materials and Methods

4.2.1 Participants

Twenty participants were recruited from the student population in Lübeck. Data from 20 participants (Women = 10, age range 18–28 years, $M = 23.55$, $SD = 2.22$) were analyzed in this study. The BMI of the included participants was between 20 and 25 ($M = 22.60$, $SD = 1.84$). All participants were right-handed, had a normal or corrected-to-normal vision, had no history of neurological or psychiatric disorders (self-report), and were not taking any medication at the time. Informed consent was obtained from each participant before conducting the study. Participants were paid for their participation or received course credit.

4.2.2 Stimuli and Procedure

Participants performed a selective attention paradigm (c.f. Heinze et al. 1994, for a similar set-up), which comprised of four experimental blocks of 160 trials. Every single block

approximately lasted for 9 min. Each trial began with the presentation of bilateral stimulus configuration, one image on the left and one on the right side of the fixation symbol (</>), which remained on the screen for 100 ms. However, the fixation symbol (a left or right-pointing arrow) stayed in the middle of the screen throughout the trial. The next trial started after an inter-trial interval of 2.3–3.85 s ($M = 3.06$, $SD = 0.47$). The fixation symbol indicated the side to which participants need to covertly shift their attention. For the first 80 trials, participants paid attention either to the left or right side; whereas for the remaining 80 trials, participants paid attention to the other side. Participants paid attention to the left side at the beginning of two blocks and to the right side at the beginning of the other two. Presentation order was counterbalanced across participants. Initially, at the beginning of each block, the fixation cross appeared in the middle of the screen for 5 s. Following the fixation cross, the message "Pay attention to the left/right side!" appeared in the middle of the screen for 9 s. After the first 80 trials, the message "BREAK!!!" appeared in the middle of the screen for 30 s to give participants some time to rest their eyes. Subsequently, the message "Pay attention to the left/right side!" appeared in the middle of the screen for 9 s.

Throughout the experiment, four combinations of bilateral stimuli were used: (i) food image on the left side/object image on the right side, (ii) object image on the left side/food image on the right side, (iii) object images on both sides, and (iv) food images on both sides. Moreover, green vertical bars were superimposed on the task-irrelevant food and object images, which were presented on the left and right side of the fixation symbol. Twenty percent of the bars on either side were smaller than the standard bars and, if appearing on the attended side, had to be responded to. Sixty percent of the trials contained the standard size vertical bars on both sides. The smaller vertical bar appeared either on the left or right side, but not on both sides at the same time. The participants' task was to fix their eyes at the fixation symbol, shift their covert attention

to the indicated side, and react to smaller bars when they appeared on the attended side using their right index finger. To ensure that participants were fixating on the fixation symbol, a MR compatible high-resolution binocular eye-tracking system was used to monitor their eye gaze. Real-time (1000 Hz sampling) binocular gaze position was determined using an Eyelink 1000 system (SR Research, Ltd., ON, Canada) calibrated using a 9-point grid at the start of each block. This system has a spatial resolution of 0.02° (RMS) and accuracy of (average bias up to) 0.25°.

Participants were instructed to refrain from food and drink, except water, for at least twelve hours before the start of the experiment. All the participants were measured in the morning between 08:00 and 10:00 am. Moreover, participants were not informed in advance that they would see images of food and object while performing the task. The selective attention paradigm was programmed and presented using Presentation software (Neurobehavioral System Inc., Albany, Ca) and visualized on MR compatible goggles inside the scanner.

4.2.3 MR Data Acquisition

Structural and functional imaging were performed using a 3-T Siemens MAGNETOM Skyra scanner (Siemens Healthcare, Erlangen, Germany) at the center for brain behavior and metabolism, University of Lübeck. Functional images were acquired in a simultaneous multi-slice fashion with a gradient-echo EPI sequence (voxel dimensions 3 × 3 × 3 mm, 50 slices, 512 x 512 matrix size, TE = 25 ms, TR = 1.34 s, 70° flip angle, 3 mm slice thickness). Four additional dummy volumes, which were subsequently discarded, were acquired at the beginning of each experimental block to account for T1 equilibrium effects. Further, structural images were acquired using a T1-weighted sequence (voxel dimensions 1 × 1 × 1 mm, 256 × 256 matrix size, TE = 2.44 ms, TR = 1.9 ms, 9° flip angle, 1 mm slice thickness).

4.2.4 Behavioral Data Analysis

To assess behavioral performance during the selective attention task, three-way repeated-measures ANOVA (rmANOVA) with the factors attended side (left, right), attended item (food, object) and distracted item (food, object) was calculated for the response times, that is, the time which participants took to press the button after a small vertical bar appeared on the attended side. Behavioral data were analyzed using IBM SPSS Statistics for Windows, version 22 (IBM Corp., Armonk, N.Y., USA). Degrees of freedom and *p*-values were Huynh-Feldt-corrected when necessary.

4.2.5 fMRI Data Analysis

Data preprocessing and analyses were performed using SPM12 (http://www.fil.ion.ucl.ac.uk/spm/software/spm12/) running on MATLAB R2016b (Mathworks, Natick, US). Slice timing correction for each block was carried out with reference to the middle slice using Fourier phase interpolation. Subsequently, volumes from all four functional blocks were realigned spatially with respect to the first functional volume of the first block using rigid body transformation. In the next step, the mean functional image of the four blocks was then co-registered to the structural image of each subject. Finally, the functional images were spatially normalized to 3 mm isotropic voxels in Montreal Neurological Institute (MNI) space and smoothed with an 8-mm full width at half maximum – FWHM- Gaussian kernel.

For each participant, an event-related design matrix was created containing the conditions of interest: food image on the left side/object image on the right side, object image on the left side/food image on the right side, object images on both sides, and food images on both sides. These conditions of interest were included in the design matrix for the left and right attended side individually. All conditions of interest comprised only trials in which standard vertical bars

superimposed on images presented on the left and right side of the fixation symbol. The trials in which smaller vertical bars were superimposed on either attended or unattended images were included in the design matrix as regressors of no interest. Furthermore, movement parameters estimated from realignment were also introduced as effects of no interest in the design matrix. Low-frequency noise was removed using a high-pass filter (cut-off 128 s). The standard SPM autoregressive AR(1) model was applied, and the onset regressors were convolved with the canonical hemodynamic response function. First-level contrast images were generated using a one-sample t-test for the conditions of interest against the fixation symbols. On the group level, we conducted a three-way rmANOVA with the factors attended side (left, right), attended item (food, object) and distracter item (food, object).

Since three-way rmANOVA neither revealed any main effect nor interaction, we then performed an exploratory analysis to investigate the impact of attended and distracted items on the brain by eliminating the factor attended side. Earlier, it was hypothesized that the experimental conditions of both attended sides might yield similar activations on the brain but in a lateralize manner, therefore we flipped the contrasts of right attended side to increase the statistical power for left attended side. The contrasts were flipped using Imcalc "flipud (X)" function on SPM12. To avoid doubling the degree of freedom on the group-level, the mean contrast of similar left and flipped right side conditions (i.e. food on attended side, food on distracted side, food on both sides, and object on both sides) was estimated for each participant individually.

Finally, a paired sample t-test was carried out on the group-level to compare the following mean contrasts: (i) $Food_{attended\_side}\_Object_{unattended\_side}$ versus $Object_{attended\_side}\_Object_{unattended\_side}$ (henceforth, $Food_{attended} > Object_{attended}$), (ii) $Object_{attended\_side}\_Food_{unattended\_side}$ versus

$Object_{attended\_side}\_Object_{unattended\_side}$ (henceforth, $Food_{unattended} > Object_{unattended}$), (iii) $Food_{attended\_side}\_Object_{unattended\_side}$ versus $Food_{attended\_side}\_Food_{unattended\_side}$ (henceforth, $Object_{unattended\_side} > Food_{unattended}$), and (iv) $Object_{attended\_side}\_Food_{unattended\_side}$ versus $Food_{attended\_side}\_Food_{unattended\_side}$ (henceforth, $Object_{attended} > Food_{attended}$). The main aim of this study was to demonstrate that food stimuli significantly biased attention towards their location as compared to object stimuli and induced contralateral activation. Therefore, instead of carrying out a two-way rmANOVA, we directly compared food in attended and unattended conditions against two control stimuli.

The rmANOVAs were specified as flexible factorial designs in SPM12 with each subject treated as a random effects variable. All main effects, two-way interactions, and comparisons between conditions were investigated using F-contrasts. The three-way interaction was examined using GLM Flex (http://nmr.mgh.harvard.edu/harvardagingbrain/People/AaronSchultz/Aarons_Scripts.html). An uncorrected voxel-level threshold of $p < .005$ was selected for all the analyses, with a family-wise error rate (FWE) corrected threshold of $p < .05$ at the cluster level. This voxel-level threshold was chosen to sufficiently avoid Type I errors while also reducing Types II errors (Lieberman and Cunningham 2009).

4.3 Results

4.3.1 Behavioral Results

A rmANOVA with factors attended side (left, right), attended item (food, object) and unattended item was performed on the response time. This showed a significant main effect of the unattended item, $F(1,19) = 4.82$, $\eta^2_p = 0.21$, $p = .041$. Compared to object items (714±20 ms),

the response time was longer when food items (723±20 ms) appeared on the distracted side. All other effects and interactions were not statistically significant, $p > .05$. The mean reaction time of each condition is shown in Table 4.1.

Condition	Reaction time (ms)
Object on both sides	715.02 (97.84)
Food on the attended side/object on the unattended side	714.07 (94.11)
Object on the attended side/food on the unattended side	728.26 (107.59)
Food on both sides	718.61 (89.13)

Table 4.1 | Behavioral results. Mean (SD) reaction time of each condition.

4.3.2 fMRI Results

Peak regions and coordinates are shown in Table 4.2.

The three-way and two-way rmANOVAs neither revealed any significant effects nor interactions. The paired t-test between attended food and object items exhibited significant activity within contralateral middle occipital and temporal gyrus (Figure 4.1 A); whereas the comparison between unattended food and object items showed significant activity within ipsilateral middle occipital and temporal gyrus, and ipsilateral superior occipital gyrus (Figure 4.1 B). The paired t-test between the attended object and food items, and unattended object and food items revealed no activity in the brain. The activated regions are contralateral and ipsilateral with respect to the left and flipped to the left attended side.

Region	BA	x	y	z	k	Peak *F*	p_{FWE}-value
$Food_{attended} > Object_{attended}$							
Contralat middle occipital gyrus	19	45	-82	8	119	18.5	.010
Contralat middle temporal gyrus	19	51	-68	6	72	14.5	< .05
$Food_{unattended} > Object_{unattended}$							
Ipsilat middle occipital gyrus	19	-45	-82	2	162	26.84	.015
Ipsilat middle temporal gyrus	19	-48	-75	17	72	18.7	< .05
Ipsilat superior occipital gyrus	19	-19	-88	20	12	12.83	< .05
$Object_{attended} > Food_{attended}$							
No significant clusters							
$Object_{unattended} > Food_{unattended}$							
No significant clusters							

Table 4.2 | Whole-brain results for the Paired t-tests. All results are FWE-corrected at the cluster level, $p < .05$. Abbreviations: Contralat: contralateral, Ipsilat: ipsilateral, BA: Brodmann's area and *k*: cluster size. The activated regions are contralateral and ipsilateral concerning the left and flipped to the left attended side.

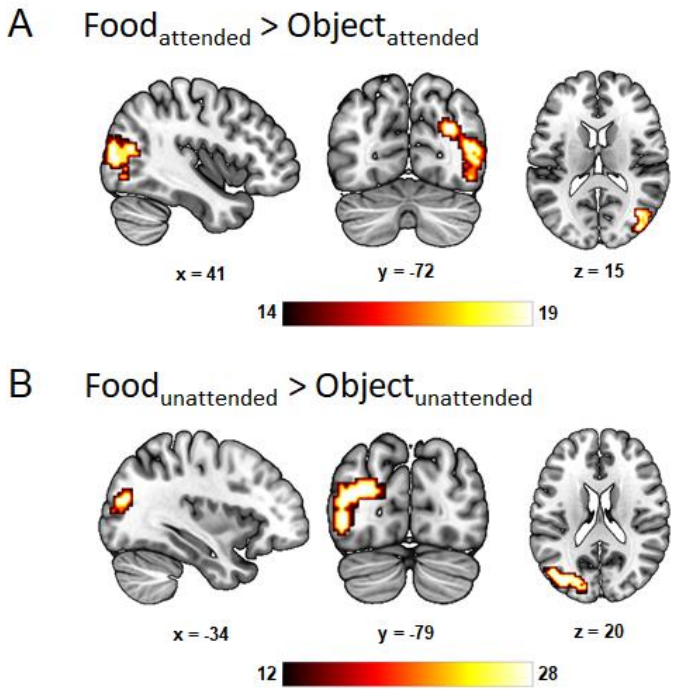

Figure 4.1 | Whole-brain results for the Paired t-tests. The *F*-values are thresholded at $p < .05$ (FWE-corrected for multiple comparisons at the cluster level) and superimposed on a T1-weighted structural MNI template. Significant brain activations in the contrasts (A) $food_{attended} > Object_{attended}$, (B) $Food_{unattended} > Object_{unattended}$

4.4 Discussion

In the current study, we tested the attentional bias towards food-related stimuli. The behavioral data demonstrated no significant difference in response time to targets when food or object appeared on the attended side. However, participants were slower in responding to the target when a food images appeared on the unattended side as compared to an object image. This result is line with previous results suggesting that task-irrelevant salient distracter stimuli attract spatial attention towards their location rapidly resulting in a slower response time to target stimuli (Hickey et al. 2010).

Regarding functional activity, our data revealed significant activity in contralateral and ipsilateral extrastriate areas of occipital and temporal cortices when food images appeared on attended and unattended side, respectively, relative to attended side. These individual activations in the contralateral and ipsilateral cortices are observed when contrasting food in attended and unattended conditions against control stimuli of an object on both sides. However, no activations were found in the whole brain when comparing food in attended or unattended condition against control stimuli of food on both sides.

Extrastriate cortex encompasses a number of distinct cortical areas that subserve different functions during visual perception (Felleman 2009). With regard to visual attention, in particular visuospatial attention, the extrastriate areas implicated in the current study have roughly grouped into two major systems: First, part of the parietal lobes appear to be involved in the control of attention (Corbetta et al. 1993; Posner et al. 1984; Mountcastle et al. 1981) whereas, second, occipitotemporal areas are involved in the implementation of attentional selection (Heinze et al. 1994; Chelazzi et al. 1993; Corbetta et al. 1991; Moran and Desimone 1985). Thus, the parietal lobes may initiate a shift of attention to the location of a salient item such as the food distracters

in the current study (Corbetta et al. 1995) which is followed by further selection implemented in the occipitotemporal region (Heinze et al. 1994). The current experiment thus delivered behavioral and brain imaging evidence for attentional capture by task-irrelevant food pictures. This is in line with our initial hypothesis. Automatic attentional capture by food items seems important for survival of the organism. Indeed, in animals, food cues have been shown to attract attention as well (Brandner 2002). The current experiment also had several shortcomings. The design was complicated leading to a complex three-factor ANOVA analysis and to a rather modest signal to noise ratio. A follow-up experiment should use a simpler setup to investigate the important question of attentional capture by food. Moreover, connectivity analyses should be implemented to look at whether and how the higher visual areas driven in the current experiment by food items are communicating with brain areas involved in assessing the hedonic value of food (see chapter 2 of the current thesis).

5 Summary of findings from food reward-related fMRI study

In summary, we used an associative learning task, in which participants received monetary or food feedback in the form of images, to explore the neural networks underlying food and monetary reward, and their modulation by hunger and satiation. Both food and money engage common reward-related regions, including VS, medial OFC, and amygdala. Food images additionally engage areas of the primary but not secondary gustatory cortex. Our findings are consistent with the view that the SMG plays an important role in integrating both interoceptive and exteroceptive awareness, as it is more sensitive to food stimuli when hungry and to monetary incentives when satiated. Furthermore, the connectivity strength between SMG and VS is regulated flexibly depending on both the metabolic state and the available incentive type.

6 Summary of findings from EEG study on goal-directed and habitual behavior

In summary, we adapted a well-established behavioral and neuroimaging outcome devaluation paradigm to identify the electrophysiological markers of goal-directed vs habitual control. We showed how decreased N2 and increased ERN amplitudes are associated to slips of action in conditions that can be resolved by goal-directed control, with participants that display more sensitivity to devaluation also showing larger N2 decreases and ERN increases. This provides further evidence of the functional dissociation between these two components in instrumental learning contexts, suggesting that the N2 might be linked to conflict monitoring, whereas the ERN likely reflects a RL signal. Furthermore, we show how the ERN and P3 components elicited during instrumental learning can predict subsequent sensitivity to

devaluation, with ERN amplitudes during learning additionally predicting ERN amplitudes associated to slips of action during outcome devaluation. Our data demonstrate that these neurophysiological signals of performance monitoring also correspond to the individual tendency to engage goal-directed vs habitual control, and further emphasize the value of the ERN as an electrophysiological trait.

7 Summary of findings from attention related fMRI study

In summary, we used a selective attention task with bilateral stimuli setup. In that study, we aimed to corroborate previous findings on the N2pc component of the event-related potential, suggesting that salient stimuli significantly bias attention towards their location and evoke contralateral brain activity in secondary visual areas. The behavioral data demonstrated that participants were slower in responding to the target when a food object image appeared on the distracted side. Regarding functional activity, our exploratory analysis revealed significant activity in the contralateral and ipsilateral (with respect to attended side) extrastriate cortex when food stimuli compared to object stimuli appeared on the attended and unattended side, respectively.

8 Future directions

The first fMRI study has certain limitations that might be addressed in the future. Even though the subjective ratings of hunger, satiation and desire to eat implied that the manipulation of the participants' metabolic state was successful, the short duration of the fasting period, only lasting six hours, might explain the absence of a main effect of metabolic state in the fMRI results. We would suggest increasing the fasting period to at least 12 hours and then test the effect of fasting on the brain. Besides, to limit the variance of our observations, the current study only included normal weight men. Previous studies have suggested gender differences in neural activity when exposed to food stimuli (e.g. see review Chao et al. 2017). This suggests that future experiments should also include women as well as lean and obese participants.

Regarding our EEG study, previous studies have highlighted the importance of DA in maintaining the balance between goal-directed and habitual control during outcome devaluation test (San Martín 2012; de Wit et al. 2011). For instance, one behavioral study (de Wit et al. 2012a) has tested the effect of reduced DA in healthy male and female participants and demonstrated that lower DA has no impact on male participants'performance during outcome devaluation test. However, for female participants, it has been shown that lower DA shifted the balance more towards habitual as compared to goal-directed control. In light of these observations, we would suggest conducting an EEG study after reducing DA levels, for example after dietary manipulation (Badawy 2013).

Regarding our third fMRI study, it was already stressed in the discussion of chapter 4 that the selective attention paradigm had a number of short-comings that could be improved in future studies. While our exploratory analysis showed significant activity in contralateral and ipsilateral extrastriate areas when food with a combination of object image appeared on the attended and

unattended side, respectively, the main analysis did not yield significant effects most likely due to an overly complex design. We would suggest repeating the experiment with a simplified set up, capitalizing on well-known behavioral effects such as inhibition of return (Wang et al. 2018).

References

Aarts, K., De Houwer, J., & Pourtois, G. (2013). Erroneous and correct actions have a different affective valence: Evidence from ERPs. *Emotion, 13*(5), 960-973, doi:10.1037/a0032808.

Alexander, W. H., & Brown, J. W. (2011). Medial prefrontal cortex as an action-outcome predictor. [Article]. *Nature Neuroscience, 14*, 1338, doi:10.1038/nn.2921.

Arana, F. S., Parkinson, J. A., Hinton, E., Holland, A. J., Owen, A. M., & Roberts, A. C. (2003). Dissociable Contributions of the Human Amygdala and Orbitofrontal Cortex to Incentive Motivation and Goal Selection. *The Journal of Neuroscience, 23*(29), 9632-9638, doi:10.1523/jneurosci.23-29-09632.2003.

Araujo, H. F., Kaplan, J., Damasio, H., & Damasio, A. (2015). Neural correlates of different self domains. *Brain and Behavior, 5*(12), e00409, doi:10.1002/brb3.409.

Aron, A. R., Robbins, T. W., & Poldrack, R. A. (2014). Inhibition and the right inferior frontal cortex: one decade on. *Trends in cognitive sciences, 18*(4), 177-185, doi:10.1016/j.tics.2013.12.003.

Ashburner, J. (2007). A fast diffeomorphic image registration algorithm. *NeuroImage, 38*(1), 95-113, doi:10.1016/j.neuroimage.2007.07.007.

Badawy, A. A. B. (2013). Appropriate amino acid mixtures for tryptophan depletion and tyrosine/phenylalanine depletion and the safety of long-term amino acid depletion in humans: reply. *Psychopharmacology, 230*(4), 673-676, doi:10.1007/s00213-013-3357-5.

Bakeman, R. (2005). Recommended effect size statistics for repeated measures designs. *Behavior Research Methods, 37*(3), 379-384, doi:10.3758/bf03192707.

Baker, T. E., & Holroyd, C. B. (2011). Dissociated roles of the anterior cingulate cortex in reward and conflict processing as revealed by the feedback error-related negativity and N200. *Biological Psychology, 87*(1), 25-34, doi:10.1016/j.biopsycho.2011.01.010.

Balleine, B. W., Delgado, M. R., & Hikosaka, O. (2007). The Role of the Dorsal Striatum in Reward and Decision-Making. *The Journal of Neuroscience, 27*(31), 8161-8165, doi:10.1523/jneurosci.1554-07.2007.

Balleine, B. W., & O'Doherty, J. P. (2009). Human and Rodent Homologies in Action Control: Corticostriatal Determinants of Goal-Directed and Habitual Action. [Neuropsychopharmacology Reviews]. *Neuropsychopharmacology, 35*, 48, doi:10.1038/npp.2009.131.

Balleine, B. W., & Ostlund, S. B. (2007). Still at the Choice-Point. *Annals of the New York Academy of Sciences, 1104*(1), 147-171, doi:10.1196/annals.1390.006.

Balthasar, N. (2006). Genetic Dissection of Neuronal Pathways Controlling Energy Homeostasis. *Obesity, 14*(S8), 222S-227S, doi:10.1038/oby.2006.313.

Barto, A. G. (1995). Adaptive critics and the basal ganglia. In *Models of information processing in the basal ganglia.* (pp. 215-232, Computational neuroscience.). Cambridge, MA, US: The MIT Press.

Beaver, J. D., Lawrence, A. D., van Ditzhuijzen, J., Davis, M. H., Woods, A., & Calder, A. J. (2006). Individual Differences in Reward Drive Predict Neural Responses to Images of Food. *The Journal of Neuroscience, 26*(19), 5160-5166, doi:10.1523/jneurosci.0350-06.2006.

Bekker, E. M., Kenemans, J. L., & Verbaten, M. N. (2005). Source analysis of the N2 in a cued Go/NoGo task. *Cognitive Brain Research, 22*(2), 221-231, doi:10.1016/j.cogbrainres.2004.08.011.

Benarroch, E. (2006). *Basic Neurosciences with Clinical Applications*: / E.E. Benarroch.

Bermudez, Maria A., Göbel, C., & Schultz, W. (2012). Sensitivity to Temporal Reward Structure in Amygdala Neurons. *Current Biology, 22*(19), 1839-1844, doi:10.1016/j.cub.2012.07.062.

Berns, G. S., McClure, S. M., Pagnoni, G., & Montague, P. R. (2001). Predictability Modulates Human Brain Response to Reward. *The Journal of Neuroscience, 21*(8), 2793-2798, doi:10.1523/jneurosci.21-08-02793.2001.

Binder, M. D., Hirokawa, N., & Windhorst, U. (2009). Encyclopedia of Neuroscience: Springer, Berlin, Heidelberg.

Bjork, J. M., Smith, A. R., Chen, G., & Hommer, D. W. (2010). Adolescents, Adults and Rewards: Comparing Motivational Neurocircuitry Recruitment Using fMRI. *PLOS ONE, 5*(7), e11440, doi:10.1371/journal.pone.0011440.

Blechert, J., Klackl, J., Miedl, S. F., & Wilhelm, F. H. (2016). To eat or not to eat: Effects of food availability on reward system activity during food picture viewing. *Appetite, 99*, 254-261, doi:10.1016/j.appet.2016.01.006.

Block, M. L. (2011). Ventral Tegmental Area of Midbrain. In J. S. Kreutzer, J. DeLuca & B. Caplan (Eds.), Encyclopedia of Clinical Neuropsychology (pp. 2597–2598). New York, NY: Springer.

Boksem, M. A. S., Tops, M., Kostermans, E., & De Cremer, D. (2008). Sensitivity to punishment and reward omission: Evidence from error-related ERP components. *Biological Psychology, 79*(2), 185-192, doi:10.1016/j.biopsycho.2008.04.010.

Boksem, M. A. S., Tops, M., Wester, A. E., Meijman, T. F., & Lorist, M. M. (2006). Error-related ERP components and individual differences in punishment and reward sensitivity. *Brain Research, 1101*(1), 92-101, doi:10.1016/j.brainres.2006.05.004.

Bokura, H., Yamaguchi, S., & Kobayashi, S. (2001). Electrophysiological correlates for response inhibition in a Go/NoGo task. *Clinical Neurophysiology, 112*(12), 2224-2232, doi:10.1016/s1388-2457(01)00691-5.

Boldt, A., & Yeung, N. (2015). Shared Neural Markers of Decision Confidence and Error Detection. *The Journal of Neuroscience, 35*(8), 3478-3484, doi:10.1523/jneurosci.0797-14.2015.

Botvinick, M. M. (2007). Conflict monitoring and decision making: Reconciling two perspectives on anterior cingulate function. *Cognitive, Affective, & Behavioral Neuroscience, 7*(4), 356-366, doi:10.3758/cabn.7.4.356.

Botvinick, M. M., Braver, T. S., Barch, D. M., Carter, C. S., & Cohen, J. D. (2001). Conflict monitoring and cognitive control. *Psychological Review, 108*(3), 624-652, doi:10.1037/0033-295x.108.3.624.

Braet, C., & Crombez, G. (2003). Cognitive Interference Due to Food Cues in Childhood Obesity. *Journal of Clinical Child & Adolescent Psychology, 32*(1), 32-39, doi:10.1207/s15374424jccp3201_04.

Brandner, C. (2002). Perinatal choline treatment modifies the effects of a visuo–spatial attractive cue upon spatial memory in naive adult rats. *Brain Research, 928*(1), 85-95, doi:10.1016/S0006-8993(01)03363-7.

Brett, M., Anton, J., Valabregue, R., & J, P. (2002). Region of interest analysis using an SPM toolbox. *Region of interest analysis using an SPM toolbox, NeuroImage, Vol 16, No 2*.

Brody, A. L., Mandelkern, M. A., Lee, G., Smith, E., Sadeghi, M., Saxena, S., et al. (2004). Attenuation of cue-induced cigarette craving and anterior cingulate cortex activation in bupropion-treated smokers: a preliminary study. *Psychiatry Research: Neuroimaging, 130*(3), 269-281, doi:10.1016/j.pscychresns.2003.12.006.

Bruin, K. J., Wijers, A. A., & van Staveren, A. S. J. (2001). Response priming in a go/nogo task: Do we have to explain the go/nogo N2 effect in terms of response activation instead of inhibition? *Clinical Neurophysiology, 112*(9), 1660-1671, doi:10.1016/s1388-2457(01)00601-0.

Burle, B., Roger, C., Allain, S., Vidal, F., & Hasbroucq, T. (2008). Error Negativity Does Not Reflect Conflict: A Reappraisal of Conflict Monitoring and Anterior Cingulate Cortex Activity. *Journal of Cognitive Neuroscience, 20*(9), 1637-1655, doi:10.1162/jocn.2008.20110 %M 18345992.

Calitri, R., Pothos, E. M., Tapper, K., Brunstrom, J. M., & Rogers, P. J. (2010). Cognitive Biases to Healthy and Unhealthy Food Words Predict Change in BMI. *Obesity, 18*(12), 2282-2287, doi:10.1038/oby.2010.78.

Camara, E., Rodriguez-Fornells, A., & Münte, T. (2009). Functional connectivity of reward processing in the brain. [Original Research]. *Frontiers in Human Neuroscience, 2*(19), doi:10.3389/neuro.09.019.2008.

Camille, N., Griffiths, C. A., Vo, K., Fellows, L. K., & Kable, J. W. (2011). Ventromedial Frontal Lobe Damage Disrupts Value Maximization in Humans. *The Journal of Neuroscience, 31*(20), 7527-7532, doi:10.1523/jneurosci.6527-10.2011.

Carbonnell, L., & Falkenstein, M. (2006). Does the error negativity reflect the degree of response conflict. *Brain Research, 1095*(1), 124-130, doi:10.1016/j.brainres.2006.04.004.

Carter, C. S., & van Veen, V. (2007). Anterior cingulate cortex and conflict detection: An update of theory and data. *Cognitive, Affective, & Behavioral Neuroscience, 7*(4), 367-379, doi:10.3758/cabn.7.4.367.

Castellanos, E. H., Charboneau, E., Dietrich, M. S., Park, S., Bradley, B. P., Mogg, K., et al. (2009). Obese adults have visual attention bias for food cue images: evidence for altered reward system function. [Original Article]. *International Journal Of Obesity, 33*, 1063, doi:10.1038/ijo.2009.138.

Cauda, F., Cavanna, A. E., D'agata, F., Sacco, K., Duca, S., & Geminiani, G. C. (2011). Functional Connectivity and Coactivation of the Nucleus Accumbens: A Combined Functional Connectivity and Structure-Based Meta-analysis. *Journal of Cognitive Neuroscience, 23*(10), 2864-2877, doi:10.1162/jocn.2011.21624.

Chao, A. M., Loughead, J., Bakizada, Z. M., Hopkins, C. M., Geliebter, A., Gur, R. C., et al. (2017). Sex/gender differences in neural correlates of food stimuli: a systematic review of functional neuroimaging studies. *Obesity reviews : an official journal of the International Association for the Study of Obesity, 18*(6), 687-699, doi:10.1111/obr.12527.

Chase, H. W., Swainson, R., Durham, L., Benham, L., & Cools, R. (2011). Feedback-related Negativity Codes Prediction Error but Not Behavioral Adjustment during Probabilistic Reversal Learning. *Journal of Cognitive Neuroscience, 23*(4), 936-946, doi:10.1162/jocn.2010.21456 %M 20146610.

Cheer, J. F., Aragona, B. J., Heien, M. L. A. V., Seipel, A. T., Carelli, R. M., & Wightman, R. M. (2007). Coordinated Accumbal Dopamine Release and Neural Activity Drive Goal-Directed Behavior. *Neuron, 54*(2), 237-244, doi:10.1016/j.neuron.2007.03.021.

Chelazzi, L., Miller, E. K., Duncan, J., & Desimone, R. (1993). A neural basis for visual search in inferior temporal cortex. *Nature, 363*(6427), 345-347, doi:10.1038/363345a0.

Chmielewski, W. X., Mückschel, M., Stock, A.-K., & Beste, C. (2015). The impact of mental workload on inhibitory control subprocesses. *NeuroImage, 112*, 96-104, doi:10.1016/j.neuroimage.2015.02.060.

Cho, Y. T., Ernst, M., & Fudge, J. L. (2013). Cortico–Amygdala–Striatal Circuits Are Organized as Hierarchical Subsystems through the Primate Amygdala. *The Journal of Neuroscience, 33*(35), 14017-14030, doi:10.1523/jneurosci.0170-13.2013.

Cockburn, J., & Holroyd, C. B. (2018). Feedback information and the reward positivity. *International Journal of Psychophysiology, 132*, 243-251, doi:10.1016/j.ijpsycho.2017.11.017.

Corbetta, M., Miezin, F., Dobmeyer, S., Shulman, G., & Petersen, S. (1991). Selective and divided attention during visual discriminations of shape, color, and speed: functional anatomy by positron emission tomography. *The Journal of Neuroscience, 11*(8), 2383-2402, doi:10.1523/jneurosci.11-08-02383.1991.

Corbetta, M., Miezin, F., Shulman, G., & Petersen, S. (1993). A PET study of visuospatial attention. *The Journal of Neuroscience, 13*(3), 1202-1226, doi:10.1523/jneurosci.13-03-01202.1993.

Corbetta, M., Shulman, G. L., Miezin, F. M., & Petersen, S. E. (1995). Superior Parietal Cortex Activation During Spatial Attention Shifts and Visual Feature Conjunction. *Science, 270*(5237), 802-805, doi:10.1126/science.270.5237.802.

Critchley, H. D., Mathias, C. J., & Dolan, R. J. (2002). Fear Conditioning in Humans: The Influence of Awareness and Autonomic Arousal on Functional Neuroanatomy. *Neuron, 33*(4), 653-663, doi:10.1016/S0896-6273(02)00588-3.

Dagher, A. (2012). Functional brain imaging of appetite. *Trends in Endocrinology & Metabolism, 23*(5), 250-260, doi:10.1016/j.tem.2012.02.009.

Daniel, R., & Pollmann, S. (2010). Comparing the Neural Basis of Monetary Reward and Cognitive Feedback during Information-Integration Category Learning. *The Journal of Neuroscience, 30*(1), 47-55, doi:10.1523/jneurosci.2205-09.2010.

Davies, P. L., Segalowitz, S. J., Dywan, J., & Pailing, P. E. (2001). Error-negativity and positivity as they relate to other ERP indices of attentional control and stimulus processing. *Biological Psychology, 56*(3), 191-206, doi:10.1016/s0301-0511(01)00080-1.

Daw, N. D., Gershman, S. J., Seymour, B., Dayan, P., & Dolan, R. J. (2011). Model-based influences on humans' choices and striatal prediction errors. *Neuron, 69*(6), 1204-1215, doi:10.1016/j.neuron.2011.02.027.

Dayan, P. (2009). Goal-directed control and its antipodes. *Neural Networks, 22*(3), 213-219, doi:10.1016/j.neunet.2009.03.004.

de Araujo, I. E. T., Kringelbach, M. L., Rolls, E. T., & Hobden, P. (2003a). Representation of Umami Taste in the Human Brain. *Journal of Neurophysiology, 90*(1), 313-319, doi:10.1152/jn.00669.2002.

de Araujo, I. E. T., Rolls, E. T., Kringelbach, M. L., McGlone, F., & Phillips, N. (2003b). Taste-olfactory convergence, and the representation of the pleasantness of flavour, in the human brain. *European Journal of Neuroscience, 18*(7), 2059-2068, doi:doi:10.1046/j.1460-9568.2003.02915.x.

de Wit, S., Barker, R. A., Dickinson, A. D., & Cools, R. (2011). Habitual versus Goal-directed Action Control in Parkinson Disease. *Journal of Cognitive Neuroscience, 23*(5), 1218-1229, doi:10.1162/jocn.2010.21514 %M 20429859.

de Wit, S., Corlett, P. R., Aitken, M. R., Dickinson, A., & Fletcher, P. C. (2009). Differential Engagement of the Ventromedial Prefrontal Cortex by Goal-Directed and Habitual Behavior toward Food Pictures in Humans. *The Journal of Neuroscience, 29*(36), 11330-11338, doi:10.1523/jneurosci.1639-09.2009.

de Wit, S., Standing, H. R., DeVito, E. E., Robinson, O. J., Ridderinkhof, K. R., Robbins, T. W., et al. (2012a). Reliance on habits at the expense of goal-directed control following dopamine precursor depletion. [journal article]. *Psychopharmacology, 219*(2), 621-631, doi:10.1007/s00213-011-2563-2.

de Wit, S., van de Vijver, I., & Ridderinkhof, K. R. (2014). Impaired acquisition of goal-directed action in healthy aging. *Cognitive, Affective, & Behavioral Neuroscience, 14*(2), 647-658, doi:10.3758/s13415-014-0288-5.

de Wit, S., Watson, P., Harsay, H. A., Cohen, M. X., van de Vijver, I., & Ridderinkhof, K. R. (2012b). Corticostriatal Connectivity Underlies Individual Differences in the Balance between Habitual and Goal-Directed Action Control. *The Journal of Neuroscience, 32*(35), 12066-12075, doi:10.1523/jneurosci.1088-12.2012.

Debener, S., Ullsperger, M., Siegel, M., Fiehler, K., von Cramon, D. Y., & Engel, A. K. (2005). Trial-by-Trial Coupling of Concurrent Electroencephalogram and Functional Magnetic Resonance Imaging Identifies the Dynamics of Performance Monitoring. *The Journal of Neuroscience, 25*(50), 11730-11737, doi:10.1523/jneurosci.3286-05.2005.

Delgado, M. R., Labouliere, C. D., & Phelps, E. A. (2006). Fear of losing money? Aversive conditioning with secondary reinforcers. *Social Cognitive and Affective Neuroscience, 1*(3), 250-259, doi:10.1093/scan/nsl025.

Delgado, M. R., Locke, H. M., Stenger, V. A., & Fiez, J. A. (2003). Dorsal striatum responses to reward and punishment: Effects of valence and magnitude manipulations. [journal article]. *Cognitive, Affective, & Behavioral Neuroscience, 3*(1), 27-38, doi:10.3758/cabn.3.1.27.

Delgado, M. R., Nystrom, L. E., Fissell, C., Noll, D. C., & Fiez, J. A. (2000). Tracking the Hemodynamic Responses to Reward and Punishment in the Striatum. *Journal of Neurophysiology, 84*(6), 3072-3077, doi:10.1152/jn.2000.84.6.3072.

Delorme, A., & Makeig, S. (2004). EEGLAB: an open source toolbox for analysis of single-trial EEG dynamics including independent component analysis. *Journal of neuroscience methods, 134*(1), 9-21, doi:10.1016/j.jneumeth.2003.10.009.

Desimone, R., & Duncan, J. (1995). Neural Mechanisms of Selective Visual Attention. *Annual Review of Neuroscience, 18*(1), 193-222, doi:10.1146/annurev.ne.18.030195.001205.

Dezfouli, A., & Balleine, B. W. (2012). Habits, action sequences and reinforcement learning. *The European journal of neuroscience, 35*(7), 1036-1051, doi:10.1111/j.1460-9568.2012.08050.x.

Dickinson, A., & Balleine, B. W. (1994). Motivational control of goal-directed action. *Animal Learning & Behavior, 22*(1), 1-18, doi:10.3758/bf03199951.

Dickinson, A., & Weiskrantz, L. (1985). Actions and habits: the development of behavioural autonomy. *Philosophical Transactions of the Royal Society of London. B, Biological Sciences, 308*(1135), 67-78, doi:10.1098/rstb.1985.0010.

Dietrich, A., Hollmann, M., Mathar, D., Villringer, A., & Horstmann, A. (2016). Brain regulation of food craving: relationships with weight status and eating behavior. [Original Article]. *International Journal Of Obesity, 40*, 982, doi:10.1038/ijo.2016.28.

DiLeone, R. J. (2009). The influence of leptin on the dopamine system and implications for ingestive behavior. [Review]. *International Journal Of Obesity, 33*, S25, doi:10.1038/ijo.2009.68.

Doherty, J. O., Rolls, E. T., Francis, S., Bowtell, R., & McGlone, F. (2001). Representation of Pleasant and Aversive Taste in the Human Brain. *Journal of Neurophysiology, 85*(3), 1315-1321, doi:10.1152/jn.2001.85.3.1315.

Dolan, Ray J., & Dayan, P. (2013). Goals and Habits in the Brain. *Neuron, 80*(2), 312-325, doi:10.1016/j.neuron.2013.09.007.

Dombrowe, I., Donk, M., & Olivers, C. N. L. (2011). The costs of switching attentional sets. *Attention, Perception, & Psychophysics, 73*(8), 2481-2488, doi:10.3758/s13414-011-0198-3.

Donaldson, K. R., Ait Oumeziane, B., Hélie, S., & Foti, D. (2016). The temporal dynamics of reversal learning: P3 amplitude predicts valence-specific behavioral adjustment. *Physiology & Behavior, 161*, 24-32, doi:10.1016/j.physbeh.2016.03.034.

Donchin, E. (1981). Surprise!… Surprise? *Psychophysiology, 18*(5), 493-513, doi:10.1111/j.1469-8986.1981.tb01815.x.

Donkers, F. C. L., & van Boxtel, G. J. M. (2004). The N2 in go/no-go tasks reflects conflict monitoring not response inhibition. *Brain and Cognition, 56*(2), 165-176, doi:10.1016/j.bandc.2004.04.005.

Draganski, B., Kherif, F., Klöppel, S., Cook, P. A., Alexander, D. C., Parker, G. J. M., et al. (2008). Evidence for Segregated and Integrative Connectivity Patterns in the Human Basal Ganglia. *The Journal of Neuroscience, 28*(28), 7143-7152, doi:10.1523/jneurosci.1486-08.2008.

Eimer, M. (1993). Effects of attention and stimulus probability on ERPs in a Go/Nogo task. *Biological Psychology, 35*(2), 123-138, doi:10.1016/0301-0511(93)90009-W.

Eimer, M. (1996). The N2pc component as an indicator of attentional selectivity. *Electroencephalography and Clinical Neurophysiology, 99*(3), 225-234, doi:10.1016/0013-4694(96)95711-9.

Elliott, R., Newman, J. L., Longe, O. A., & Deakin, J. F. W. (2003). Differential Response Patterns in the Striatum and Orbitofrontal Cortex to Financial Reward in Humans: A Parametric Functional Magnetic Resonance Imaging Study. *The Journal of Neuroscience, 23*(1), 303-307, doi:10.1523/jneurosci.23-01-00303.2003.

Endrass, T., Franke, C., & Kathmann, N. (2005). Error Awareness in a Saccade Countermanding Task. *Journal of Psychophysiology, 19*(4), 275-280, doi:10.1027/0269-8803.19.4.275.

Endrass, T., Reuter, B., & Kathmann, N. (2007). ERP correlates of conscious error recognition: aware and unaware errors in an antisaccade task. *European Journal of Neuroscience, 26*(6), 1714-1720, doi:10.1111/j.1460-9568.2007.05785.x.

Engelmann, J. B., Damaraju, E., Padmala, S., & Pessoa, L. (2009). Combined effects of attention and motivation on visual task performance: transient and sustained motivational effects. [Original Research]. *Frontiers in Human Neuroscience, 3*(4), doi:10.3389/neuro.09.004.2009.

Engelmann, J. B., & Pessoa, L. (2007). Motivation sharpens exogenous spatial attention. *Emotion, 7*(3), 668-674, doi:10.1037/1528-3542.7.3.668.

Enriquez-Geppert, S., Konrad, C., Pantev, C., & Huster, R. J. (2010). Conflict and inhibition differentially affect the N200/P300 complex in a combined go/nogo and stop-signal task. *NeuroImage, 51*(2), 877-887, doi:10.1016/j.neuroimage.2010.02.043.

Erlanson-Albertsson, C. (2005). Appetite regulation and energy balance. *Acta Paediatrica, 94*(s448), 40-41, doi:10.1111/j.1651-2227.2005.tb02128.x.

Falkenstein, M., Hohnsbein, J., Hoormann, J., & Blanke, L. (1991). Effects of crossmodal divided attention on late ERP components. II. Error processing in choice reaction tasks. *Electroencephalography and Clinical Neurophysiology, 78*(6), 447-455, doi:10.1016/0013-4694(91)90062-9.

Falkenstein, M., Hoormann, J., & Hohnsbein, J. (1999). ERP components in Go/Nogo tasks and their relation to inhibition. *Acta psychologica, 101*(2-3), 267-291, doi:10.1016/s0001-6918(99)00008-6.

Faure, A., Haberland, U., Condé, F., & Massioui, N. E. (2005). Lesion to the Nigrostriatal Dopamine System Disrupts Stimulus-Response Habit Formation. *The Journal of Neuroscience, 25*(11), 2771-2780, doi:10.1523/jneurosci.3894-04.2005.

Felleman, D. J. (2009). Extrastriate Visual Cortex. In M. D. Binder, N. Hirokawa, & U. 13 Windhorst (Eds.), Encyclopedia of Neuroscience (pp. 1526-1532). Berlin, Heidelberg: 14 Springer Berlin Heidelberg.

Fellows, L. K. (2006). Deciding how to decide: ventromedial frontal lobe damage affects information acquisition in multi-attribute decision making. *Brain, 129*(4), 944-952, doi:10.1093/brain/awl017.

Felsted, J. A., Ren, X., Chouinard-Decorte, F., & Small, D. M. (2010). Genetically Determined Differences in Brain Response to a Primary Food Reward. *The Journal of Neuroscience, 30*(7), 2428-2432, doi:10.1523/jneurosci.5483-09.2010.

Frank, M. J., Woroch, B. S., & Curran, T. (2005). Error-related negativity predicts reinforcement learning and conflict biases. *Neuron, 47*(4), 495-501, doi:10.1016/j.neuron.2005.06.020.

Frank, S., Laharnar, N., Kullmann, S., Veit, R., Canova, C., Hegner, Y. L., et al. (2010). Processing of food pictures: Influence of hunger, gender and calorie content. *Brain Research, 1350*, 159-166, doi:10.1016/j.brainres.2010.04.030.

Friederich, H.-C., Wu, M., Simon, J. J., & Herzog, W. (2013). Neurocircuit function in eating disorders. *International Journal of Eating Disorders, 46*(5), 425-432, doi:10.1002/eat.22099.

Führer, D., Zysset, S., & Stumvoll, M. (2008). Brain Activity in Hunger and Satiety: An Exploratory Visually Stimulated fMRI Study. *Obesity, 16*(5), 945-950, doi:10.1038/oby.2008.33.

Fujiwara, J., Tobler, P. N., Taira, M., Iijima, T., & Tsutsui, K.-I. (2009). Segregated and Integrated Coding of Reward and Punishment in the Cingulate Cortex. *Journal of Neurophysiology, 101*(6), 3284-3293, doi:10.1152/jn.90909.2008.

Gajewski, P. D., & Falkenstein, M. (2013). Effects of task complexity on ERP components in Go/Nogo tasks. *International Journal of Psychophysiology, 87*(3), 273-278, doi:10.1016/j.ijpsycho.2012.08.007.

Gehring, W. J., & Fencsik, D. E. (2001). Functions of the Medial Frontal Cortex in the Processing of Conflict and Errors. *The Journal of Neuroscience, 21*(23), 9430-9437, doi:10.1523/jneurosci.21-23-09430.2001.

Gehring, W. J., Goss, B., Coles, M. G. H., Meyer, D. E., & Donchin, E. (1993). A Neural System for Error Detection and Compensation. *Psychological Science, 4*(6), 385-390, doi:10.1111/j.1467-9280.1993.tb00586.x.

Gentsch, A., Ullsperger, P., & Ullsperger, M. (2009). Dissociable medial frontal negativities from a common monitoring system for self- and externally caused failure of goal achievement. *NeuroImage, 47*(4), 2023-2030, doi:10.1016/j.neuroimage.2009.05.064.

Gläscher, J., Daw, N., Dayan, P., & O'Doherty, J. P. (2010). States versus rewards: dissociable neural prediction error signals underlying model-based and model-free reinforcement learning. *Neuron, 66*(4), 585-595, doi:10.1016/j.neuron.2010.04.016.

Glazer, J. E., Kelley, N. J., Pornpattananangkul, N., Mittal, V. A., & Nusslock, R. (2018). Beyond the FRN: Broadening the time-course of EEG and ERP components implicated in reward processing. *International Journal of Psychophysiology, 132*, 184-202, doi:10.1016/j.ijpsycho.2018.02.002.

Goldstone, A. P., Prechtl de Hernandez, C. G., Beaver, J. D., Muhammed, K., Croese, C., Bell, G., et al. (2009). Fasting biases brain reward systems towards high-calorie foods. *European Journal of Neuroscience, 30*(8), 1625-1635, doi:10.1111/j.1460-9568.2009.06949.x.

Goto, Y., & Grace, A. A. (2005). Dopaminergic modulation of limbic and cortical drive of nucleus accumbens in goal-directed behavior. [Article]. *Nature Neuroscience, 8*, 805, doi:10.1038/nn1471.

Gottfried, J. A., O'Doherty, J., & Dolan, R. J. (2003). Encoding Predictive Reward Value in Human Amygdala and Orbitofrontal Cortex. *Science, 301*(5636), 1104-1107, doi:10.1126/science.1087919.

Göttlich, M., Beyer, F., & Krämer, U. (2015). BASCO: a toolbox for task-related functional connectivity. [Methods]. *Frontiers in Systems Neuroscience, 9*(126), doi:10.3389/fnsys.2015.00126.

Grace, A. A. (2000). Gating of information flow within the limbic system and the pathophysiology of schizophrenia. *Brain research. Brain research reviews, 31*(2-3), 330-341, doi:10.1016/s0165-0173(99)00049-1.

Greenhouse, I., & Wessel, J. R. (2013). EEG signatures associated with stopping are sensitive to preparation. *Psychophysiology, 50*(9), 900-908, doi:10.1111/psyp.12070.

Grimm, O., Jacob, M. J., Kroemer, N. B., Krebs, L., Vollstädt-Klein, S., Kobiella, A., et al. (2012). The personality trait self-directedness predicts the amygdala's reaction to appetizing cues in fMRI. *Appetite, 58*(3), 1023-1029, doi:10.1016/j.appet.2012.02.007.

Grosbras, M.-H., & Paus, T. (2005). Brain Networks Involved in Viewing Angry Hands or Faces. *Cerebral Cortex, 16*(8), 1087-1096, doi:10.1093/cercor/bhj050.

Gruendler, T. O. J., Ullsperger, M., & Huster, R. J. (2011). Event-Related Potential Correlates of Performance-Monitoring in a Lateralized Time-Estimation Task. *PLOS ONE, 6*(10), e25591, doi:10.1371/journal.pone.0025591.

Haber, S. N. (2011). *Neuroanatomy of Reward: A View from the Ventral Striatum. In: Gottfried JA, editor. Neurobiology of Sensation and Reward. Boca Raton (FL): CRC Press/Taylor & Francis; 2011. Chapter 11.*

Haber, S. N., & Knutson, B. (2010). The reward circuit: linking primate anatomy and human imaging. *Neuropsychopharmacology : official publication of the American College of Neuropsychopharmacology, 35*(1), 4-26, doi:10.1038/npp.2009.129.

Haber, S. N., Lynd-Balta, E., & Spooren, W. P. J. M. (1994). Integrative Aspects of Basal Ganglia Circuitry. In G. Percheron, J. S. McKenzie, & J. Féger (Eds.), *The Basal Ganglia IV: New Ideas and Data on Structure and Function* (pp. 71-80). Boston, MA: Springer US.

Hajcak, G., Franklin, M. E., Foa, E. B., & Simons, R. F. (2008). Increased Error-Related Brain Activity in Pediatric Obsessive-Compulsive Disorder Before and After Treatment. *American Journal of Psychiatry, 165*(1), 116-123, doi:10.1176/appi.ajp.2007.07010143.

Hajcak, G., McDonald, N., & Simons, R. F. (2003). Anxiety and error-related brain activity. *Biological Psychology, 64*(1-2), 77-90, doi:10.1016/s0301-0511(03)00103-0.

Hajcak, G., McDonald, N., & Simons, R. F. (2004). Error-related psychophysiology and negative affect. *Brain and Cognition, 56*(2), 189-197, doi:10.1016/j.bandc.2003.11.001.

Hajcak, G., Moser, J. S., Holroyd, C. B., & Simons, R. F. (2006). The feedback-related negativity reflects the binary evaluation of good versus bad outcomes. *Biological Psychology, 71*(2), 148-154, doi:10.1016/j.biopsycho.2005.04.001.

Hajcak, G., Moser, J. S., Yeung, N., & Simons, R. F. (2005). On the ERN and the significance of errors. *Psychophysiology, 42*(2), 151-160, doi:10.1111/j.1469-8986.2005.00270.x.

Hall, J. R., Bernat, E. M., & Patrick, C. J. (2007). Externalizing Psychopathology and the Error-Related Negativity. *Psychological Science, 18*(4), 326-333, doi:10.1111/j.1467-9280.2007.01899.x.

Haruno, M., & Kawato, M. (2006). Different Neural Correlates of Reward Expectation and Reward Expectation Error in the Putamen and Caudate Nucleus During Stimulus-Action-Reward Association Learning. *Journal of Neurophysiology, 95*(2), 948-959, doi:10.1152/jn.00382.2005.

Heinze, H. J., Mangun, G. R., Burchert, W., Hinrichs, H., Scholz, M., Münte, T. F., et al. (1994). Combined spatial and temporal imaging of brain activity during visual selective attention in humans. *Nature, 372*(6506), 543-546, doi:10.1038/372543a0.

Henri-Bhargava, A., Simioni, A., & Fellows, L. K. (2012). Ventromedial frontal lobe damage disrupts the accuracy, but not the speed, of value-based preference judgments. *Neuropsychologia, 50*(7), 1536-1542, doi:10.1016/j.neuropsychologia.2012.03.006.

Hernandez, L. F., Redgrave, P., & Obeso, J. (2015). Habitual behavior and dopamine cell vulnerability in Parkinson disease. [Opinion]. *Frontiers in Neuroanatomy, 9*(99), doi:10.3389/fnana.2015.00099.

Hickey, C., van Zoest, W., & Theeuwes, J. (2010). The time course of exogenous and endogenous control of covert attention. *Experimental Brain Research, 201*(4), 789-796, doi:10.1007/s00221-009-2094-9.

Hiebert, N. M., Vo, A., Hampshire, A., Owen, A. M., Seergobin, K. N., & MacDonald, P. A. (2014). Striatum in stimulus–response learning via feedback and in decision making. *NeuroImage, 101*, 448-457, doi:10.1016/j.neuroimage.2014.07.013.

Hitchcott, P. K., Quinn, J. J., & Taylor, J. R. (2007). Bidirectional Modulation of Goal-Directed Actions by Prefrontal Cortical Dopamine. *Cerebral Cortex, 17*(12), 2820-2827, doi:10.1093/cercor/bhm010.

Holroyd, C. B., & Coles, M. G. H. (2002). The neural basis of human error processing: Reinforcement learning, dopamine, and the error-related negativity. *Psychological Review, 109*(4), 679-709, doi:10.1037/0033-295x.109.4.679.

Holroyd, C. B., Dien, J., & Coles, M. G. (1998). Error-related scalp potentials elicited by hand and foot movements: evidence for an output-independent error-processing system in humans. *Neuroscience Letters, 242*(2), 65-68, doi:10.1016/s0304-3940(98)00035-4.

Holroyd, C. B., Pakzad-Vaezi, K. L., & Krigolson, O. E. (2008). The feedback correct-related positivity: Sensitivity of the event-related brain potential to unexpected positive feedback. *Psychophysiology, 45*(5), 688-697, doi:10.1111/j.1469-8986.2008.00668.x.

Holroyd, C. B., & Umemoto, A. (2016). The research domain criteria framework: The case for anterior cingulate cortex. *Neuroscience & Biobehavioral Reviews, 71*, 418-443, doi:10.1016/j.neubiorev.2016.09.021.

Hopf, J.-M., Luck, S. J., Girelli, M., Hagner, T., R., G., Scheich, M. H., et al. (2000). Neural Sources of Focused Attention in Visual Search. *Cerebral Cortex, 10*(12), 1233-1241, doi:10.1093/cercor/10.12.1233.

Hübner, R., & Schlösser, J. (2010). Monetary reward increases attentional effort in the flanker task. *Psychonomic Bulletin & Review, 17*(6), 821-826, doi:10.3758/pbr.17.6.821.

Huster, R. J., Enriquez-Geppert, S., Lavallee, C. F., Falkenstein, M., & Herrmann, C. S. (2013). Electroencephalography of response inhibition tasks: Functional networks and cognitive contributions. *International Journal of Psychophysiology, 87*(3), 217-233, doi:10.1016/j.ijpsycho.2012.08.001.

Huys, Q. J. M., Cruickshank, A., & Seriès, P. (2013). Reward-Based Learning, Model-Based and Model-Free. In D. Jaeger, & R. Jung. In E. o. C. N. p. 1-10) (Ed.): New York, NY: Springer New York.

Jacobson, A., Green, E., & Murphy, C. (2010). Age-related functional changes in gustatory and reward processing regions: An fMRI study. *NeuroImage, 53*(2), 602-610, doi:10.1016/j.neuroimage.2010.05.012.

Jenkins, M., Grubert, A., & Eimer, M. (2018). The speed of voluntary and priority-driven shifts of visual attention. *Journal of Experimental Psychology: Human Perception and Performance, 44*(1), 27-37, doi:10.1037/xhp0000438.

Jenkinson, M., Bannister, P., Brady, M., & Smith, S. (2002). Improved Optimization for the Robust and Accurate Linear Registration and Motion Correction of Brain Images. *NeuroImage, 17*(2), 825-841, doi:10.1006/nimg.2002.1132.

Jiang, Y., Kim, S.-i., & Bong, M. (2014). Effects of reward contingencies on brain activation during feedback processing. [Original Research]. *Frontiers in Human Neuroscience, 8*(656), doi:10.3389/fnhum.2014.00656.

Jodo, E., & Kayama, Y. (1992). Relation of a negative ERP component to response inhibition in a Go/No-go task. *Electroencephalography and Clinical Neurophysiology, 82*(6), 477-482, doi:10.1016/0013-4694(92)90054-L.

Joel, D., Niv, Y., & Ruppin, E. (2002). Actor–critic models of the basal ganglia: new anatomical and computational perspectives. *Neural Networks, 15*(4), 535-547, doi:10.1016/S0893-6080(02)00047-3.

Jonides, J. (1981). *Voluntary versus automatic control over the mind's eye's movement.* Paper presented at the Attention and performance IX Proceedings of the ninth international symposium on attention and performance, Jesus college, Cambridge, England, July 13–18 1980.,

Kashkouli Nejad, K., Sugiura, M., Nozawa, T., Kotozaki, Y., Furusawa, Y., Nishino, K., et al. (2015). Supramarginal activity in interoceptive attention tasks. *Neuroscience Letters, 589*, 42-46, doi:10.1016/j.neulet.2015.01.031.

Kastner, S., & Ungerleider, L. G. (2000). Mechanisms of Visual Attention in the Human Cortex. *Annual Review of Neuroscience, 23*(1), 315-341, doi:10.1146/annurev.neuro.23.1.315.

Keen-Rhinehart, E., Ondek, K., & Schneider, J. (2013). Neuroendocrine regulation of appetitive ingestive behavior. [Review]. *Frontiers in Neuroscience, 7*(213), doi:10.3389/fnins.2013.00213.

Kelly, S. P., & O'Connell, R. G. (2013). Internal and External Influences on the Rate of Sensory Evidence Accumulation in the Human Brain. *The Journal of Neuroscience, 33*(50), 19434-19441, doi:10.1523/jneurosci.3355-13.2013.

Killgore, W. D. S., Young, A. D., Femia, L. A., Bogorodzki, P., Rogowska, J., & Yurgelun-Todd, D. A. (2003). Cortical and limbic activation during viewing of high- versus low-calorie foods. *NeuroImage, 19*(4), 1381-1394, doi:10.1016/s1053-8119(03)00191-5.

Kim, M. J., Solomon, K. M., Neta, M., Davis, F. C., Oler, J. A., Mazzulla, E. C., et al. (2016). A face versus non-face context influences amygdala responses to masked fearful eye whites. *Social Cognitive and Affective Neuroscience, 11*(12), 1933-1941, doi:10.1093/scan/nsw110.

Knutson, B., Fong, G. W., Bennett, S. M., Adams, C. M., & Hommer, D. (2003). A region of mesial prefrontal cortex tracks monetarily rewarding outcomes: characterization with rapid event-related fMRI. *NeuroImage, 18*(2), 263-272, doi:10.1016/s1053-8119(02)00057-5.

Knutson, B., & Greer, S. M. (2008). Anticipatory affect: neural correlates and consequences for choice. *Philosophical Transactions of the Royal Society B: Biological Sciences, 363*(1511), 3771-3786, doi:doi:10.1098/rstb.2008.0155.

Knutson, B., Rick, S., Wimmer, G. E., Prelec, D., & Loewenstein, G. (2007). Neural Predictors of Purchases. *Neuron, 53*(1), 147-156, doi:10.1016/j.neuron.2006.11.010.

Knutson, B., Westdorp, A., Kaiser, E., & Hommer, D. (2000). FMRI Visualization of Brain Activity during a Monetary Incentive Delay Task. *NeuroImage, 12*(1), 20-27, doi:10.1006/nimg.2000.0593.

Ko, C.-H., Liu, G.-C., Hsiao, S., Yen, J.-Y., Yang, M.-J., Lin, W.-C., et al. (2009). Brain activities associated with gaming urge of online gaming addiction. *Journal of Psychiatric Research, 43*(7), 739-747, doi:10.1016/j.jpsychires.2008.09.012.

Koch, K., Schachtzabel, C., Wagner, G., Reichenbach, J. R., Sauer, H., & Schlösser, R. (2008). The neural correlates of reward-related trial-and-error learning: An fMRI study with a probabilistic learning task. *Learning & Memory, 15*(10), 728-732, doi:10.1101/lm.1106408.

Koelsch, S. (2012). *Brain and Music*: Wiley-Blackwell.

Kok, A., Ramautar, J. R., De Ruiter, M. B., Band, G. P. H., & Ridderinkhof, K. R. (2004). ERP components associated with successful and unsuccessful stopping in a stop-signal task. *Psychophysiology, 41*(1), 9-20, doi:10.1046/j.1469-8986.2003.00127.x.

Kopp, B., Mattler, U., Goertz, R., & Rist, F. (1996). N2, P3 and the lateralized readiness potential in a nogo task involving selective response priming. *Electroencephalography & Clinical Neurophysiology, 99*(1), 19-27, doi:10.1016/0921-884x(96)95617-9.

Krajbich, I., Hare, T., Bartling, B., Morishima, Y., & Fehr, E. (2015). A Common Mechanism Underlying Food Choice and Social Decisions. *PLOS Computational Biology, 11*(10), e1004371, doi:10.1371/journal.pcbi.1004371.

Krämer, U. M., Cunillera, T., Càmara, E., Marco-Pallarés, J., Cucurell, D., Nager, W., et al. (2007). The Impact of Catechol-O-Methyltransferase and Dopamine D4 Receptor Genotypes on Neurophysiological Markers of Performance Monitoring. *The Journal of Neuroscience, 27*(51), 14190-14198, doi:10.1523/jneurosci.4229-07.2007.

Kringelbach, M. L. (2004). Food for thought: hedonic experience beyond homeostasis in the human brain. *Neuroscience, 126*(4), 807-819, doi:10.1016/j.neuroscience.2004.04.035.

Kringelbach, M. L. (2005). The human orbitofrontal cortex: linking reward to hedonic experience. [Review Article]. *Nature Reviews Neuroscience, 6*, 691, doi:10.1038/nrn1747.

Kringelbach, M. L., de Araujo, I. E. T., & Rolls, E. T. (2004). Taste-related activity in the human dorsolateral prefrontal cortex. *NeuroImage, 21*(2), 781-788, doi:10.1016/j.neuroimage.2003.09.063.

Kringelbach, M. L., O'Doherty, J., Rolls, E. T., & Andrews, C. (2003). Activation of the Human Orbitofrontal Cortex to a Liquid Food Stimulus is Correlated with its Subjective Pleasantness. *Cerebral Cortex, 13*(10), 1064-1071, doi:10.1093/cercor/13.10.1064.

Kringelbach, M. L., & Rolls, E. T. (2004). The functional neuroanatomy of the human orbitofrontal cortex: evidence from neuroimaging and neuropsychology. *Progress in Neurobiology, 72*(5), 341-372, doi:10.1016/j.pneurobio.2004.03.006.

Krug, M. K., & Braver, T. S. (2014). Motivation and cognitive control: Going beyond monetary incentives. *In: Bijleveld E., Aarts H. (eds) The Psychological Science of Money (pp. 137–162). Springer, New York, NY*, doi:10.1007/978-1-4939-0959-9_10.

Kühn, S., & Gallinat, J. (2011). A Quantitative Meta-Analysis on Cue-Induced Male Sexual Arousal. *The Journal of Sexual Medicine, 8*(8), 2269-2275, doi:10.1111/j.1743-6109.2011.02322.x.

Kumar, S., Higgs, S., Rutters, F., & Humphreys, G. W. (2016). Biased towards food: Electrophysiological evidence for biased attention to food stimuli. *Brain and Cognition, 110*, 85-93, doi:10.1016/j.bandc.2016.04.007.

Larson, M. J., Clayson, P. E., & Baldwin, S. A. (2012). Performance monitoring following conflict: internal adjustments in cognitive control? *Neuropsychologia, 50*(3), 426-433, doi:10.1016/j.neuropsychologia.2011.12.021.

Larson, M. J., Clayson, P. E., & Clawson, A. (2014). Making sense of all the conflict: A theoretical review and critique of conflict-related ERPs. *International Journal of Psychophysiology, 93*(3), 283-297, doi:10.1016/j.ijpsycho.2014.06.007.

Lehéricy, S., Ducros, M., Van De Moortele, P.-F., Francois, C., Thivard, L., Poupon, C., et al. (2004). Diffusion tensor fiber tracking shows distinct corticostriatal circuits in humans. *Annals of Neurology, 55*(4), 522-529, doi:10.1002/ana.20030.

Leidy, H. J., Lepping, R. J., Savage, C. R., & Harris, C. T. (2011). Neural responses to visual food stimuli after a normal vs. higher protein breakfast in breakfast-skipping teens: a pilot fMRI study. *Obesity (Silver Spring, Md.), 19*(10), 2019-2025, doi:10.1038/oby.2011.108.

Lieberman, M. D., & Cunningham, W. A. (2009). Type I and Type II error concerns in fMRI research: re-balancing the scale. *Social Cognitive and Affective Neuroscience, 4*(4), 423-428, doi:10.1093/scan/nsp052.

Liljeholm, M., Dunne, S., & O'Doherty, J. P. (2014). Anterior Insula Activity Reflects the Effects of Intentionality on the Anticipation of Aversive Stimulation. *The Journal of Neuroscience, 34*(34), 11339-11348, doi:10.1523/jneurosci.1126-14.2014.

Liljeholm, M., Dunne, S., & O'Doherty, J. P. (2015). Differentiating neural systems mediating the acquisition vs. expression of goal-directed and habitual behavioral control. *European Journal of Neuroscience, 41*(10), 1358-1371, doi:10.1111/ejn.12897.

Liotti, M., Pliszka, S. R., Perez, R., Kothmann, D., & Woldorff, M. G. (2005). Abnormal Brain Activity Related to Performance Monitoring and Error Detection in Children with ADHD. *Cortex, 41*(3), 377-388, doi:10.1016/S0010-9452(08)70274-0.

Lopez-Calderon, J., & Luck, S. J. (2014). ERPLAB: an open-source toolbox for the analysis of event-related potentials. [Technology Report]. *Frontiers in Human Neuroscience, 8*(213), doi:10.3389/fnhum.2014.00213.

Luck, S. J., Girelli, M., McDermott, M. T., & Ford, M. A. (1997). Bridging the Gap between Monkey Neurophysiology and Human Perception: An Ambiguity Resolution Theory of Visual Selective Attention. *Cognitive Psychology, 33*(1), 64-87, doi:10.1006/cogp.1997.0660.

Luck, S. J., & Hillyard, S. A. (1994a). Electrophysiological correlates of feature analysis during visual search. *Psychophysiology, 31*(3), 291-308, doi:10.1111/j.1469-8986.1994.tb02218.x.

Luck, S. J., & Hillyard, S. A. (1994b). Spatial filtering during visual search: Evidence from human electrophysiology. *Journal of Experimental Psychology: Human Perception and Performance, 20*(5), 1000-1014, doi:10.1037/0096-1523.20.5.1000.

Luque, D., Beesley, T., Morris, R. W., Jack, B. N., Griffiths, O., Whitford, T. J., et al. (2017). Goal-Directed and Habit-Like Modulations of Stimulus Processing during Reinforcement Learning. *The Journal of Neuroscience, 37*(11), 3009-3017, doi:10.1523/jneurosci.3205-16.2017.

Luu, P., Collins, P., & Tucker, D. M. (2000). Mood, personality, and self-monitoring: Negative affect and emotionality in relation to frontal lobe mechanisms of error monitoring. *Journal of Experimental Psychology: General, 129*(1), 43-60, doi:10.1037/0096-3445.129.1.43.

Luus, B. M., Van Snellenberg, J. X., & Liotti, M. (2007). To stop or not to stop: A high spatio-temporal resolution study of response inhibition using MEG. *International Congress Series, 1300*, 425-428, doi:10.1016/j.ics.2007.03.016.

Maheux, M., & Jolicœur, P. (2017). Differential engagement of attention and visual working memory in the representation and evaluation of the number of relevant targets and their spatial relations: Evidence from the N2pc and SPCN. *Biological Psychology, 125*, 28-35, doi:10.1016/j.biopsycho.2017.01.011.

Mannella, F., Gurney, K., & Baldassarre, G. (2013). The nucleus accumbens as a nexus between values and goals in goal-directed behavior: a review and a new hypothesis. [Hypothesis and Theory]. *Frontiers in Behavioral Neuroscience, 7*(135), doi:10.3389/fnbeh.2013.00135.

McNamee, D., Liljeholm, M., Zika, O., & O'Doherty, J. P. (2015). Characterizing the Associative Content of Brain Structures Involved in Habitual and Goal-Directed Actions in Humans: A Multivariate fMRI Study. *The Journal of Neuroscience, 35*(9), 3764-3771, doi:10.1523/jneurosci.4677-14.2015.

Metereau, E., & Dreher, J.-C. (2012). Cerebral Correlates of Salient Prediction Error for Different Rewards and Punishments. *Cerebral Cortex, 23*(2), 477-487, doi:10.1093/cercor/bhs037.

Miltner, W. H. R., Braun, C. H., & Coles, M. G. H. (1997). Event-Related Brain Potentials Following Incorrect Feedback in a Time-Estimation Task: Evidence for a "Generic" Neural System for Error Detection. *Journal of Cognitive Neuroscience, 9*(6), 788-798, doi:10.1162/jocn.1997.9.6.788.

Mogenson, G. J., Jones, D. L., & Yim, C. Y. (1980). From motivation to action: Functional interface between the limbic system and the motor system. *Progress in Neurobiology, 14*(2), 69-97, doi:10.1016/0301-0082(80)90018-0.

Mogg, K., Bradley, B. P., Hyare, H., & Lee, S. (1998). Selective attention to food-related stimuli in hunger: Are attentional biases specific to emotional and psychopathological states, or are they also found in normal drive states? *Behaviour Research and Therapy, 36*(2), 227-237, doi:10.1016/s0005-7967(97)00062-4.

Mohanty, A., Gitelman, D. R., Mesulam, M. M., & Small, D. M. (2008). The Spatial Attention Network Interacts with Limbic and Monoaminergic Systems to Modulate Motivation-Induced Attention Shifts. *Cerebral Cortex, 18*(11), 2604-2613, doi:10.1093/cercor/bhn021.

Moore, T., & Zirnsak, M. (2017). Neural Mechanisms of Selective Visual Attention. *Annual Review of Psychology, 68*(1), 47-72, doi:10.1146/annurev-psych-122414-033400.

Moran, J., & Desimone, R. (1985). Selective attention gates visual processing in the extrastriate cortex. *Science, 229*(4715), 782-784, doi:10.1126/science.4023713.

Morris, J. S., & Dolan, R. J. (2001). Involvement of Human Amygdala and Orbitofrontal Cortex in Hunger-Enhanced Memory for Food Stimuli. *The Journal of Neuroscience, 21*(14), 5304-5310, doi:10.1523/jneurosci.21-14-05304.2001.

Moser, J. S., Hajcak, G., & Simons, R. F. (2005). The effects of fear on performance monitoring and attentional allocation. *Psychophysiology, 42*(3), 261-268, doi:10.1111/j.1469-8986.2005.00290.x.

Moser, J. S., & Simons, R. F. (2009). The neural consequences of flip-flopping: The feedback-related negativity and salience of reward prediction. *Psychophysiology, 46*(2), 313-320, doi:10.1111/j.1469-8986.2008.00760.x.

Mountcastle, V., Andersen, R., & Motter, B. (1981). *The Influence of Attentive Fixation upon the Excitability of the Light-Sensitive Neurons of the Posterior Parietal Cortex* (Vol. 1).

Murray, E. A. (2007). The amygdala, reward and emotion. *Trends in cognitive sciences, 11*(11), 489-497, doi:10.1016/j.tics.2007.08.013.

Nestler, E. J., & Lutter, M. (2009). Homeostatic and Hedonic Signals Interact in the Regulation of Food Intake. *The Journal of Nutrition, 139*(3), 629-632, doi:10.3945/jn.108.097618.

Nieuwenhuis, S., Heslenfeld, D. J., von Geusau, N. J. A., Mars, R. B., Holroyd, C. B., & Yeung, N. (2005). Activity in human reward-sensitive brain areas is strongly context dependent. *NeuroImage, 25*(4), 1302-1309, doi:10.1016/j.neuroimage.2004.12.043.

Nieuwenhuis, S., Holroyd, C. B., Mol, N., & Coles, M. G. H. (2004). Reinforcement-related brain potentials from medial frontal cortex: Origins and functional significance. *Neuroscience and Biobehavioral Reviews, 28*(4), 441-448, doi:10.1016/j.neubiorev.2004.05.003.

Nieuwenhuis, S., Ridderinkhof, K. R., Blom, J., Band, G. P. H., & Kok, A. (2001). Error-related brain potentials are differentially related to awareness of response errors: Evidence from an antisaccade task. *Psychophysiology, 38*(5), 752-760, doi:10.1111/1469-8986.3850752.

Nieuwenhuis, S., Yeung, N., van den Wildenberg, W., & Ridderinkhof, K. R. (2003). Electrophysiological correlates of anterior cingulate function in a go/no-go task: Effects of response conflict and trial type frequency. *Cognitive, Affective, & Behavioral Neuroscience, 3*(1), 17-26, doi:10.3758/cabn.3.1.17.

Nijs, I. M. T., Muris, P., Euser, A. S., & Franken, I. H. A. (2010). Differences in attention to food and food intake between overweight/obese and normal-weight females under conditions of hunger and satiety. *Appetite, 54*(2), 243-254, doi:10.1016/j.appet.2009.11.004.

Nuwer, M. R., Comi, G., Emerson, R., Fuglsang-Frederiksen, A., Guérit, J. M., Hinrichs, H., et al. (1998). IFCN standards for digital recording of clinical EEG. International Federation of Clinical Neurophysiology. *Electroencephalography and Clinical Neurophysiology, 106*(3), 259-261, doi:10.1016/s0013-4694(97)00106-5.

O'Connell, R. G., Dockree, P. M., Bellgrove, M. A., Kelly, S. P., Hester, R., Garavan, H., et al. (2007). The role of cingulate cortex in the detection of errors with and without awareness: a high-density electrical mapping study. *European Journal of Neuroscience, 25*(8), 2571-2579, doi:10.1111/j.1460-9568.2007.05477.x.

O'Connell, R. G., Dockree, P. M., & Kelly, S. P. (2012). A supramodal accumulation-to-bound signal that determines perceptual decisions in humans. [Article]. *Nature Neuroscience, 15*, 1729, doi:10.1038/nn.3248.

O'Doherty, J., Critchley, H., Deichmann, R., & Dolan, R. J. (2003). Dissociating Valence of Outcome from Behavioral Control in Human Orbital and Ventral Prefrontal Cortices. *The Journal of Neuroscience, 23*(21), 7931-7939, doi:10.1523/jneurosci.23-21-07931.2003.

O'Doherty, J., Dayan, P., Schultz, J., Deichmann, R., Friston, K., & Dolan, R. J. (2004). Dissociable Roles of Ventral and Dorsal Striatum in Instrumental Conditioning. *Science, 304*(5669), 452-454, doi:10.1126/science.1094285.

Oliveira-Maia, A. J., Roberts, C. D., Simon, S. A., & Nicolelis, M. A. L. (2011). Gustatory and reward brain circuits in the control of food intake. In J. D. Pickard, N. Akalan, V. Benes, C. Di Rocco, V. V. Dolenc, J. L. Antunes, et al. (Eds.), *Advances and Technical Standards in Neurosurgery* (pp. 31-59). Vienna: Springer Vienna.

Overbeek, T. J. M., Nieuwenhuis, S., & Ridderinkhof, K. R. (2005). Dissociable Components of Error Processing. *Journal of Psychophysiology, 19*(4), 319-329, doi:10.1027/0269-8803.19.4.319.

Pailing, P. E., Segalowitz, S. J., Dywan, J., & Davies, P. L. (2002). Error negativity and response control. *Psychophysiology, 39*(2), 198-206, doi:10.1111/1469-8986.3920198.

Palminteri, S., Justo, D., Jauffret, C., Pavlicek, B., Dauta, A., Delmaire, C., et al. (2012). Critical Roles for Anterior Insula and Dorsal Striatum in Punishment-Based Avoidance Learning. *Neuron, 76*(5), 998-1009, doi:10.1016/j.neuron.2012.10.017.

Pishnamazi, M., Tafakhori, A., Loloee, S., Modabbernia, A., Aghamollaii, V., Bahrami, B., et al. (2016). Attentional bias towards and away from fearful faces is modulated by developmental amygdala damage. *Cortex; a journal devoted to the study of the nervous system and behavior, 81*, 24-34, doi:10.1016/j.cortex.2016.04.012.

Plassmann, H., O'Doherty, J., Shiv, B., & Rangel, A. (2008). Marketing actions can modulate neural representations of experienced pleasantness. *Proceedings of the National Academy of Sciences, 105*(3), 1050-1054, doi:10.1073/pnas.0706929105.

Plata-Salamán, C. R. (1991). Regulation of Hunger and Satiety in Man. *Digestive Diseases, 9*(5), 253-268, doi:10.1159/000171310.

Polich, J. (2007). Updating p300: An integrative theory of P3a and P3b. *Clinical Neurophysiology, 118*(10), 2128-2148, doi:10.1016/j.clinph.2007.04.019.

Porubská, K., Veit, R., Preissl, H., Fritsche, A., & Birbaumer, N. (2006). Subjective feeling of appetite modulates brain activity: An fMRI study. *NeuroImage, 32*(3), 1273-1280, doi:10.1016/j.neuroimage.2006.04.216.

Posner, M., Walker, J., Friedrich, F., & Rafal, R. (1984). Effects of parietal injury on covert orienting of attention. *The Journal of Neuroscience, 4*(7), 1863-1874, doi:10.1523/jneurosci.04-07-01863.1984.

Potts, G. F., George, M. R. M., Martin, L. E., & Barratt, E. S. (2006). Reduced punishment sensitivity in neural systems of behavior monitoring in impulsive individuals. *Neuroscience Letters, 397*(1-2), 130-134, doi:10.1016/j.neulet.2005.12.003.

Pritchard, T. C., Macaluso, D. A., & Eslinger, P. J. (1999). Taste perception in patients with insular cortex lesions. *Behavioral Neuroscience, 113*(4), 663-671, doi:10.1037/0735-7044.113.4.663.

Proudfit, G. (2015). The reward positivity: From basic research on reward to a biomarker for depression. *Psychophysiology, 52*(4), 449-459, doi:10.1111/psyp.12370.

Proudfit, G., Inzlicht, M., & Mennin, D. (2013). Anxiety and error monitoring: the importance of motivation and emotion. [Opinion]. *Frontiers in Human Neuroscience, 7*(636), doi:10.3389/fnhum.2013.00636.

Pruim, R. H. R., Mennes, M., Buitelaar, J. K., & Beckmann, C. F. (2015a). Evaluation of ICA-AROMA and alternative strategies for motion artifact removal in resting state fMRI. *NeuroImage, 112*, 278-287, doi:10.1016/j.neuroimage.2015.02.063.

Pruim, R. H. R., Mennes, M., van Rooij, D., Llera, A., Buitelaar, J. K., & Beckmann, C. F. (2015b). ICA-AROMA: A robust ICA-based strategy for removing motion artifacts from fMRI data. *NeuroImage, 112*, 267-277, doi:10.1016/j.neuroimage.2015.02.064.

Pursey, K. M., Stanwell, P., Callister, R. J., Brain, K., Collins, C. E., & Burrows, T. L. (2014). Neural Responses to Visual Food Cues According to Weight Status: A Systematic Review of Functional Magnetic Resonance Imaging Studies. [Review]. *Frontiers in Nutrition, 1*(7), doi:10.3389/fnut.2014.00007.

Ramautar, J. R., Kok, A., & Ridderinkhof, K. R. (2004). Effects of stop-signal probability in the stop-signal paradigm: The N2/P3 complex further validated. *Brain and Cognition, 56*(2), 234-252, doi:10.1016/j.bandc.2004.07.002.

Ramirez, D. R., & Savage, L. M. (2007). Differential involvement of the basolateral amygdala, orbitofrontal cortex, and nucleus accumbens core in the acquisition and use of reward expectancies. *Behavioral Neuroscience, 121*(5), 896-906, doi:10.1037/0735-7044.121.5.896.

Randall, W. M., & Smith, J. L. (2011). Conflict and inhibition in the cued-Go/NoGo task. *Clinical Neurophysiology, 122*(12), 2400-2407, doi:10.1016/j.clinph.2011.05.012.

Reber, J., Feinstein, J. S., O'Doherty, J. P., Liljeholm, M., Adolphs, R., & Tranel, D. (2017). Selective impairment of goal-directed decision-making following lesions to the human ventromedial prefrontal cortex. *Brain, 140*(6), 1743-1756, doi:10.1093/brain/awx105.

Ridderinkhof, K. R., Forstmann, B. U., Wylie, S. A., Burle, B., & van den Wildenberg, W. P. M. (2011). Neurocognitive mechanisms of action control: resisting the call of the Sirens. *Wiley Interdisciplinary Reviews: Cognitive Science, 2*(2), 174-192, doi:10.1002/wcs.99.

Ridderinkhof, K. R., Ramautar, J. R., & Wijnen, J. G. (2009). To PE or not to PE: A P3-like ERP component reflecting the processing of response errors. *Psychophysiology, 46*(3), 531-538, doi:10.1111/j.1469-8986.2009.00790.x.

Riesel, A., Weinberg, A., Endrass, T., Meyer, A., & Hajcak, G. (2013). The ERN is the ERN is the ERN? Convergent validity of error-related brain activity across different tasks. *Biological Psychology, 93*(3), 377-385, doi:10.1016/j.biopsycho.2013.04.007.

Rietdijk, W. J. R., Franken, I. H. A., & Thurik, A. R. (2014). Internal Consistency of Event-Related Potentials Associated with Cognitive Control: N2/P3 and ERN/Pe. *PLOS ONE, 9*(7), e102672, doi:10.1371/journal.pone.0102672.

Rissman, J., Gazzaley, A., & D'Esposito, M. (2004). Measuring functional connectivity during distinct stages of a cognitive task. *NeuroImage, 23*(2), 752-763, doi:10.1016/j.neuroimage.2004.06.035.

Robbins, T. W., & Everitt, B. J. (1992). Functions of dopamine in the dorsal and ventral striatum. *Seminars in Neuroscience, 4*(2), 119-127, doi:10.1016/1044-5765(92)90010-Y.

Robinson, T. E., & Berridge, K. C. (1993). The neural basis of drug craving: An incentive-sensitization theory of addiction. *Brain Research Reviews, 18*(3), 247-291, doi:10.1016/0165-0173(93)90013-p.

Roche, R. A. P., Garavan, H., Foxe, J. J., & O'Mara, S. M. (2005). Individual differences discriminate event-related potentials but not performance during response inhibition. *Experimental Brain Research, 160*(1), 60-70, doi:10.1007/s00221-004-1985-z.

Rolls, E. T. (1999). *The Brain and Emotion*: Oxford University Press.

Rolls, E. T. (2000). The Orbitofrontal Cortex and Reward. *Cerebral Cortex, 10*(3), 284-294, doi:10.1093/cercor/10.3.284.

Rolls, E. T. (2006). Brain mechanisms underlying flavour and appetite. *Philosophical Transactions of the Royal Society B: Biological Sciences, 361*(1471), 1123-1136, doi:10.1098/rstb.2006.1852.

Rolls, E. T. (2008). Functions of the orbitofrontal and pregenual cingulate cortex in taste, olfaction, appetite and emotion. *Acta Physiologica Hungarica, 95*(2), 131-164, doi:10.1556/APhysiol.95.2008.2.1.

Rolls, E. T. (2016). Functions of the anterior insula in taste, autonomic, and related functions. *Brain and Cognition, 110*, 4-19, doi:10.1016/j.bandc.2015.07.002.

Rolls, E. T., & McCabe, C. (2007). Enhanced affective brain representations of chocolate in cravers vs. non-cravers. *European Journal of Neuroscience, 26*(4), 1067-1076, doi:doi:10.1111/j.1460-9568.2007.05724.x.

Rolls, E. T., Yaxley, S., & Sienkiewicz, Z. J. (1990). Gustatory responses of single neurons in the caudolateral orbitofrontal cortex of the macaque monkey. *Journal of Neurophysiology, 64*(4), 1055-1066, doi:10.1152/jn.1990.64.4.1055.

Ruchsow, M., Spitzer, M., Grön, G., Grothe, J., & Kiefer, M. (2005). Error processing and impulsiveness in normals: Evidence from event-related potentials. *Cognitive Brain Research, 24*(2), 317-325, doi:10.1016/j.cogbrainres.2005.02.003.

Ryan, R. M., & Deci, E. L. (2000). Intrinsic and Extrinsic Motivations: Classic Definitions and New Directions. *Contemporary Educational Psychology, 25*(1), 54-67, doi:10.1006/ceps.1999.1020.

San Martín, R. (2012). Event-related potential studies of outcome processing and feedback-guided learning. [Review]. *Frontiers in Human Neuroscience, 6*(304), doi:10.3389/fnhum.2012.00304.

Saper, C. B., Chou, T. C., & Elmquist, J. K. (2002). The Need to Feed: Homeostatic and Hedonic Control of Eating. *Neuron, 36*(2), 199-211, doi:10.1016/S0896-6273(02)00969-8.

Schienle, A., Schäfer, A., Hermann, A., & Vaitl, D. (2009). Binge-Eating Disorder: Reward Sensitivity and Brain Activation to Images of Food. *Biological Psychiatry, 65*(8), 654-661, doi:10.1016/j.biopsych.2008.09.028.

Schiffer, A.-M., Siletti, K., Waszak, F., & Yeung, N. (2017). Adaptive behaviour and feedback processing integrate experience and instruction in reinforcement learning. *NeuroImage, 146*, 626-641, doi:10.1016/j.neuroimage.2016.08.057.

Schmajuk, M., Liotti, M., Busse, L., & Woldorff, M. G. (2006). Electrophysiological activity underlying inhibitory control processes in normal adults. *Neuropsychologia, 44*(3), 384-395, doi:10.1016/j.neuropsychologia.2005.06.005.

Schmidt, R. F., Lüthold, P., Kittel, R., Tetzlaff, A., & Hilbert, A. (2016). Visual attentional bias for food in adolescents with binge-eating disorder. *Journal of Psychiatric Research, 80*, 22-29, doi:10.1016/j.jpsychires.2016.05.016.

Schoenbaum, G., Roesch, M. R., Stalnaker, T. A., & Takahashi, Y. K. (2009). A new perspective on the role of the orbitofrontal cortex in adaptive behaviour. [Perspective]. *Nature Reviews Neuroscience, 10*, 885, doi:10.1038/nrn2753.

Schultz, W. (2002). Getting Formal with Dopamine and Reward. *Neuron, 36*(2), 241-263, doi:10.1016/s0896-6273(02)00967-4.

Schultz, W. (2015). Neuronal Reward and Decision Signals: From Theories to Data. *Physiological Reviews, 95*(3), 853-951, doi:10.1152/physrev.00023.2014.

Schultz, W., Dayan, P., & Montague, P. R. (1997). A Neural Substrate of Prediction and Reward. *Science, 275*(5306), 1593-1599, doi:10.1126/science.275.5306.1593.

Schur, E. A., Kleinhans, N. M., Goldberg, J., Buchwald, D., Schwartz, M. W., & Maravilla, K. (2009). Activation in brain energy regulation and reward centers by food cues varies with choice of visual stimulus. *International journal of obesity (2005), 33*(6), 653-661, doi:10.1038/ijo.2009.56.

Schwartz, M. W., Woods, S. C., Porte Jr, D., Seeley, R. J., & Baskin, D. G. (2000). Central nervous system control of food intake. *Nature, 404*, 661, doi:10.1038/35007534.

Sescousse, G., Caldú, X., Segura, B., & Dreher, J.-C. (2013). Processing of primary and secondary rewards: A quantitative meta-analysis and review of human functional neuroimaging studies. *Neuroscience & Biobehavioral Reviews, 37*(4), 681-696, doi:10.1016/j.neubiorev.2013.02.002.

Simmons, W. K., Martin, A., & Barsalou, L. W. (2005). Pictures of Appetizing Foods Activate Gustatory Cortices for Taste and Reward. *Cerebral Cortex, 15*(10), 1602-1608, doi:10.1093/cercor/bhi038.

Simon, J. J., Skunde, M., Wu, M., Schnell, K., Herpertz, S. C., Bendszus, M., et al. (2014). Neural dissociation of food- and money-related reward processing using an abstract incentive delay task. *Social Cognitive and Affective Neuroscience, 10*(8), 1113-1120, doi:10.1093/scan/nsu162.

Simon, J. J., Wetzel, A., Sinno, M. H., Skunde, M., Bendszus, M., Preissl, H., et al. (2017). Integration of homeostatic signaling and food reward processing in the human brain. *JCI Insight, 2*(15), doi:10.1172/jci.insight.92970.

Small, D. M., Gregory, M. D., Mak, Y. E., Gitelman, D., Mesulam, M. M., & Parrish, T. (2003). Dissociation of Neural Representation of Intensity and Affective Valuation in Human Gustation. *Neuron, 39*(4), 701-711, doi:10.1016/s0896-6273(03)00467-7.

Smith, S. M. (2002). Fast robust automated brain extraction. *Human Brain Mapping, 17*(3), 143-155, doi:10.1002/hbm.10062.

Solbakk, A.-K., Funderud, I., Løvstad, M., Endestad, T., Meling, T., Lindgren, M., et al. (2014). Impact of Orbitofrontal Lesions on Electrophysiological Signals in a Stop Signal Task. *Journal of Cognitive Neuroscience, 26*(7), 1528-1545, doi:10.1162/jocn_a_00561.

Spreckelmeyer, K. N., Krach, S., Kohls, G., Rademacher, L., Irmak, A., Konrad, K., et al. (2009). Anticipation of monetary and social reward differently activates mesolimbic brain structures in men and women. *Social Cognitive and Affective Neuroscience, 4*(2), 158-165, doi:10.1093/scan/nsn051.

Steinhauser, M., Maier, M., & Hübner, R. (2008). Modeling behavioral measures of error detection in choice tasks: Response monitoring versus conflict monitoring. *Journal of Experimental Psychology: Human Perception and Performance, 34*(1), 158-176, doi:10.1037/0096-1523.34.1.158.

Steinhauser, M., & Yeung, N. (2010). Decision Processes in Human Performance Monitoring. *The Journal of Neuroscience, 30*(46), 15643-15653, doi:10.1523/jneurosci.1899-10.2010.

Steward, T., Picó-Pérez, M., Mata, F., Martínez-Zalacaín, I., Cano, M., Contreras-Rodríguez, O., et al. (2016). Emotion Regulation and Excess Weight: Impaired Affective Processing Characterized by Dysfunctional Insula Activation and Connectivity. *PLOS ONE, 11*(3), e0152150, doi:10.1371/journal.pone.0152150.

Stockburger, J., Weike, A. I., Hamm, A. O., & Schupp, H. T. (2008). Deprivation selectively modulates brain potentials to food pictures. *Behavioral Neuroscience, 122(4), pp. 936-942*, doi:10.1037/a0012517.

Stoeckel, L. E., Kim, J., Weller, R. E., Cox, J. E., Cook, E. W., & Horwitz, B. (2009). Effective connectivity of a reward network in obese women. *Brain Research Bulletin, 79*(6), 388-395, doi:10.1016/j.brainresbull.2009.05.016.

Tricomi, E., Balleine, B. W., & O'Doherty, J. P. (2009). A specific role for posterior dorsolateral striatum in human habit learning. *European Journal of Neuroscience, 29*(11), 2225-2232, doi:10.1111/j.1460-9568.2009.06796.x.

Tsotsos, J. K. (1990). Analyzing vision at the complexity level. *Behavioral and Brain Sciences, 13*(3), 423-445, doi:10.1017/s0140525x00079577.

Turken, A. U., & Swick, D. (2008). The effect of orbitofrontal lesions on the error-related negativity. *Neuroscience Letters, 441*(1), 7-10, doi:10.1016/j.neulet.2008.05.115.

Uher, R., Treasure, J., Heining, M., Brammer, M. J., & Campbell, I. C. (2006). Cerebral processing of food-related stimuli: Effects of fasting and gender. *Behavioural Brain Research, 169*(1), 111-119, doi:10.1016/j.bbr.2005.12.008.

Ullsperger, M., Fischer, A. G., Nigbur, R., & Endrass, T. (2014). Neural mechanisms and temporal dynamics of performance monitoring. *Trends in cognitive sciences, 18*(5), 259-267, doi:10.1016/j.tics.2014.02.009.

Valentin, V. V., Dickinson, A., & O'Doherty, J. P. (2007). Determining the Neural Substrates of Goal-Directed Learning in the Human Brain. *The Journal of Neuroscience, 27*(15), 4019-4026, doi:10.1523/jneurosci.0564-07.2007.

van der Laan, L. N., de Ridder, D. T. D., Viergever, M. A., & Smeets, P. A. M. (2011). The first taste is always with the eyes: A meta-analysis on the neural correlates of processing visual food cues. *NeuroImage, 55*(1), 296-303, doi:10.1016/j.neuroimage.2010.11.055.

van Veen, V., & Carter, C. S. (2002a). The anterior cingulate as a conflict monitor: fMRI and ERP studies. *Physiology & Behavior, 77*(4-5), 477-482, doi:10.1016/s0031-9384(02)00930-7.

van Veen, V., & Carter, C. S. (2002b). The timing of action-monitoring processes in the anterior cingulate cortex. *Journal of Cognitive Neuroscience, 14*(4), 593-602, doi:10.1162/08989290260045837.

Verdejo-Román, J., Fornito, A., Soriano-Mas, C., Vilar-López, R., & Verdejo-García, A. (2017a). Independent functional connectivity networks underpin food and monetary reward sensitivity in excess weight. *NeuroImage, 146*, 293-300, doi:10.1016/j.neuroimage.2016.11.011.

Verdejo-Román, J., Vilar-López, R., Navas, J. F., Soriano-Mas, C., & Verdejo-García, A. (2017b). Brain reward system's alterations in response to food and monetary stimuli in overweight and obese individuals. *Human Brain Mapping, 38*(2), 666-677, doi:10.1002/hbm.23407.

Verleger, R., Koerbs, A., Graf, J., Śmigasiewicz, K., Schroll, H., & Hamker, F. H. (2014). Patients with Parkinson's disease are less affected than healthy persons by relevant response-unrelated features in visual search. *Neuropsychologia, 62*, 38-47, doi:10.1016/j.neuropsychologia.2014.07.004.

Verleger, R., Zurawska Vel Grajewska, B., & Jaśkowski, P. (2012). Time-course of hemispheric preference for processing contralateral relevant shapes: P1pc, N1pc, N2pc, N3pc. *Advances in cognitive psychology, 8*(1), 19-28, doi:10.2478/v10053-008-0098-9.

Vilkka, L. (1997). *The Intrinsic Value of Nature*.

Völlm, B., Richardson, P., McKie, S., Elliott, R., Dolan, M., & Deakin, B. (2007). Neuronal correlates of reward and loss in Cluster B personality disorders: a functional magnetic resonance imaging study. *Psychiatry research, 156*(2), 151-167, doi:10.1016/j.pscychresns.2007.04.008.

Wang, B., Yan, C., Klein, R. M., & Wang, Z. (2018). Inhibition of return revisited: Localized inhibition on top of a pervasive bias. *Psychonomic Bulletin & Review, 25*(5), 1861-1867, doi:10.3758/s13423-017-1410-9.

Warren, C., & Holroyd, C. (2012). The Impact of Deliberative Strategy Dissociates ERP Components Related to Conflict Processing vs. Reinforcement Learning. [Original Research]. *Frontiers in Neuroscience, 6*(43), doi:10.3389/fnins.2012.00043.

Watson, P., & de Wit, S. (2018). Current limits of experimental research into habits and future directions. *20*, 33-39, doi:10.1016/j.cobeha.2017.09.012.

Weaver, M. R., & Brittin, H. C. (2001). Food Preferences of Men and Women by Sensory Evaluation Versus Questionnaire. *Family and Consumer Sciences Research Journal, 29*(3), 288-301, doi:10.1177/1077727x01293006.

Wright, H., Li, X., Fallon, N. B., Crookall, R., Giesbrecht, T., Thomas, A., et al. (2016). Differential effects of hunger and satiety on insular cortex and hypothalamic functional connectivity. *European Journal of Neuroscience, 43*(9), 1181-1189, doi:10.1111/ejn.13182.

Yarkoni, T., Poldrack, R. A., Nichols, T. E., Van Essen, D. C., & Wager, T. D. (2011). Large-scale automated synthesis of human functional neuroimaging data. [Article]. *Nature Methods, 8*, 665, doi:10.1038/nmeth.1635.

Yeung, N., Botvinick, M. M., & Cohen, J. D. (2004). The Neural Basis of Error Detection: Conflict Monitoring and the Error-Related Negativity. *Psychological Review, 111*(4), 931-959, doi:10.1037/0033-295x.111.4.931.

Yeung, N., & Cohen, J. D. (2006). The Impact of Cognitive Deficits on Conflict Monitoring:Predictable Dissociations Between the Error-Related Negativity and N2. *Psychological Science, 17*(2), 164-171, doi:10.1111/j.1467-9280.2006.01680.x.

Yin, H. H., Knowlton, B. J., & Balleine, B. W. (2004). Lesions of dorsolateral striatum preserve outcome expectancy but disrupt habit formation in instrumental learning. *European Journal of Neuroscience, 19*(1), 181-189, doi:10.1111/j.1460-9568.2004.03095.x.

Yin, H. H., Ostlund, S. B., Knowlton, B. J., & Balleine, B. W. (2005). The role of the dorsomedial striatum in instrumental conditioning. *European Journal of Neuroscience, 22*(2), 513-523, doi:doi:10.1111/j.1460-9568.2005.04218.x.

Acknowledgements

First, I would like to thank my supervisor and mentor, Prof. Thomas F. Münte and Dr. Nuria Doñamayor Alonso, for their support, guidance, constructive criticism and help in carrying out PhD thesis. I am also much thankful to them for their invaluable support for financing my PhD work. Without their help, this PhD would not be completed on time.

It has been a pleasure to be part of the Münte group at CBBM (Center of Brain, Behavior and Metabolism). I am especially grateful to all my colleagues at CBBM for the excellent work environment they offered to me. Furthermore, I would like to express my gratitude to my family and to my friends for their continuous support.